

# RESTON AND ZAIRE EBOLAVIRUS LIFE CYCLE AND HOST CELLULAR RESPONSE

A comparative study



## FRIEDRICH-SCHILLER- UNIVERSITÄT JENA

Dissertation zur Erlangung des Akademischen Grades  
doctor rerum naturalium (Dr. rer. nat.)

vorgelegt dem Rat der Fakultät für Mathematik und Informatik  
der Friedrich Schiller Universität Jena

von

NELLY FERNANDA MOSTAJO BERROSPI

geboren am 29. Jan. 1988 in Lima, Peru

June 2020

BETREUER: Prof. Dr. Manja Marz

BETREUER: Prof. Dr. Stephan Becker

GUTACHTER:

1. Prof. Dr. Manja Marz, Friedrich-Schiller-Universität Jena
2. Prof. Dr. Stephan Becker, Philipps Universität Marburg

TAG DER ÖFFENTLICHEN VERTEIDIGUNG: 14.04.2021

Nelly Fernanda Mostajo Berrospi: *Reston and Zaire ebolavirus life cycle and host cellular response*, A comparative study , © June 2020



## ABSTRACT

---

Ebolaviruses are negative strand RNA viruses which are known to cause Ebola virus disease (EVD) with a fatal outcome in primates. All five species of Ebolavirus can infect humans, but only four lead to EVD. The Ebolavirus with the most provoked outbreaks and highest fatality rate (above 80%) is Zaire ebolavirus (EBOV), while the one without any provoke symptoms in humans is Reston ebolavirus (RESTV). In order to determine the features which lead to the different outcomes from EBOV and RESTV the cellular response against these viruses, and the divergence between RESTV and EBOV life cycle inside human cells was investigated. To study the cellular response RNA of two human cell lines (HuH7 and THP1) infected with RESTV, EBOV and uninfected (Mock) at two different time points was analyzed. Using whole transcriptome screening with smallRNAseq, Microarray, *de novo* annotation and expression profiles it was possible to elucidate that the cellular response against RESTV and EBOV infection differs the most at 3 h p.i., this was consistent in HuH7 and THP1 cell lines. The transcriptomic study showed RESTV and EBOV stimulate a distinct set of genes related to cellular entry. Also, the transcriptomic data suggests EBOV transcribes and replicates faster than RESTV, supported by cellular components like snoRNAs, while RESTV is similar to Mock in this aspect. This finding was backed with an entry assay which showed EBOV releases its content into the cytosol faster than RESTV, pointing to differences in entry pathway or a better time controlled response from the cell against RESTV. To understand the life cycle of RESTV and EBOV in human cells transcription/replication, inclusion bodies, nucleocapsid (NC) transport, viral particle formation, and infection was studied. Selected genes which were differentially expressed between RESTV and EBOV infected cells were further analyzed on the virus life cycle context. Evaluation of different steps in the viral replication cycle revealed no clear difference between RESTV and EBOV, but in the formation and composition of the produced viral particles where it was found a different viral protein ratio. It was also observed RESTV NP amino acid sequence differences with EBOV could already limit protein-protein interactions, explaining the viral life cycle disruption found when EBOV VP35 and EBOV VP40 are combined with RESTV NP. This points to RESTV NP being the limiting factor for the virus to have the same success in humans as EBOV.

Furthermore, it was found that the miRNA miR-204 is up-regulated 3 h.p.i. only in RESTV infected cells. Over-expression of miR-204 in the presence of EBOV components caused similar effects observed in RESTV life cycle, like reduced incorporation of NP into new viral particles and a reduced transcription/replication. This could be explained with miR-204 over-expression altered NP inclusion bodies morphology, which would affect viral transcription/replication. Taken together, these results suggest the viral protein NP and its cellular interactions are the main difference in the pathogenicity between RESTV and EBOV. In addition, miR-204 negatively affects the life cycle of the virus by disrupting its propagation and limiting the possibility of further infections. However, it needs to be further explored what triggers miR-204 at such an early time post infection and the target genes of this miRNA which could affect the virus life cycle. To conclude, this study proposes the differences between RESTV and EBOV outcome in humans is due to a combination of intrinsic and cellular factors. Finally, a further exploration of NP interactome and miR-204 can lead to a better understanding to fight EVD.

## ZUSAMMENFASSUNG

---

Ebolaviren sind Negativstrang-RNA-Viren von denen bekannt ist, dass sie eine Ebola-Virus-Krankheit (EVD) verursachen, welche für Primaten oft tödlich endet. Alle fünf Arten des Ebolavirus können Menschen infizieren, wobei aber nur vier zu EVD führen. Das Ebolavirus mit den häufigsten Infektionen und der höchsten Todesrate (über 80%) ist das Zaire-Ebolavirus (EBOV), während hingegen das Reston-Ebolavirus (RESTV) keine Symptome beim Menschen auslöst. Um die Eigenschaften zu bestimmen, welche zu diesen unterschiedlichen Verhalten von EBOV und RESTV führen, wurde die zelluläre Antwort gegen diese Viren, und der Unterschied zwischen den "Lebenszyklen" von RESTV und EBOV in menschlichen Zellen untersucht. Zur Untersuchung der zellulären RNA-Antwort wurden zwei menschliche Zelllinien (HuH7 und THP1) zu zwei verschiedenen Zeitpunkten unter verschiedenen Bedingungen analysiert: infiziert mit RESTV oder EBOV und eine nicht infizierte Kontrollgruppe (Mock). Unter Verwendung des gesamten Transkriptom-Screenings mit smallRNAseq-, Microarray-, *de novo* -Annotationen und Expressionsprofilen konnte aufgeklärt werden, dass sich die zelluläre Antwort gegen RESTV- und EBOV-Infektionen am stärksten bei

3 h p.i. unterscheidet, sowohl in HuH7 als auch in THP1-Zelllinien. Die transkriptomische Studie zeigte, dass RESTV und EBOV eine bestimmte Menge von Genen stimuliert, die in Zusammenhang mit dem Zelleintritt stehen. Die transkriptomischen Daten legen auch nahe, dass EBOV schneller als RESTV transkribiert und sich repliziert, unterstützt durch zelluläre Komponenten wie snoRNAs. In diesem Aspekt verhält sich RESTV ähnlich dem Mock. Diese Entdeckung wird durch ein Eintrittsassay gestützt, welches zeigte, dass EBOV seinen Inhalt schneller als RESTV in das Cytosol abgibt, was auf Unterschiede im Eintrittsweg oder eine bessere zeitgesteuerte Reaktion der Zelle gegen RESTV hinweist. Um den "Lebenszyklus" von RESTV und EBOV bei der Transkription/Replikation menschlicher Zellen zu verstehen, wurden Einschlusskörperchen, Nucleocapsid (NC) Transporte, Bildung viraler Partikel und Infektionen untersucht. Im Hinblick auf den "Lebenszyklus" des Virus wurden ausgewählte Gene weiter analysiert, welche zwischen RESTV- und EBOV-infizierten Zellen unterschiedlich exprimiert wurden. Die Auswertung verschiedener Phasen im viralen Replikationszyklus ergab keinen signifikanten Unterschied zwischen RESTV und EBOV. Bei der Bildung und Zusammensetzung der produzierten viralen Partikel hingegen konnte ein unterschiedliches virales Proteinverhältnis festgestellt werden. Weiterhin wurde beobachtet, dass Aminosäuresequenzunterschiede zwischen RESTV NP und EBOV bereits Protein-Protein-Wechselwirkungen begrenzen könnten, was die Störung im viralen "Lebenszyklus" erklärt, welche auftritt, wenn EBOV VP35 und EBOV VP40 mit RESTV NP kombiniert wird. Dies deutet darauf hin, dass RESTV NP der limitierende Faktor ist um beim Menschen den gleichen Erfolg zu erzielen wie EBOV. Zudem wurde gefunden, dass die miRNA miR-204 3 h p.i lediglich in RESTV-infizierten Zellen hochreguliert ist. Eine Überexpression von miR-204 in Gegenwart von EBOV-Komponenten verursachte ähnliche Effekte, welche im RESTV "Lebenszyklus" beobachtet werden konnte; wie zum Beispiel eine verringerte Inkorporation von NP in neue Viruspartikel oder eine verringerte Transkription/Replikation. Dies könnte mit einer durch miR-204-Überexpression veränderten Morphologie der NP-Einschlusskörperchen erklärt werden, die die virale Transkription/Replikation beeinflussen würde. Zusammengefasst legen diese Ergebnisse nahe, dass das virale Protein NP und seine zellulären Wechselwirkungen den Hauptunterschied in der Pathogenität zwischen RESTV und EBOV darstellen. Darüber hinaus beeinflusst miR-204 den "Lebenszyklus" des Virus negativ, wobei es seine Vermehrung stört und dadurch die Möglichkeit weiterer Infektionen einschränkt. Es muss jedoch weiter untersucht werden, was miR-204 zu einem so frühen Zeitpunkt nach

einer Infektion auslöst und welche Zielgene dieser miRNA den "Lebenszyklus" des Virus beeinflussen könnten. Zusammenfassend lässt sich sagen, dass die Unterschiede zwischen den Ergebnissen der RESTV und EBOV Studien mit menschlichen Zellen auf eine Kombination von intrinsischen und zellulären Faktoren zurückzuführen sind. Schließlich kann eine tiefere Untersuchung des NP-Interaktoms und miR-204 zu einem besseren Verständnis der Bekämpfung von EVD führen.

## PUBLICATIONS

---

### List of publications

- [1] Nelly F Mostajo, Marie Lataretu, Sebastian Krautwurst, Florian Mock, Daniel Desirò, Kevin Lamkiewicz, Maximilian Collatz, Andreas Schoen, Friedemann Weber, Manja Marz, et al. “A comprehensive annotation and differential expression analysis of short and long non-coding RNAs in 16 bat genomes”. In: *NAR Genomics and Bioinformatics* 2.1 (2020), lqz006.
- [2] Konstantin Riege, Martin Hölzer, Tilman E Klassert, Emanuel Barth, Julia Bräuer, Maximilian Collatz, Franziska Hufsky, Nelly Mostajo, Magdalena Stock, Bertram Vogel, et al. “Massive effect on LncRNAs in human monocytes during fungal and bacterial infections and in response to vitamins A and D”. In: *Scientific reports* 7.1 (2017), pp. 1–13.
- [3] Martin Hölzer, Verena Krähling, Fabian Amman, Emanuel Barth, Stephan H Bernhart, Victor AO Carmelo, Maximilian Collatz, Gero Doose, Florian Eggenhofer, Jan Ewald, et al. “Differential transcriptional responses to Ebola and Marburg virus infection in bat and human cells”. In: *Scientific reports* 6 (2016), p. 34589.
- [4] Richard Henze, Jan Huwald, Nelly Mostajo, Peter Dittrich, and Bashar Ibrahim. “Structural analysis of in silico mutant experiments of human inner-kinetochore structure”. In: *BioSystems* 127 (2015), pp. 47–59.
- [5] Roberto Lozano, Olga Ponce, Manuel Ramirez, Nelly Mostajo, and Gisella Orjeda. “Genome-wide identification and mapping of NBS-encoding resistance genes in *Solanum tuberosum* group phureja”. In: *PLoS One* 7.4 (2012).

### List of publications in progress

- [1] S Becker N Mostajo M Marz. “RESTV and EBOV molecular components comparison”. In: (in preparation).
- [2] M Marz N Mostajo S Becker. “Transcriptome analysis of cells infected with RESTV and EBOV”. In: (in preparation).



*The most exciting phrase to hear in science,  
the one that heralds new discoveries,  
is not "Eureka!" but "That's funny..."*

–Isaac Asimov

## ACKNOWLEDGMENTS

---

There are many people I would like to thank who have accompanied me on my way to this thesis. First of all I want to thank my supervisors Manja Marz and Stephan Becker, who made this experience possible. I feel really lucky and fortunate for the opportunity of combining wet- and dry-lab in one project, and for the great people I got to share this experience with.

Nadine Biedenkopf and Dirk Becker were part of the heads and hands which did the viral experiments that allowed the start of the whole thesis. Martin Hoelzer was since the first stage making sure that the sequencing and the Bioinformatic part was properly arranged to have a great start.

Furthermore, Science is about exchanging ideas and knowledge, and helping each other. I have colleagues from the Bioinformatics/High-Throughput Analysis group in Jena and the Virology Institute in Marburg, who I can call friends, which made this work successful and gratifying. Additionally to Nadine, Dirk and Martin, are Emanuel B., Max C., S. Krauty, Franzi H., Verena K., Corni R., Sandro H., Katharina K., Yuki T., Astrid H., and hopefully not many more...

Last but not least, I am thankful to my family who from the distance always supported my crazy journey to Germany and kept me going. Also, friends who also helped with their own experience, Felipe and Kari, and friends who push me forward. Finally, my sweet husband Richard H. who had the worst and best of me during the whole experience, and stayed.

**Financial support:** This thesis was financially supported by **Scholarship:** The German Academic Exchange Service (DAAD).





# CONTENTS

---

<b>1</b>	<b>Introduction</b>	<b>1</b>
1.1	Ebolavirus . . . . .	2
1.1.1	Viral morphology and protein function . . . . .	2
1.1.2	Ebolavirus life cycle . . . . .	3
	Viral entry . . . . .	3
	Transcription and replication . . . . .	4
	Nucleocapsid transport . . . . .	4
	Filamentous particle formation and release . . . . .	4
1.2	EBOV and RESTV known differences . . . . .	6
1.3	Studying viral Ebolavirus protein function outside BSL4 . . . . .	6
1.3.1	Minigenome . . . . .	7
1.3.2	Infectious virus-like particle . . . . .	7
1.3.3	NC movement via Live cell imaging . . . . .	8
1.4	Human ncRNAs . . . . .	8
1.5	Aim of this study . . . . .	9
<b>2</b>	<b>Materials</b>	<b>11</b>
2.1	Genomes . . . . .	11
2.2	Primers . . . . .	12
2.3	Plasmids encoding recombinant proteins . . . . .	14
2.4	Cells . . . . .	15
2.5	Agomir . . . . .	15
2.6	Programs and tools . . . . .	16
<b>3</b>	<b>Methods</b>	<b>19</b>
3.1	Biochemical and molecular methods . . . . .	19
3.1.1	Gel electrophoresis . . . . .	19
3.1.2	Protein visualization . . . . .	20
	Western blot . . . . .	20
	Silver staining . . . . .	20
3.1.3	Cloning . . . . .	21
3.1.4	Immunofluorescence analysis . . . . .	22
3.2	Cell biological methods . . . . .	22
3.2.1	Cell preparation . . . . .	22

3.2.2	Transfection . . . . .	22
	HEK293 cell line treatment . . . . .	23
	HuH7 cell line treatment . . . . .	23
3.2.3	Minigenome . . . . .	24
3.2.4	Infectious viral-like particle (iVLP) . . . . .	24
	iVLP purification . . . . .	25
	Filamentous iVLP purification . . . . .	26
	Infection of naive and pre-transfected cells . . . . .	27
3.2.5	Luciferase measurement . . . . .	28
3.2.6	Entry assay . . . . .	29
3.2.7	Nucleocapsid study and evaluation . . . . .	29
3.2.8	Agomir transfection and analysis . . . . .	30
3.2.9	BSL4 infections . . . . .	31
3.2.10	Infection and RNA preparation for transcriptome analysis . . . . .	31
3.3	Bioinformatic methods . . . . .	32
3.3.1	Small RNA sequencing and analysis . . . . .	32
3.3.2	Microarray analysis . . . . .	32
3.3.3	Ebolavirus sequence comparison . . . . .	33
3.4	Overview of study: Graphical summary . . . . .	33
<b>4</b>	<b>Results</b>	<b>37</b>
4.1	Differences in cellular response caused by RESTV and EBOV infection . . . . .	37
4.1.1	Different cellular response to viral infection observed at early time point . . . . .	37
	The small RNA-Seq data shows EBOV and RESTV cause a different cellular response at early infection in both cell lines . . . . .	39
4.1.2	THP1 and HuH7 cell lines share ncRNAs triggered by RESTV and EBOV infection . . . . .	40
	snoRNAs expression discriminates better between RESTV and EBOV treatments . . . . .	41
	Specific miRNAs are only triggered by RESTV . . . . .	42
4.1.3	THP1 cells show that RESTV triggers a ncRNA-immune response pathway . . . . .	44
4.1.4	Microarray data shows early time point of infection as a common feature between cell lines against a pathogenic virus . . . . .	45

4.2	RESTV vs EBOV: from assay establishment to evaluation of viral compatibility . . . . .	46
4.2.1	Antibody selection for RESTV studies . . . . .	47
4.2.2	RESTV and EBOV show minor differences in the minigenome assay . . . . .	48
	RESTV minigenome establishment . . . . .	49
	Transcription/replication components evaluation . . .	50
	Minigenome inhibitors evaluation . . . . .	51
4.2.3	Major difference between EBOV and RESTV found on protein incorporation into filamentous particles . . . .	53
	Virus filamentous particles composition of RESTV and EBOV . . . . .	53
	Filamentous particle release analyses . . . . .	56
	Comparison of transcription and replication in iVLP context . . . . .	57
	iVLP infectivity . . . . .	59
4.2.4	RESTV NP and EBOV VP35 do not form a stable NC .	61
4.2.5	Cell entry: EBOV releases its content into the cytosol faster than RESTV . . . . .	64
4.3	Ebolavirus intrinsic differences . . . . .	66
4.3.1	Ebolaviruses protein sequences comparison . . . . .	66
4.3.2	Ebolavirus non-coding regions comparison . . . . .	67
	Transcription start sites suggest common regulation with other ebolaviruses . . . . .	69
	Viral putative small ncRNAs could represent a new factor for host response . . . . .	69
4.4	Cellular candidates and their influence in viral fitness . . . .	70
4.4.1	Mir-204 and miR-10a affect viral transcription/replication . . . . .	72
4.4.2	miR-204 affects NP/VP40 ratio on filamentous particles	72
4.4.3	miR-204 effect in the viral proteins cellular distribution	73
	Aggregates formed by EBOV NP alone and with minigenome components do not get affected by miR-204 . . . . .	75
4.4.4	EBOV infection and inclusion bodies are affected by miR-204 . . . . .	75
4.5	Results' graphical summary . . . . .	80
<b>5</b>	<b>Discussion</b>	<b>83</b>

<b>6 Conclusion</b>	<b>91</b>
<b>7 Supplementary data</b>	<b>93</b>
7.1 Cellular response . . . . .	93
7.2 Minigenome . . . . .	93
7.3 iVLP . . . . .	93
7.4 miR-204 . . . . .	93

## LIST OF FIGURES

---

1.1	Ebolavirus summarized life cycle . . . . .	5
3.1	Human transcriptome response against EBOV and RESTV approach . . . . .	34
3.2	Viral life cycle studied via minigenome assay, iVLPs and LCI systems method summary . . . . .	35
4.1	PCA of HuH7's and THP1's small RNA-Seq data based on two annotations . . . . .	41
4.2	Heatmap of ncRNAs with the highest FC in both HuH7 and THP1 cells . . . . .	42
4.3	PCA of snoRNAs and miRNAs from HuH7 and THP1 cells . . . . .	43
4.4	Heatmap of differentially expressed miRNAs . . . . .	44
4.5	Visualization of reads from RESTV treatment mapping on IFIT2 and CXCL10 in THP1 cells . . . . .	45
4.6	Heatmap of microarray DEG in HuH7 and THP1 cells . . . . .	46
4.7	Stripe WB of RESTV with different available antibodies . . . . .	48
4.8	RESTV minigenome relative reporter activity comparison with different RESTV components concentrations . . . . .	50
4.9	Minigenome reporter activity measurement after exchanging protein components between EBOV and RESTV . . . . .	52
4.10	Minigenome reporter activity measurement after the addition of viral transcription/replication inhibitors between EBOV and RESTV . . . . .	54
4.11	Silver gel of collected supernatant from cells infected with RESTV, EBOV (Makona and Mayinga) . . . . .	56
4.12	iVLP preparation with different combinations of NP, GP and VP40 from RESTV and EBOV in HuH7 cells . . . . .	58
4.13	MG relative reporter activity from iVLPs formed by the combination of RESTV and EBOV components in HuH7 cells . . . . .	59
4.14	Maximum intensity projection of moving NC formed with different combinations of NP, VP35 and VP24 from RESTV and EBOV . . . . .	62
4.15	Detailed evaluation of chimeric RESTV (R) and EBOV (Z) NCs . . . . .	65
4.16	Entry assay result summary . . . . .	66

4.17	Predicted secondary structure of TSS from all ebolaviruses . . . . .	70
4.18	Putative ncRNA in VP40-TSS . . . . .	71
4.19	Effect of different miRNAs on the minigenome reporter activity of RESTV and EBOV . . . . .	73
4.20	Effect of miR-204 on EBOV's protein ratio NP/VP40 measured by WB . . . . .	74
4.21	Immunofluorescence of HuH7 cells treated with miR-204 and transfected with iVLP components from RESTV and EBOV collected at 24 h p. t. and 48 h p. t. . . . .	76
4.22	Immunofluorescence of HuH7 cells treated with miR-204 and transfected with NP or minigenome components . . . . .	77
4.23	Immunofluorescence of HuH7 cells treated with miR-204 and infected with RESTV or EBOV . . . . .	78
4.24	RESTV vs EBOV summary . . . . .	81

## LIST OF TABLES

---

2.1	Genome sequences used in the present study . . . . .	12
2.2	RESTV cloning primers . . . . .	13
2.3	Mutagenesis primers . . . . .	14
2.4	Plasmids encoding recombinant proteins . . . . .	15
2.5	Agomir sequences . . . . .	16
2.6	Programs used for the analysis of sequences and data . . . . .	17
3.1	Polyacrylamide gel ingredients for different gel concentrations.	20
3.2	Antibodies usage for western blot. . . . .	21
3.3	Immunofluorescence antibodies list . . . . .	22
3.4	Human cells used and quantities . . . . .	23
3.5	Minigenome plasmid concentration used for EBOV and RESTV	24
3.6	Minigenome plasmid concentration tried for RESTV study . . .	24
3.7	Minigenome plasmid concentration of RESTV and EBOV components to evaluate transcription/replication inhibition . . .	25
3.8	Plasmid concentration of RESTV and EBOV components for iVLP assay . . . . .	25
3.9	Ultracentrifugation settings . . . . .	26

3.10	Viral plasmids and amounts used for transfecting cells before iVLP infection . . . . .	28
3.11	Plasmid concentrations for LCI . . . . .	29
4.1	HuH7 sequencing results . . . . .	38
4.2	THP1 sequencing results . . . . .	39
4.3	Protein ratio calculation from RESTV and EBOV strains Makona and Mayinga. . . . .	55
4.4	Chimeric iVLP infection ratio in HuH7 pre-transfected cells .	61
4.5	NP, VP35 and VP40 aa differences between RESTV and other ebolaviruses . . . . .	68
4.6	L most common substitutios between RESTV and other ebolaviruses . . . . .	69
4.7	Ratio of EBOV infected cells with different NP distribution observed in miR-NC and miR-204 treated samples after 18 and 42 h.p.i.. . . . .	79
7.1	Top 80 commonly differentially expressed genes in HuH7 and THP1 cells genomic location . . . . .	94
7.2	Top 80 differentially expressed genes in THP1 cells genomic location . . . . .	95
7.3	Top 80 differentially expressed genes in HuH7 cells genomic location . . . . .	96
7.4	RESTV MG reporter activity standardization . . . . .	97
7.5	Relative EBOV MG reporter activity in the combination of RESTV and EBOV components . . . . .	97
7.6	Relative RESTV MG reporter activity in the combination of RESTV and EBOV components . . . . .	98
7.7	Relative EBOV MG reporter activity in the presence of viral inhibitors . . . . .	98
7.8	Relative RESTV MG reporter activity in the presence of viral inhibitors . . . . .	99
7.9	Relative MG reporter activity of EBOV and RESTV iVLPs after protein exchange . . . . .	99
7.10	Relative reporter MG activity of RESTV and EBOV after AgoMiR treatments . . . . .	100
7.11	Effect of miR-204 on EBOV's protein amount inside the cells and filamentous particles measured by WB . . . . .	100

## ACRONYMS

---

ANKRD2	Ankyrin Repeat Domain 2
AP1S3	Adaptor-related protein complex 1 sigma subunit
APS	Ammonium persulfate
BDBV	Bundibugyo ebolavirus
bp	Base pairs
BSL4	Biosafety level 4
C-terminus	Carboxy-terminus
CXCL10	C-X-C Motif Chemokine Ligand 10
DAPI	4',6-Diamidino-2-phenylindol
DEG	Differentially expressed genes
DMEM	Dulbecco's Modified Eagle Medium
DMEM++	DMEM penicillin/streptomycin
DNA	Desoxyribonucleic acid
dNTP	Deoxynucleoside triphosphate
E.coli	Escherichia coli
EBOV	Ebola virus (former Zaire)
EVD	Ebola virus disease
FC	Fold change
FCS	Fetal calf serum
FITC	Fluorescein isothiocyanate
GFP	Green fluorescent protein
GP	Glycoprotein
h	Hour



HBV Hepatitis B virus  
HCV Hepatitis C virus  
HEK293 Human kidney cells  
HuH7 Human hepatome cells  
IFA Immunofluorescence analysis  
IFIT2 Interferon Induced Protein With Tetratricopeptide Repeats 2  
IFN Interferon  
IL-6 Interleukin 6  
IL6R Interleukin 6 Receptor  
iVLP Infectious virus-like particle  
kb Kilo bases  
KCNQ5 Potassium Voltage-gated Channel Subfamily Q Member 5  
kDa Kilo Dalton  
KLK8 Kallikrein Related Peptidase 8  
L Polymerase large protein  
LCI Live cell imaging  
MARV Marburg virus  
MG Viral minigenome: 3'-reporter gene-5'  
min minutes  
MIP Maximum intensity projection  
miR-10a hsa-miR-10a-5p  
miR-10b hsa-miR-10b-5p  
miR-204 hsa-miR-204-5p  
miR-NC MiR-Negative control  
miRNAs microRNA  
MOI Multiplicity of infection

mRNA messenger RNA

MT Mitochondria

NC Nucleocapsid

ncRNAs Non coding RNAs

NP Nucleoprotein

NPC1 Niemann Pick 1

nt Nucleotide

N-terminus Amino-terminus

ORF Open reading frame

p.i. Post infection

p.t Post transfection

PAGE Polyacrylamide gel electrophoresis

PBSdef Phosphate-buffered saline deficient in magnesium and calcium

PCA Principal component analysis

PCR Polymerase chain reaction

pH potentia hydrogenii

PKR Eukaryotic Translation Initiation Factor 2 Alpha Kinase 2

REBOV Reston ebolavirus

RNA-Seq RNA sequencing

RNA Ribonucleic acid

RNAi RNA interference

rpm Revolutions per minute

rRNA ribosomal RNA

RT Room temperature

SCN10A Sodium Voltage-gated Channel Alpha Subunit 10

SDS Sodium dodecyl sulfate

siRNA Short interference ribonucleic acid

snoRNA small nucleolar RNA

snRNA small nuclear RNA

STAT3 Signal Transducer And Activator Of Transcription 3

SUDV Sudan virus

T7 T7 DNA-dependent RNA polymerase

TAFV Tai Forest virus

TCID50 Tissue culture infectious dose 50

TEMED Tetramethylethylenediamine

THP1 Human monocytic cell

TIM-1 human T-cell immunoglobulin and mucin domain protein 1

TNE Tris-HCL NaCL EDTA buffer

tRNAs transfer RNA

TRPM3 Transient receptor potential cation channel subfamily M member 3

TSS Transcription starting site

UTRs Untranslated region

VLP Virus-like particle

VP24 Viral protein 24

VP30 Viral protein 30

VP35 Viral protein 35

VP40 Viral protein 40

WB Western blot

ZG16 Zymogen Granule Protein 16



## INTRODUCTION

---

Ebolaviruses are known to cause ebola virus disease (EVD) which affects primates including humans with high fatality rates. Zaire ebolavirus (EBOV) has caused the highest amount of outbreaks and deaths since the discovery of the disease. Reston ebolavirus (RESTV), was discovered later than EBOV, and was found to infect humans but without causing them any symptoms. The current thesis explores all the possible comparisons between EBOV and RESTV including: life cycle, from infection to particle formation; intrinsic and functional protein divergence; differences on the cellular response towards both viruses at different times after infection; and to evaluate regulated genes which could explain the contrasting outcome of both viruses on humans. The aim is to use this knowledge to improve the understanding of EBOV and RESTV pathogenicity and to expose targets for the control of EVD.

Ebola virus disease (EVD) is caused by Ebolaviruses and provokes severe infection in primates which can lead to severe fever and death. EVD was discovered in 1976 after two simultaneous outbreaks in Central Africa. The first outbreak was in Sudan and registered a fatality rate of 53 % with Sudan ebolavirus (SUDV) being the causative agent. The second outbreak was in the Democratic Republic of Congo with an 88 % fatality rate and was caused by Zaire ebolavirus (EBOV). In 1989 a virus was discovered in *Cynomolgus macaques*. The virus caused hemorrhagic fever symptoms with a high fatality rate, but did not cause symptoms in humans. This virus was named Reston ebolavirus (RESTV) [1, 2]. Humans can get infected by all ebolavirus species and the fatality rate varies from 0 % to 90 % [3]. This means ebolavirus contains species which represent the extremes of human pathogenicity. Since EVD discovery there have been reports of ebolaviruses almost every year. SUDV and EBOV are the cause of most of the reported cases. In 2014 the largest outbreak of EVD was reported with more than 28,000 confirmed cases and was caused by EBOV [2]. EVD has an incubation period of 2 to 21 days, and it starts with symptoms of a cold and can be mistaken for influenza or malaria. The development of the disease to fatal cases or survival

depends on the clinical care and the immune system of the patient. However, there is not a licensed treatment to combat EVD and the outbreaks are getting more common, even one ongoing, and the fatality rates are above 40% [2, 4, 5]. Altogether, there is a need to understand better the ebolaviruses in order to fight them properly.

## 1.1 Ebolavirus

Filoviruses are single-stranded, negative-sense RNA viruses. Three genera are known to belong to the family *Filoviridae*: Cuevavirus, Marburgvirus, and Ebolavirus [6]. The genus Ebolavirus comprises five species: Bundibugyo ebolavirus (BDBV), RESTV, SUDV, TaiForest ebolavirus (TAFV) and EBOV [6, 7]. RESTV is the only Ebolavirus species which is known to infect humans without causing symptoms, in contrast with other non-human primates. [8].

### 1.1.1 Viral morphology and protein function

Ebolaviruses have a filamentous shape, as the name Filovirus implies, but can also form a six-like and a donut-like shape. The viral particle has a relatively constant width of 80 nm, and a variety of length between 10-13  $\mu$ m [9]. The Ebolavirus genome is *ca.* 19 Kb, it contains seven non-consecutive open reading frames (ORFs), and it is bordered by 3' and 5' secondary structures. The ORFs are located in the genome in the following order: the nucleoprotein (NP), the viral protein 35 (VP35), VP40, glycoprotein (GP), VP30, VP24 and the polymerase (L) [10, 11]. The particle is formed by GP attached to a host derived membrane which has also attached VP40 in the inner side; Inside the viral particle is the nucleocapsid (NC), which is the viral genome encapsidated by NP, VP35 and VP24, VP30 and L [12].

EBOV proteins have been better studied than those of other sister species, and their main functions established. Here are presented the roles directly related to the virus life cycle. NP is essential for transcription/replication, NC assembly and transport, and subsequent infections due to its role as the envelope of the viral RNA. VP35, as NP, is necessary for transcription/replication and NC transport, and also has known effects in the infected cells. VP40 is a protein which assembles in different homo-polymers: not all its forms are understood; it is responsible for the formation of the filamentous particles (assembly and budding); and is one of the main components of the viral matrix. GP surrounds all the outer filamentous particle. It is known to

be the first contact with the surface of the target cell, and its cleavage is necessary for the release of the filamentous content into the cytosol. GP's ORF codifies three forms: full length GP, soluble GP and small soluble GP. The different forms of GP are produced by L editing, and have different roles in the life cycle of the virus. VP30 is a co-factor of viral transcription/replication, and it is suggested to be the switch between transcription and replication. L is the RNA dependent polymerase, which is in charge of the viral transcription/replication with NP and VP35. VP24 is also known as a matrix component. It seems to compress the NC and is necessary for the NC movement. VP24 also seems to promote NC incorporation into the viral particles via VP40 interaction. VP24 has cellular roles which help EBOV establish the infection. It is interesting to mention that VP35, VP30 and VP40 seem to disrupt the RNA interference (RNAi) machinery, due to their ability of RNA binding, but the implication in the viral life cycle is not known [11, 13].

### 1.1.2 Ebolavirus life cycle

EBOV initially and preferentially replicates in immune cells i.e. macrophages and dendritic cells [14, 15]. Thus, the virus replication is supported by the immune response. Additionally, EBOV can infect a variety of organs including liver and brain [16]. The ebolavirus life cycle is not entirely understood, but it can be divided into three parts (summarized in fig. 1.1). Firstly: viral contact is made with the cell surface via GP, viral particle engulfment and macropinocytosis, GP cleavage inside the late endosome, binding to the receptor Niemann-Pick type C1 (NPC1) and fusing with the endosomal membrane, and release of the NC into the cytosol (see fig. 1.1 A). Secondly: the virus establishes transcription/replication inside viral inclusion bodies, with a high presence of NP, which are perinuclear allowing translation and further protein modifications only possible with the host machinery (see fig. 1.1 B). Thirdly: the NC is formed and transported via actin filaments until reaching the plasma membrane where with VP40 (inner membrane) and GP (outer membrane) can form filamentous particles, and form a new viral particle [11]. However, the assembly is not entirely synchronized because the virus can form empty particles (see fig. 1.1 C).

#### *Viral entry*

Little is known about the whole process of Ebolavirus entry into the cell. GP first adheres to the cell, activates macropinocytosis allowing the virus to enter the cellular endosomal compartment. Then, GP is cleaved by cysteine

proteases during the maturation of the vesicle [17]. This cleavage exposes EBOV GP position 82 allowing the interaction with NPC1, and GP position 544 with the membrane for fusion [18]. Then the NC gets released into the cytosol, allowing the start of primary transcription/replication.

#### *Transcription and replication*

The transcription and replication of Ebolaviruses have been explored in more detail than other viral processes. These are mainly observed in NP aggregations, referred to as NP inclusion bodies. These inclusion bodies work as hot-spots where viral proteins, namely NP, VP35, VP30, L, and cellular components get recruited and where the viral genome is processed. The order of events is still not entirely comprehended, but each step for transcription or replication needs the coordination of NP, VP35, VP30 and L, and the recognition of two motives 3' CUC/ACUUCUAAUU and 3' UAAUUC(U). For replication the negative-sense RNA is used as a template to synthesize a positive-sense RNA copy. Then, the newly synthesized positive RNA is used as template to produce more copies of the viral genome. For transcription the negative-sense RNA can be used directly for transcribing each ORFs individually [19].

#### *Nucleocapsid transport*

There is still a gap of knowledge regarding the synchronization of events, but there must be a switch which determines the transition from transcription/replication to NC formation. VP35 and NP interaction seems to determine the switch from transcription-replication to NC [20, 21]. NP wraps the viral genome to protect it from the host RNases. VP24 binds the complex NP-RNA and compacts it, blocking the entire access to the genome by any protein. The protein complex, composed of NP, VP35 and VP24, forms a transport-competent NC which is able to move around the cell via actin filamentous/polymerization, in a directed manner [22].

#### *Filamentous particle formation and release*

The building blocks of filamentous particles are GP and VP40. VP40 hexamers are formed at the inner layer of the plasma membrane to build a matrix, and likely form membrane protrusions and recruit the NC. Also, GP reaches the plasma membrane after going through post-translational modifications, most notably glycosylation. However, it is not understood if there is a coordination between VP40 and GP to form the filamentous particles, or at least



to favor it, but it is possible to release GP-vesicles and GP-VP40 empty particles. Furthermore, once the NC is completely surrounded by VP40, which is attached to the inner cellular membrane, and GP located in the transmembrane region towards the outer membrane, a viable filamentous particle is formed and released. It is not known how the filamentous particle closes or detaches from the membrane. Neither is it known where or how L and VP30 are incorporated into the NC, but it is not possible to have viable infectious virus without L and VP30 proteins inside the filamentous particles [23–25].

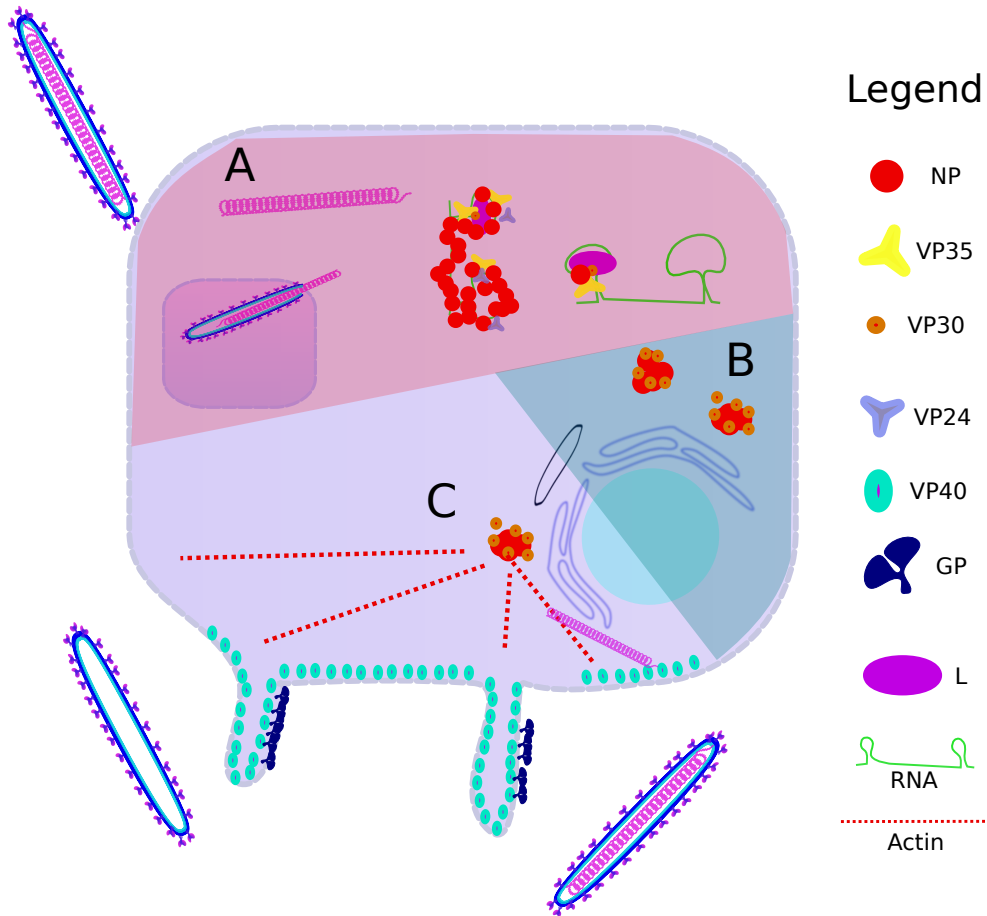


Figure 1.1: Ebolavirus summarized life cycle. (A) Entry: The virus contacts the cellular membrane. This englobes the virus into a vesicle, where different proteins will cause the fusion to the vesicle membrane and NC release into the cytosol. (B) Established replication: Viral fabric loci are formed around the cytosol. Here active transcription and replication for further translation are ongoing. (C) Viral particle assembly and release: The NC is transported via actin filamentous. Once it reaches the membrane the NC can assemble with the matrix proteins into a protrusion which ends on a viral particle: there is a lack of synchronization of this process, allowing the release of empty viral particles.

## 1.2 EBOV and RESTV known differences

Despite the lack of fully developed tools for RESTV research outside BSL4 facilities, there are advances in the comparison of RESTV and EBOV. Various studies propose a different cellular response towards RESTV and EBOV which can be triggered by viral factors. RESTV GP and VP35 were suggested to contribute to the virulence in different primates, GP interaction with TIM-1 and CD209 and VP35 with PKR inhibiting the effect of IFN [26]. The protein interactions, viral and cellular, seem to be interrupted due to the cellular domains variance in the different species. The differences on VP35 between EBOV and RESTV would give less affinity to RESTV VP35 towards double strand RNA (dsRNA), but more stability to the system, and are thought to be directly related to the difference on the IFN stimulation [27, 28]. Also, it has been shown that Marburg virus (MARV) and EBOV are able to suppress the IFN response, while RESTV stimulates it [29]. Moreover, recent reports suggest the IFN stimulation difference is mainly related to GP, and EBOV is able to activate many more factors related to the immune response than RESTV [30]. Nevertheless, it was shown that exchanging GP between RESTV and EBOV leads to the same outcome, only it took longer [31]; also, it was observed that RESTV and EBOV symptoms differ only significantly on the liver pathology [31, 32], but it is not enough to explain the difference between both viruses. Interestingly, EBOV can activate Interleukin 6 (IL-6) and not RESTV [30]. MARV and EBOV do not seem to control the IFN response with the same viral protein, but EBOV affects IFN alpha/beta via VP24 and MARV affects IFN alpha/beta/gamma via VP40, including the phosphorylation of STAT3 and IL-6 [33]. However, it has not been explored if RESTV VP40 has any effect on IFN stimulation. Therefore, the cause remains unknown for the difference between the outcome or pathogenicity of these two viruses. In order to investigate fully the differences between EBOV and RESTV in BSL1 or BSL2 facilities it is necessary to establish tools for the study of RESTV, like that already developed for EBOV.

## 1.3 Studying viral Ebolavirus protein function outside BSL4

RESTV is a virus poorly investigated compared to the pathogenic sister species SUDV and EBOV. The study of Ebolaviruses is challenging. The virus is highly mortal and all the species contained in this family are considered BSL4 agents. EBOV has been extensively studied outside BSL4 conditions because of available tools and methods such as: minigenome, for the study

of transcription and replication; infectious viral like particle (iVLP), for the study of particle formation and infectivity; live cell imaging (LCI), for the study of nucleocapsid (NC) transport [22, 34]. These tools are a plasmid-based transfection system, based on the possibility to produce viral proteins inside the cells and replace the whole viral genome for a reporter gene or truncated genome for hindering the production of viable viral particles.

### 1.3.1 Minigenome

The minigenome assay can be used to understand viral transcription/replication in the cellular context. EBOV and RESTV share the same proteins, and basics for transcription and replication. The components needed for this process are the proteins NP, VP35, VP30 L and the 3' and 5' sequences of the viral genome. The only necessary signal for recruiting the proteins for transcription and replication and then starting the process are in the secondary structure formed by the 3' and 5' sequences of the viral genome. In order to measure the activity and efficiency of the process outside BSL4 conditions, it is possible to replace everything between the 3' and 5' for a reporter gene. This is named minigenome (MG: viral 3'-reporter gene-5') in EBOV and RESTV [34, 35]. Notwithstanding the possible role or effect of the viral secondary structures formed along the genome. Moreover, this assay has to be properly established to ensure that the reporter control (for normalization) does not get affected by any added extracellular component.

### 1.3.2 Infectious virus-like particle

To evaluate the viral capability to infect new cells one needs to produce viral-like particles (VLPs). The viral particles can be formed with VP40 and GP. The inclusion of NP, VP35, VP30, L and MG with VP40 and GP can produce viral particles which are able to infect new cells and transcribe/replicate the reporter gene of the MG in a measurable manner. The addition of VP24 into the system improves the production of formed particles. The formed particles are named transcription and replication competent virus-like particle or infectious virus-like particles (iVLP). They can be used to understand the viral molecular biology, pathogenesis and life cycle of the virus [34]. However, there is currently no iVLP system for RESTV available.

### 1.3.3 NC movement via Live cell imaging

EBOV's NCs have long directed trajectories in the cell. NP, VP35 and VP24 are the only necessary components for the NC movement. Live cell imaging (LCI)T is used for the study of the NC-like structures under BSL1 conditions [22]. This technique allows a direct analysis of the protein interactions and their behaviors inside the cell. Since the NC assembly is necessary for an efficient transport of the NC, it will influence the production of viable iVLPs. This is a relatively new technique and has not been tried with RESTV components, and could help to see if RESTV has an impaired NC in human cells.

Moreover, the above mentioned tools do not take in account the cellular context. The host non-coding RNAs (ncRNAs) response towards EBOV and RESTV has not been studied.

## 1.4 Human ncRNAs

EBOV has been extensively studied, and triggered cascades as well as miRNA markers during virus infection have been determined [36, 37]. But there is not a study of the ncRNA population during infection of RESTV and EBOV. NcRNAs are RNA molecules that are not translated into a protein. The number of ncRNAs is still uncertain, but they fulfill a variety of functions. Until now, mostly small RNAs have been studied, for example transfer (t)RNAs, micro (mi)RNAs, small nucleolar (sno)RNAs, and small nuclear (sn)RNAs (see [38] for details). MiRNAs are small ncRNAs of 22 nucleotides (nt) found in all eukaryotes but also in prokaryotes and viruses. In animals they mediate post-transcriptional gene silencing while regulating the translation of mRNAs into proteins [39]. It is estimated that miRNAs govern the translation of 60% of protein-coding genes [40]. SnoRNAs are 60-300 nt long and can be divided into two types: C/D and H/ACA box snoRNAs. They facilitate the folding of the rRNA and stabilize it. In addition, snoRNAs are involved in the post-transcriptional regulation of mRNA expression via methylation or pseudouridylation [41]. Moreover, new studies suggest that snoRNAs are involved in splicing regulation [42, 43].

Current research shows that ncRNAs are part of the cellular virus infection response which can be triggered to combat the pathogen or warn the immune system. Therefore, the specific cell response acts as a footprint for each virus. [44–46]. Components of this footprint can be required by the pathogen in order to replicate and survive. For example, mir-122 is a miRNA found

commonly in the liver, and reported to be part of the replication cycle of Hepatitis C virus (HCV) (see [47] for a review). Vaccinia virus was observed to change the snoRNA human expression profile. This change was necessary for the virus to survive [48]. Therefore, the determination and study of these footprints are needed to understand the pathogenicity of viral infections.

### 1.5 Aim of this study

EVD continues to cause human loses. The differences between RESTV and EBOV could expose the traits which make EBOV pathogenic to humans. However, most of the research focus has been mainly on EBOV. Few reports compared RESTV and EBOV. Some include aspects of the viral replication cycle but none compares ncRNA-related cell response to these viruses. As mentioned above, ncRNAs are known to be relevant during a viral infection, and understanding the complete cell response could give a better picture of the viral effects in humans. The aim of this study was to determine differences and similarities between RESTV and EBOV infection, cellular response and life cycle in order to pinpoint the traits which are responsible for the different pathogenicity of these two viruses in humans. Specifically, the focus of this study is on the comparison of cellular RNA-related differential expression against the highly pathogenic EBOV and the non-pathogenic RESTV. These results could give a detailed comprehension of the cellular responses and have the potential to unveil new targets for the development of antiviral countermeasures against the deadly EBOV.



## MATERIALS

---

[ Here are listed the materials used in this study without detailing materials for well established and known protocols. ]

This document was typeset using an adapted version of the `classicthesis` template developed by André Miede, available for both  $\text{\LaTeX}$  and  $\text{\LyX}$  (<http://www.miede.de/#classicthesis>).

### 2.1 Genomes

The human and viral genomes used for the reads mapping were merged into one consecutive genome. This allowed the localization of most of the outcome reads expected from the sequencing. A merged genome also allows a better discrimination of the reads mapping to its origin. The genomes versions are listed in table 2.1 "RNA-Seq reference genome". The identification of differences between ebolaviruses was done using more viral genomes for each species. Most ebolaviruses have more than one complete genome sequence publicly available, except for TAFV which only has one (to date). The genomes versions are listed in table 2.1 "TSS alignment".

Table 2.1: Genome sequences used in the present study

Analysis	Species	Entry
RNA-Seq reference genome	Human	GRCh38
	EBOV	AF086833.2
	RESTV	AB050936.1
TSS alignment	BDBV	Gi:302371213
	EBOV	Gi:10313991
	RESTV	Gi:22789222
	SUDV	Gi:55770807
	TAFV	Gi:302315369
Sequence Comparison	BDBV	FJ217161, KC545393, KC545394, KC545395, KC545396, KR063673, KU182911
	EBOV	AF054908, EU224440, AF086833, J04337, AF272001, KF113528, AF499101, KF113529, AJ001707, KJ660346, AY058896, KJ660347, AY058897, AY142960, AY354458
	MARV	Z29337.1
	RESTV	AB050936, AF522874, AY769362, FJ621583, FJ621584, FJ621585, JX477165, JX477166, KY008770, KY798004, KY798005, KY798006, KY798007, KY798008, KY798009, KY798010, KY798011, KY798012, FJ621583
	SUDV	AY729654, EU338380, FJ968794, JN638998, KC242783, KC545389, KC545390, KC545391, KC545392, KC589025, KT750754, KT878488, KY425631, KY425644, KC545391
	TAFV	FJ217162

## 2.2 Primers

The primers are nucleotide sequences used for the direct amplification of RNA or DNA sequences. These were used for RESTV proteins cloning (see table 2.2). Also were used for the sequence edition of RESTV coding sequences, also known as mutagenesis, (see table 2.3).



Table 2.2: RESTV cloning primers

RESTV product	Primer number and sequence 5'-3'	Orientation	Size (nt)	Restriction enzymes
NP	4137: GCAGAATTCATAATGGATCGTGGGACCAGAAG	Forward	2233	EcoRI, KpnI
	4138: GCAGGTACCTTACTGATGGTGTGCAAGATTG	Reverse		
VP35	4139: GCACCCGGGTAAATGTACAATAATAAATTGAAGTATGTTC	Forward	1000	XmaI, NotI
	4140: GCAGCGGCCGCTTAGATCTTAAAGTCCAAGCGTTTTA	Reverse		
VP40	4143: GCAGAATTCATAATGAGCGCGGAGTGTAC	Forward	1005	EcoRI, XmaI
	4144: GCACCCGGGTATTGGTAACTAATCTGCTTGTC	Reverse		
GP	4145: GCACCCGGGATGGGGTCAGGATATCAACTTCT	Forward	2047	XmaI, SacI
	4146: GCAGAGCTCATCAACACAAAATCTTACATATACAAAAGT	Reverse		
VP30	4147: GCAGAATTCATAATGGAGCAITCAAGAGAACGG	Forward	874	EcoRI, NotI
	4148: GCAGCGCCGCTAATCAACTGTACTTGACCAGG	Reverse		
VP24	4150: GCACCTCGAGTAAATGGCTAAAGCCACAGGCC	Forward	765	XhoI, XmaI
	4151: GCACCCGGGTAAATGGCCAAACAACCTGTGAACT	Reverse		
L	4152: GCACCCGGGTAAATGGCTACCCAGCATACCCA	Forward	2302	XmaI, NheI
	4157: GCAGCTAGCCTATGTGTGATTGGAATATATTAACC	Reverse		
3'-Renilla-5'	4158: GCATTCGAAGTCATGGTGGTATGAGAATCGACTTCCCTTGTTCGA	Forward	527	BstBI, RsRII
	4159: GCAGCCACCCGGAGGAGTGGAGATGCCATGCCGACCCCGGACACACAAAAAGAAAAAAGG	Reverse		
	4160: GCACCCGGTTAATACGACTCACTATAGGACACACAAAAAGGAAAAAATTGG	Forward		
	4161: GCAGCGGCCGCTACTAAATCATCATAGTATGAGGA	Reverse	741	XmaI, NotI

Table 2.3: Mutagenesis primers

<b>Primer</b>	<b>Mutagenesis primer</b>	<b>Sequence 5'-3'</b>
4214	GP A extension	TGGGCCTTCTGGGAAACTAAAAAAAAACTTTTCCC
4215	GP T896C	TGCATTTCCAAATTCCATCAACCCAC
4216	GP C1526T	TACTATTGGACAGCTGTTGATGAGGGGGC
4217	NP C1112A	GGCCTGGACGATCAGGAAAGAAGAATAC

### 2.3 Plasmids encoding recombinant proteins

A plasmid is genetic material which can be replicated, transcribed and transferred independent of the organism's chromosomes. It can include coding sequences of choice to be introduced and produced in target cells. Plasmid constructs used for the expression of viral proteins are listed in table 2.4.

Table 2.4: Plasmids encoding recombinant proteins

<b>Vector</b>	<b>Encoded protein</b>	<b>Virus</b>	<b>Name</b>
pAndy	3E-5E Renilla luciferase	EBOV	pAndy-3E5E-luciferase
pCAGGS	T7 polymerase	-	pCAGGS-T7
pCAGGS	GP	EBOV	EBOV pCAGGS-GP
pCAGGS	L	EBOV	EBOV pCAGGS-L
pCAGGS	NP	EBOV	EBOV pCAGGS-NP
pCAGGS	VP24	EBOV	EBOV pCAGGS-VP24
pCAGGS	VP30	EBOV	EBOV pCAGGS-VP30
pCAGGS	VP35	EBOV	EBOV pCAGGS-VP35
pCAGGS	VP40	EBOV	EBOV pCAGGS-VP30
pCAGGS	VP30-Firefly	EBOV	EBOV pCAGGS-VP30-FF
pCAGGS	VP30-GFP	EBOV	EBOV pCAGGS-VP30-GFP
pAndy	3R-5R Renilla luciferase	RESTV	pAndy-3R5R-luciferase
pCAGGS	GP	RESTV	RESTV pCAGGS-GP
pCAGGS	NP	RESTV	RESTV pCAGGS-NP
pCAGGS	L	RESTV	RESTV pCAGGS-L
pCAGGS	VP24	RESTV	RESTV pCAGGS-VP24
pCAGGS	VP30	RESTV	RESTV pCAGGS-VP30
pCAGGS	VP35	RESTV	RESTV pCAGGS-VP35
pCAGGS	VP40	RESTV	RESTV pCAGGS-VP40
pGL4	Firefly	-	pGL4-FF

## 2.4 Cells

HuH7, HEK293, THP1 cell lines were available in the Institute of Virology from Marburg (Germany).

## 2.5 Agomir

The Agomir was used to mimic the miRNA of interest and evaluate their effect in the cells. The sequences of the Agomir which were obtained from shanghai GenePharma are listed in table 2.5.

Table 2.5: Agomir sequences

Name	Sequence 5'-3'
hsa-miR-10b-5p agomiR	uaccuguagaaccgaauuugug caauucgguucuacagguauu
hsa-miR-10b-5p agomiR	uaccuguagaucggaauuugug caauugccaucuacagguauu
hsa-miR-204-5p agomiR	uucccuugucauccaugccu gcauaggaugacaaaggaauu
Agomir N.C.	uucccgaacgugucacguTT acgugacacguucggagaaTT

## 2.6 Programs and tools

Available programs and software used for the developing of this thesis are listed in table 2.6. Specifications of the usage of each program is detailed in 3.

Table 2.6: Programs used for the analysis of sequences and data

<b>Program</b>	<b>Version</b>	<b>Used for</b>
BioEdit	7.0.5.3	Small sequence analysis
Blockclust	1.0.0	ncRNA prediction based on blocks
Clone Manager	9	Cloning planning
CoRal	1.1.1	ncRNA prediction
cutadapt	1.4.1	Adaptors removal
DESeq2	1.22.2	Differential expression analysis
FastQC	0.113	Quality assessment
featureCounts	1.5.3	Reads per transcript counting
Image Lab	5.2	Detection and quantification of bands
ImageJ	1.47	Immunofluorescence analysis
Inkscape	0.92.3	Picture preparation
LaTeX	3.14	Document writing
locarna	1.8.11	TSS analysis and prediction
miRDeep	2.0.08	miRNA predictions
Nikon NIS Elements	3.1	LCI picture evaluation
PoSeiDon	-	Recombination and positive selection analysis
PRINSEQ-lite	0.20.3	Quality filtering
Python	2.7, 3.7	Data analysis
R studio	3.5	Analysis and graphic preparation
TopHat	2.1.1	Reads mapping
TrackEvaluator	0928	LCI deep evaluation



## METHODS

The human transcriptome was investigated in two cell lines, HuH7 (hepatome like) and THP1 (differentiated into macrophages) in the context of virus infection with EBOV as well as RESTV (apathogenic), and compared with uninfected cells (Mock). Two time points were chosen for the analysis these are 3 h p.i., representing an early time of infection, and 24 h p.i., which shows an established infection and the release of new viral particles (see fig. 3.1). These time points were selected in accordance with previously published data where the highest amount of genes differentially expressed in EBOV was observed [36]. In addition, multiple sequence alignments were calculated to find differences between RESTV and all other Ebolavirus species, which are known to cause human EVD. Further, EBOV and RESTV transcription/replication, filamentous particle formation and infection were evaluated and compared, using a minigenome assay, iVLPs and LCI system (see fig. 3.2). These systems were first established for RESTV using EBOV's systems as reference. With a full study of all the differences between EBOV, RESTV, and other Ebolaviruses it was possible to narrow down viral protein candidates related to infection. Finally, with a proper understanding of RESTV and EBOV differences in the systems studied, cellular genes differentially expressed in RESTV treatment were explored.

### 3.1 Biochemical and molecular methods

#### 3.1.1 Gel electrophoresis

Gel electrophoresis is a technique which allows the separation of molecules by size and charge. The gel is done with polymers that form a matrix which works as a particle resistance. This resistance helps to discern the size of the molecules which are moved by an electric current across the matrix. Agarose is used as the matrix to discern big molecules, and polyacrylamide matrix is

Table 3.1: Polyacrylamide gel ingredients for different gel concentrations.

Ingredients	Stacking gel		Separation gel	
	4%	8%	10%	12%
dH <sub>2</sub> O	2.9 mL	4.7mL	4 mL	3.3 mL
30% polyacrylamide (Rotiphorese 30)	0.750 mL	2.7 mL	3.3 mL	4 mL
SDS PAGE Stacking gel buffer	1.25 mL	-	-	-
SDS PAGE Separation gel buffer	-	2.5 mL	2.5 mL	2.5 mL
APS 10% in dH <sub>2</sub> O	0.05 mL	0.1 mL	0.1 mL	0.1 mL
TEMED	0.01 mL	0.01 mL	0.01 mL	0.05 mL

used for smaller size differences. Here agarose gel was used for DNA separation and polyacrylamide gel for protein separations, as described in Koehler (2017) [49], with the additional polyacrylamide percentages depending on the study (see Table.3.1).

For the protein size determination the PageRuler Plus Prestained Protein Ladder from Thermofisher was used.

### 3.1.2 Protein visualization

#### *Western blot*

The western blot technique allows specific detection of proteins transferred (or blotted) from an SDS gel into a membrane. For all the experiments a nitrocellulose membrane and a semi-dry blotting were used. For details of the assembly and staining of the proteins the protocol from Koehler (2017) [49] was followed with the variations: a) nitrocellulose GelCondoes not need an activation with methanol b) the chamber was set up to 45 min. at 10 V c) the membrane was washed for 10 min and not 5 min in each round d) the substrate used for the protein visualization was Forte for most of the experiments unless specified The specific proteins were observed with the use of different antibodies listed in table 3.2.

#### *Silver staining*

Silver staining is a method which allows the precipitations of molecules with silver- the staining is unspecific and really sensitive. The silver staining was performed following the manufacturer's instructions from the Pierce silver stain kit.



The band intensities, which represent single protein populations, were measured with ImageView.

### 3.1.3 Cloning

Cloning refers to the technique of copying a piece of genomic information or gene into a vector to form a recombinant genome, which is going to be copied or multiplied as part of the replication cycle of the vector. The final goal to produce copies of the recombinant genome (plasmid) for further purification and production of the inserted gene. The steps are as follows: a) amplify the genomic information or gene, b) purify the gene, c) dephosphorylate the target genomic vector, d) digest the end of the gene and the genomic vector in order to have complementary sequences between them, e) ligate both gene and vector, f) transform the host, which refers to the introduction of the plasmid into the host, usually a bacteria, g) foment host replication, h) purify stock plasmid, i) sequence confirmation via sequencing, j) sequence correction via mutagenesis (if needed), k) quantification and storage.

Protocols and cloning documents already established for EBOV were used for designing a similar RESTV cloning approach. RNA was extracted from cells infected with RESTV by Nadine Biedenkopf and Dirk Becker. Primers were designed for each ORF based on the RESTV genomic available sequence. The primers included ends with the enzyme recognition sequence present in the multiple cloning site from the plasmid vector pCAGGS (see Materials for sequences). The cDNA and amplification rounds were done with the designed primers and the *Omniscript RT kit* using the manufacturer's instructions. Further steps were performed following the protocols

Table 3.2: Antibodies usage for western blot.

Primary antibody	Species	Dilution	Secondary antibody	Species	Dilution
anti VP40 (2C4)	Mouse	1:200			
anti NP (B6C5)	Mouse	1:200	anti Mouse	Donkey	1:20000
anti GP (3B11)	Mouse	1:500			
anti Sudan	Goat	1:1000	anti Goat	Donkey	1:20000
anti EBOV	Goat	1:1000			
anti NP	Chicken	1:1000	anti Chicken	Donkey	1:20000
anti VP40	Chicken	1:1000			
anti Tubulin	Mouse	1:500	anti Mouse	Donkey	1:20000

Table 3.3: Immunofluorescence antibodies list

Primary antibody	Species	Dilution	Secondary antibody	Species	Dilution	Wavelength
anti VP40	Mouse	1:50	anti Mouse	Human	1:300	Alexa 647
anti NP	Chicken	1:100	anti Chicken	Goat	1:300	Alexa 488
-	-	-	DAPI	-	1:10000	
-	-	-	Phalloidin	-	1:600	FITC

available in Koehler (2017) [49]. The polymerase L plasmid was finished by C. Rohde and A. Herwig and RESTV MG was done by N. Biedenkopf.

### 3.1.4 Immunofluorescence analysis

Immunofluorescence analysis allows the visualization of the protein's location inside the cells. It is possible to directly mark the protein of interest, or mark it indirectly. For all the experiments presented here HuH7 cells were seeded and transfected or infected with EBOV or RESTV components or virus. The viral experiments were performed in the BSL4 by Dirk Becker. The protocol from Koehler (2017) [49] was followed with variations: a) the incubation time was not 5 min but 10 min, b) the blocking buffer was left overnight to reduce background observed with the serums used, c) The direct actin marker Phalloidin was additionally used. The list of antibodies used and the specification of their usage is detailed in table 3.3

## 3.2 Cell biological methods

### 3.2.1 Cell preparation

Here is specified the preparation of cells used for transfection and study systems. The standardized cells used for EBOV life cycle study are HEK293 and HuH7 cell lines. These were counted and seeded in pre-warmed DMEM with FCS (10%) glutamine (2%) and penicillin/streptomycin mixture (2%) (10%FCS DMEM ++). The number of cells used for different study systems are specified in table 3.4.

### 3.2.2 Transfection

Transfection refers to the introduction of nucleic acids into cells with the objective of expressing the genetic information stored in the nucleic acid

Table 3.4: Human cells used and quantities

Plate size	Cells seeded	
	HEK293	HuH7
6 well	$8.0 \times 10^5$	$1.5 \times 10^5$
12 well	$3.0 \times 10^5$	$8.0 \times 10^4$
Ibidi 8 well	-	$1.0 \times 10^4$
6 well for Agomir	-	$3.0 \times 10^5$

sequence. In order to insert the material into the cells, one needs to open gaps in the cellular membrane- this process can change from cell to cell.

#### *HEK293 cell line treatment*

HEK293 is a cell line prepared from the kidney of a human embryo. These cells were kept in their growing media after 18-24 h seeded and the DNA to be transfected was prepared in 1.5 mL Micro Screw Tubes (regular bench). The transfection of the DNA into the cells was performed inside a laminar flow as follow:

- 1) 100  $\mu$ L OptiMem (reduced medium) is added to each tube containing the DNA to be introduced in the cells (mixture A).
- 2) 100  $\mu$ L OptiMem and 3  $\mu$ L/DNA  $\mu$ g of TransIT (reagent for opening of the membrane) is mixed and incubated for 5 min (mixture B).
- 3) 100  $\mu$ L of mixture B is added to mixture A and incubated for 15 min (final mixture).
- 4) The final mixture is added to the cellular medium of the corresponding well to be transfected in a drop-wise manner.

The cells are incubated at 37°C and 5% CO<sub>2</sub> for 24 h, 48 h or 72 h post transfection (p.t.) depending on the assay.

#### *HuH7 cell line treatment*

HuH7 is a cell line prepared from human liver cells. The cells were changed from their growing medium of 10% FCS DMEM ++ to 3% FCS DMEM ++ media after 18-24 h seeded. The DNA preparation and transfection continued as in HEK293 cells.

Table 3.5: Minigenome plasmid concentration used for EBOV and RESTV

Plasmids	Final [ng]
pCAGGS NP	125
pCAGGS VP35	125
pCAGGS L	1000
3'-Renilla-Luciferase-5'	250
pCAGGS T7 Polym	250
pCAGGS VP30	100
pGL4 (Firefly, control)	100

Table 3.6: Minigenome plasmid concentration tried for RESTV study

Plasmids	Final [ng]
pCAGGS NP	100
pCAGGS NP	250
pCAGGS VP30	70
pCAGGS VP30	200
pCAGGS VP35	70
pCAGGS VP35	250

### 3.2.3 Minigenome

EBOV minigenome was performed as specified in [34]. In summary, the assay was performed to quantify transcription/replication of the virus outside BSL4 conditions. Different combinations of viral proteins between RESTV and EBOV were tested to evaluate the compatibility of the proteins in this system. The amount of plasmids used for testing the combinations did not change from the original concentration specified below (see Table. 3.5). The constructs used for these experiments were prepared by Dirk Becker. It was established that the EBOV protocol can be used for RESTV study. The plasmid amounts tried for RESTV standardization are specified in Table. 3.6. The plasmid amounts used for transfection/replication inhibitors study are specified in Table. 3.7.

The cells were treated following section 3.2.5 after 48 h p.t..

### 3.2.4 Infectious viral-like particle (iVLP)

In summary, the assay was performed to quantify transcription/replication, viral particle formation and infectivity of the virus outside BSL4 conditions.

Table 3.7: Minigenome plasmid concentration of RESTV and EBOV components to evaluate transcription/replication inhibition

Plasmids	Final [ng]
pCAGGS GP	250
pCAGGS VP40	250
pCAGGS VP24	250

Table 3.8: Plasmid concentration of RESTV and EBOV components for iVLP assay

Plasmids	Final [ng]
pCAGGS VP40	250
pCAGGS VP24	60
pCAGGS GP	250
pCAGGS NP	125
pCAGGS VP35	125
pCAGGS L	1000
3'-Renilla-Luciferase-5'	250
pCAGGS T7 Polym	250
pCAGGS VP30	70
pGL4 (Firefly, control)	100

Different combinations of viral proteins were tested to evaluate the system in RESTV and to compare EBOV with RESTV. The plasmid from EBOV's used for these experiments were prepared by Dirk Becker. Most of the iVLPs here presented were prepared in HuH7 cells because there were more consistent results than in HEK293 cells. EBOV's protocol was used for RESTV iVLP production with the plasmid amounts specified in Table. 3.8.

#### *iVLP purification*

After the incubation period one needs to collect the supernatant and the cells separately. The formed and released iVLPs are in the supernatant. Inside the cells the produced proteins should be retained, including the Renilla luciferase, which is the only indication of proper viral transcription/replication. The cells were treated following the section 3.2.5. For the purification of the iVLPs from the supernatant the further steps were followed (inside the laminar flow).

- 1) after 72 h.p.t. collect the cell supernatant into 15 mL Falcon tubes
- 2) centrifuge the falcon tube for 10' 2500 rpm at 4°C to pellet dead cells

Table 3.9: Ultracentrifugation settings

Final volume	Sucrose underlay	Tube size	Speed	Time	Temperature
ca. 5mL	1mL	SW60	$4.5 \times 10^4$ rpm	2 h	4°C
ca. 12mL	2mL	SW41	$3.6 \times 10^4$ rpm	2 h	4°C
ca. 30mL	5mL	SW32	$3.0 \times 10^4$ rpm	2.5 h	4°C

- 3) transfer from step 2 only the supernatant to a new 15 mL Falcon tubes
- 4) prepare ultracentrifugation tubes with 20% Sucrose in 1x TNE depending on the collected supernatant final volume as in Table. 3.9
- 5) balance all the tubes before introducing them in the ultracentrifuge buckets, if necessary add sterile PBSdef for weight compensation
- 6) centrifuge the tubes following the tube size as described in Table. 3.9
- 7) when the run is over, collect the tubes carefully and remove the liquid by turning the tubes upside down in one movement and leaving them upside down above a paper towel (the particles are attached to the bottom of the tube)
- 8) with precision wipes and a dry sterile tweezers dry all the tube without touching the bottom of the tube (it is not always possible to observe a pellet)- do not turn the tube up until all the tube is dry
- 9) re-suspend the content while directing the desired liquid (depends on planned analysis or usage) to the bottom and mix without making any bubble (to avoid breaking the particles)

#### *Filamentous iVLP purification*

For filamentous particle purification the iVLP purification steps described above were followed until step 8. Then the particles were re-suspend in 730  $\mu$ L TNE buffer. Further:

- 1) prepare a 60% Nycodenz solution with TNE buffer.
- 2) in an SW60 tube prepare a Nycodenz gradient with a gradient pipette at the slowest speed following from bottom to top as follows: a) 730  $\mu$ L 30%, b) 490  $\mu$ L 20%, c) 490  $\mu$ L 15%, d) 490  $\mu$ L 10%, e) 490  $\mu$ L 7.5%, f) 490  $\mu$ L 5%, g) 490  $\mu$ L 2.5% At the end of the gradient one has to be able to observe the different layer between the different concentrations.

- 3) add the resuspended particles at the top of the tube
- 4) centrifuge in an SW60 rotor for 15 min at 16000 rpm (take 15 min of centrifuge at desired speed exactly)

The gradient has different densities, based on the nycodenz concentration, and the particles can go through the gradient based on their sizes. The different particle sizes can be differentiated in fractions, where the upper fraction (names fractions 1-3) of 1500  $\mu$ l contains small particles, vesicles, etc. The consecutive fraction of 1500  $\mu$ L, fractions 4 to 6, contains the filamentous iVLPs. Therefore, fractions 1 to 3 were collected in a TLA55 tube as control, and fractions 4 to 6 were also collected in a TLA55 tube for further analysis. The TLA55 tubes are centrifuged to concentrate the particles for 2 h at 45000 rpm. All the liquid has to be discarded without touching the bottom sides of the tube. Then the inside pellet can be re-suspended in 45  $\mu$ L TNE buffer and stored at 4°C until usage.

#### *Infection of naive and pre-transfected cells*

In order to see if the purified particles are properly assembled and functional it is necessary to use them for infecting new cells. It is possible to directly add the particles to the target cells (naive) or pre-transfect the cells with transcription/replication components (NP, VP35, VP30 and L with control pGL4) to increase the signal of the MG to evaluate the infection. Depending on the objective of the assay both approaches were used. EBOV's components give a higher RESTV and EBOV MG signal, therefore, only EBOV's components were pre-transfected to avoid false negatives in RESTV's infection evaluation. HuH7 cells were used for the analysis and were pre-transfected as follows:

- 1) prepare transfection components, as detailed above, using the plasmid amounts from the table 3.10 and incubate for 4-5 h (if pre-transfected)
- 2) change all the media for pre-warmed DMEM with 2% glutamine.
- 3) add concentrated iVLPs and incubate at 37°C and 5% CO<sub>2</sub> for 1.5 h with soft manual shaking every 15 min
- 4) add 2 mL 5% FCS DMEM++
- 5) incubate for 72 h. before proceeding to luciferase measurement as described below with the variations, resuspend the final cell pellet in 30  $\mu$ L Lysis buffer and do not dilute for measurement.

Table 3.10: Viral plasmids and amounts used for transfecting cells before iVLP infection

<b>Plasmids</b>	<b>Final [ng]</b>
pCAGGS NP	125
pCAGGS VP35	125
pCAGGS L	1000
pCAGGS VP30	100
pGL4 (Firefly, control)	100

### 3.2.5 Luciferase measurement

The MG contains a reporter gene which codifies a Renilla luciferase. The transcription/replication activity is measured via the Renilla luciferase signal. This was done as follows:

- 1) remove cell media.
- 2) wash the cells with 1 mL PBSdef (twice).
- 3) scrape the cells with 1 mL PBSdef and transfer all content into an 1.5 mL tube.
- 4) pull down the cells for 2 min at 3000 revolutions per minute (rpm).
- 5) remove all remaining liquid.
- 6) resuspend the cells in 100  $\mu$ L lysis buffer (2x Dual LysisJuice, PJK GmbH mixed with water in proportions 1:1).
- 7) store cell lysate at  $-20^{\circ}\text{C}$  overnight or until measurement takes place.
- 8) thaw the cells lysate, and precipitate the debris for 10 min at 13000 rpm at  $4^{\circ}\text{C}$ .
- 9) depending on the assay, 10  $\mu$ L of the direct supernatant or a dilution 1:100 in water, is put in a plate compatible with Luciferase Assay System (Promega).
- 10) measure the signal for 5sec. in Berthold Luminometer (Centro LB960) following company instructions.

The setup of the measurement correspond to Renilla for transcription/replication and Firefly for transfection normalization (unless specified otherwise).



Table 3.11: Plasmid concentrations for LCI

Plasmid	Concentration (ng)
NP	125
VP35	125
VP24	100
GFP-VP30	100

### 3.2.6 Entry assay

The speed of RESTV and EBOV content release into the cytosol was tested to evaluate the difference in the first steps of infection between both viruses. An adapted version of the entry assay from Mittler (2011) [50] was used (see fig. 4.16 A). In summary, iVLPs were prepared in a T75 flask (ca. 30mL) with EBOV VP40 , NP, and NP cofactor VP30 with a *Firefly* (VP30-luciferase) and GP from RESTV or EBOV (see fig. 4.16 B). After collecting only the filamentous particles (based on a gradient purification described above), were used to infect HEK293 cells in suspension. Then the luciferase (firefly) was collected and quantified at three time points after infection using a Luciferase Assay System (Promega) on a Berthold Luminometer (Centro LB960). The signal was then plotted to evaluate the time point where it goes above the independent background controls. For details of the controls here used refer to [50]. Additionally, the filamentous particles were also visualized in a silver gel to evaluate the integrity of the iVLPs.

### 3.2.7 Nucleocapsid study and evaluation

The NC transport involves the formation and displacement of the NC towards the cellular membrane. For details refer to section 1.3.3. The NC transport evaluation consists of following the particles inside the live cell live. One viral protein which attaches to the NC but does not interfere in the movement is VP30. Therefore, VP30 with a green fluorescent protein (GFP) (prepared by Yuki Takamatsu) was used in order to track the filamentous particles inside the cells. RESTV and EBOV components were prepared and combined as in Table. 3.11 to evaluate the NC transport of both viruses and their compatibility.

The NC components were transfected in an 8well ibidi as described above, and analyzed after at least 18 h p.t. For visualization the medium was changed to pre-warmed color-free Leibovits 20% FCS DMEM++. The

pictures were taken every two seconds for three minutes. At least three cells were taken for really active combinations and at least 10 cells in no obvious NC movement. Three independent transfections were prepared and analyzed to evaluate the NC transport of EBOV and RESTV. The images were taken and MPI was performed with Nikon NIS Elements 3.1. Deeper analysis of the acquired pictures was done with TrackEvaluator v. 0928 (implemented by Andreas Rausch, unpublished)

### 3.2.8 Agomir transfection and analysis

Agomir is the name of a synthetic molecule which resembles a mature miRNA with the addition of four thiols and a cholesterol residue in the 3' end, and 2 thiol and a 2'OMe in the 5' end. Agomir are double stranded and can imitate the selected miRNA being able to target mRNAs and reduce their translation. The advantages of these molecules compared to other available in the market are the affinity to the cell membrane, reducing the amount of transfection reagent needed and higher stability inside the cell. The Agomir molecules were acquired from Genepharma, for specific sequences refer to materials. The detailed protocol established here was performed inside the laminar flow with filter tips as follows:

- 1) re-suspend the Agomir following provider instructions, split in small aliquots to avoid freeze and defreeze rounds which can affect the efficiency of the molecules.
- 2) store the aliquots at -20C, and thaw at RT when needed.
- 3) prepare 6well dishes of HuH7 cells to have  $3 \times 10^5$  cells per well after 24 h of seeding.
- 4) change medium for 1 mL pre-warmed Optimem.
- 5) mix 100  $\mu$ L Optimem with 2.5  $\mu$ L Agomir and 2  $\mu$ L Dharmafect per desire well to transfect, this will give a final Agomir concentration of 50nM per well.
- 6) incubate for 20 min at RT.
- 7) add dropwise the prepared mixture to each well.
- 8) incubate at 37°C and 5% CO<sub>2</sub> for 4 h.
- 9) add 2 mL 3% FCS DMEM++.

- 10) incubate at 37°C and 5% CO<sub>2</sub> for 4h for iVLP transfection or 24h for virus infection
  - a) for transfection: Follow transfection protocol as described above with desired components without changing the medium and incubate for the necessary time.
  - b) for infection: change medium to 0%DMEM and infect for 1 h with the desired virus MOI, then change medium to 3 % FCS DMEM++ and incubate for the desired amount of time
- 11) every incubation was done at 37°C and 5% CO<sub>2</sub> for the desired amount of time.

The effect of the Agomir molecules was evaluated in the iVLP transcription/replication, iVLP integrity and infectivity. Therefore every treatment per experiment was prepared in 3 wells (of a 6well plate) and pulled together for analysis. The supernatant of the three wells was pulled together and filamentous particles were purified in a SW42 as described above. The cells were also pulled together and split in three: one for transcription/replication measurement, another for protein expression evaluation and the last one for RNA extraction. Every Agomir was studied at least three times independently.

### 3.2.9 BSL4 infections

The infections and collection of material from RESTV and EBOV was done following BSL4 protocols only by authorized persons. Colleagues who kindly contributed with the sample preparation for different steps are mentioned in the corresponding section.

### 3.2.10 Infection and RNA preparation for transcriptome analysis

The following steps were done by Nadine Biedenkopf and Dirk Becker following BSL4 protocols. THP1 cells were differentiated into macrophage like cells with PMA (final concentration in medium 200 nM) and grown in RPMI medium with FCS 10 % for growth (until usage) and differentiation; 0 % infection; and 3 % for growth after 1 hour post infection (h p.i.). HuH7 cells were cultivated in DMEM with FCS (10 % for growth; 0 % infection; and 3 % for growth after 1 h p.i.). The infections with EBOV (Mayinga) and RESTV

(Pennsylvania) were done with an MOI of 5 TCID<sub>50</sub> %/ml. The Mock samples and the virus samples were treated similarly. The total RNA was collected at 3 h p.i. and 24 h p.i. with mirVana miRNA Isolation kit (Ambion). The quality of the RNA was evaluated with Bioanalyzer. Every step was performed in parallel for three replicates. In total 36 samples were prepared for transcriptome analysis, each sample was distributed in three tubes (small RNA sequencing, Microarray and laboratory)

### 3.3 Bioinformatic methods

#### 3.3.1 Small RNA sequencing and analysis

For the small RNA sequencing (small RNA-Seq), the TruSeq Small RNA kit was used with strand specific preparation. Sequencing was done on an Illumina HiSeq2500 in single-end modus with 50 cycles (producing reads with a length of 50 bp). The reads from Illumina sequencing were processed previous to the mapping for adaptor removal with cutadapt 1.4.1 [51] and quality score < 20 and size (15-51 nt) with PRINSEQ-lite 0.20.3 [52]. Library quality was assessed after each step with FastQC v0.11.3 [53]. The mapping of the filtered reads was performed with TopHat 2.1.1 [54] (without gaps and at most one mismatch), against a concatenated genome of human (GRCh38), EBOV (AF086833.2) and RESTV (AB050936.1). *De novo* prediction of ncRNAs was performed with Blockclust v1.0.0 [55], miRDeep v2.0.08 [56] and CoRa1 v1.1.1 [57] using default parameters and miRBase 21 [58] data as input if required for training. A merged annotation file with the human Ensemble release 80 and the *de novo* annotated regions was used for the differential expression analysis (referred to in the results as *full annotation*). featureCounts v1.5.3 [59] was used for counting the reads and DeSeq2 [60] for the differential expression analysis, both as part of R software [61]. One replicate from EBOV treatment at 24 h p.i. was excluded because the values biased all the expression profiles (observed on a PCA).

#### 3.3.2 Microarray analysis

The 36 samples were sent and further processed by Jochen Wilhelm. The Microarray chip used for the study was "Human G3 v2 Kit 8x60k". This chip includes 26 083 coding gene probes and 30 606 long ncRNA probes. The data received was filtered based on saturation signal, signal below background,

significance on logarithm scale base 10 ( $\log_{10} > 1.5$ ) and fold change on logarithmic scale base 2 ( $FC > 2$ )

### 3.3.3 Ebolavirus sequence comparison

As a further approach to narrow down the differences between RESTV and pathogenic Ebolaviruses, genomic differences between all of the Ebolaviruses were explored. This was approached via the non-coding regions with a secondary structure analysis comparison and the coding one with a full alignment of the ORFs. The secondary structure prediction of the viral intergenic regions was performed with *locarna* [62] using max probabilities as parameter. All the input sequences from the different viruses were isolated from human samples. The seven ORF from the 5 species of Ebolavirus were aligned and mutagenesis was analyzed with *PoSeiDon* [63] using as parameters "with breaks". The input genomes for the sequence comparison are listed in section 2.1.

## 3.4 Overview of study: Graphical summary

### Cellular reponse

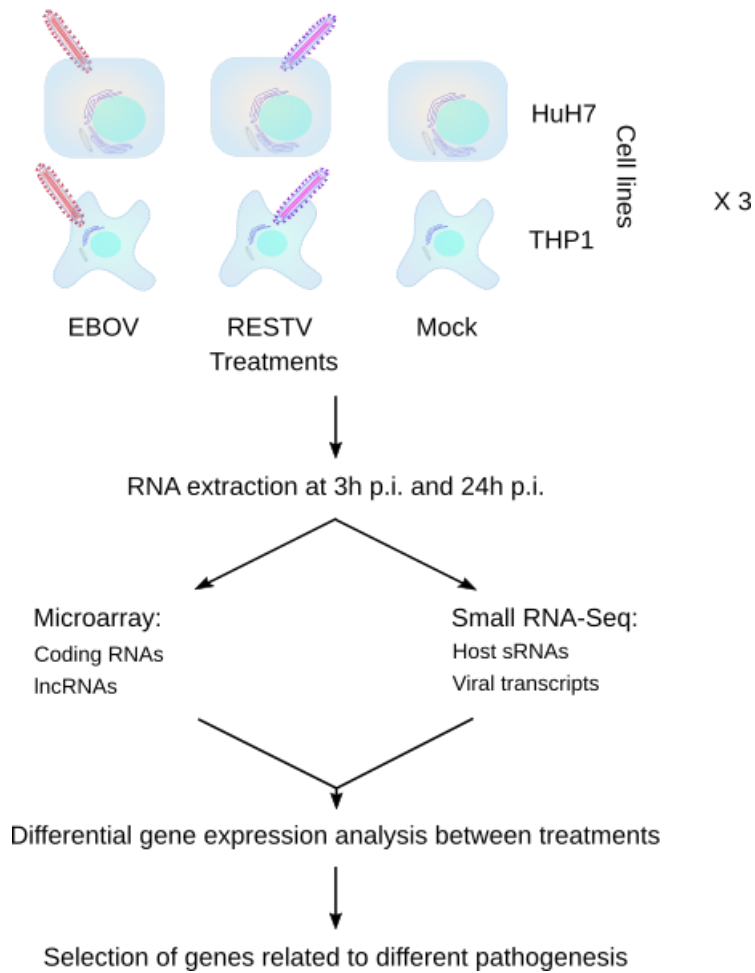


Figure 3.1: The cellular response against RESTV and EBOV, compared to Mock, was studied in two cell lines, HuH7 and THP1. RNA was extracted at 3 h p.i. and 24 h p.i. in triplicates and further processed via Microarray for coding RNAs and lncRNAs study, or small RNA-Seq, for host sRNAs and viral transcripts analysis. Differential gene expression analysis between treatments was evaluated and genes which showed a relationship to different pathogenesis were selected for further investigation.

### Viral life cycle study with artificial systems:

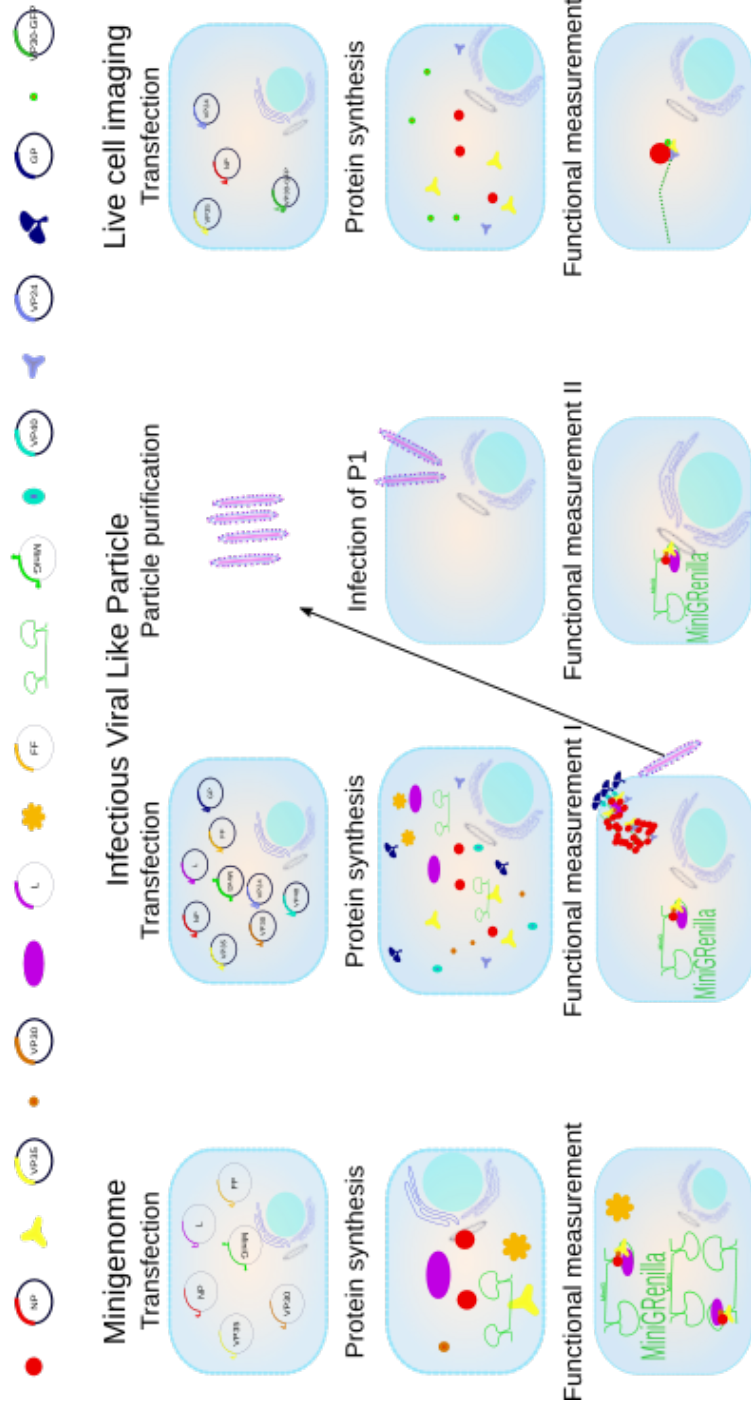


Figure 3.2: Constructs for RESTV and EBOV were prepared and their function in their native system or in combination were studied. For each approach the necessary components were transfected into the respective cells in order to produce the viral proteins and to evaluate their expression and function. The minigenome system was directly measured via the quantification of the viral MG expression. The iVLP system has different steps which were evaluated to prove the system is working properly: first, as in the minigenome system the MG quantification in the producer cells; second, the production of viral particles; and third, the infection efficiency of the purified particles via the MG quantification in the infected cells. The LCI system is evaluated live with the expression of a VP30-GFP this protein can be excited and the signal followed around the cell. This data is stored in order to determine the particle movement characteristics.





## RESULTS

---

This thesis explores, for the first time, the differences between RESTV and EBOV in early cell response, ncRNA stimulation, complete viral life cycle, and the effect of RESTV triggered genes on EBOV's life cycle. Also, Ebolaviruses can only be studied in BSL4 facilities. Thus first a study system for RESTV was established like that already determined for EBOV.

### 4.1 Differences in cellular response caused by RESTV and EBOV infection

The host transcript population in two cell lines, HuH7 (hepatome like) and THP1 (differentiated into macrophages), infected with EBOV, RESTV, and uninfected (Mock) was investigated. Two time points were chosen for the analysis, that are 3 h p.i., and 24 h p.i. Using the available annotation for humans and the *de novo* annotation based on the obtained small RNA-Seq library, small ncRNAs were quantified and evaluated, to determine their differential expression profile. Because the small RNA-Seq only covers transcripts below 200 nt and here the aim was to evaluate the whole transcriptome, the larger ncRNAs and protein-coding transcripts were quantified with microarray. The aim was to determine cellular differences triggered by EBOV, RESTV and Mock, which could give an indication on the different virus pathogenicity on the host.

#### 4.1.1 Different cellular response to viral infection observed at early time point

First, small RNA-Seq data from HuH7 and THP1 cell lines was compared and the number of reads mapping to the host and viral genomes was counted. A merged genome formed by human, RESTV and EBOV concatenation was used for the reads mapping. For HuH7 cells, at least 95% of the reads were mapped for each treatment (see Tab.4.1. total column). There was a higher amount of reads (*circa* double) mapping to the mitochondrial

Table 4.1: **HuH7 sequencing results.** reads: total number of reads that were received after sequencing; RESTV: number of reads mapping to RESTV; EBOV: number of reads mapping to EBOV genome; total (%): percentage of reads mapping to the input genomes; rRNA %: percentage of reads mapping to rRNA; MT (%): percentage of reads mapping to mitochondria;

infection	time point	replicate	reads	RESTV	EBOV	total (%)	rRNA (%)	MT (%)
Mock	3h	1	13 909 063	9	9	96	5.64	7.50
Mock	3h	2	16 388 319	8	8	96.3	5.96	7.02
Mock	3h	3	13 043 651	4	14	96.4	6.01	6.24
Mock	24h	1	23 137 302	6	8	96	4.73	7.45
Mock	24h	2	20 444 481	7	13	96.1	4.85	5.69
Mock	24h	3	15 642 097	4	9	96.3	5.95	5.15
RESTV	3h	1	19 497 826	2309	25	95.6	5.13	18.16
RESTV	3h	2	11 731 893	1260	15	95.8	6.08	13.81
RESTV	3h	3	20 287 357	2245	32	95.9	5.08	14.11
RESTV	24h	1	17 602 660	44769	157	96.5	6.18	13.18
RESTV	24h	2	23 428 788	54503	185	96.9	5.39	14.50
RESTV	24h	3	14 798 953	38303	118	96.3	6.31	13.02
EBOV	3h	1	16 993 685	36	489	96.6	5.66	25.03
EBOV	3h	2	15 998 337	30	401	96.8	5.21	17.19
EBOV	3h	3	14 830 357	26	480	96.7	5.71	16.79
EBOV	24h	1	16 543 657	562	118831	96	5.58	11.31
EBOV	24h	2	15 519 297	522	104581	96	5.01	19.08
EBOV	24h	3	9 698 044	277	57253	95.8	5.50	16.89

genome of the virus infected cells (see Tab.4.1 MT column) than in the mitochondria genome of the uninfected cells. This suggests both Filoviruses can trigger the expression of mitochondrial genes. In the THP1 cells at least 96 % of the reads were mapped for each treatment (Tab.4.2 total column). In THP1 infected cells a higher amount of reads mapping to the mitochondria genome was not observed. The increased expression of ncRNAs from the mitochondria in HuH7 infected cells might be specific to the viral infection in liver cells, such as HuH7.

For EBOV and RESTV infected cells, the number of reads mapping to the viruses increased from 3 hp.i. to 24 hp.i. (see Tab. 4.1 and 4.2 columns "RESTV" and "EBOV"). At 3 hp.i. HuH7 and THP1 cells had more reads mapping to RESTV than to EBOV (Average in: HuH7, 1938 and 457; THP1, 2337 and 65 respectively). However, at 24 hp.i. the number of reads mapping to EBOV exceeded the number of reads mapping to RESTV (average in: HuH7, 93555 and 45858; THP1, 30059 and 9272 respectively). This suggests that RESTV can infect both cell lines efficiently, but is not able to replicate or

Table 4.2: **THP1 sequencing results.** reads: total number of reads that were received after sequencing; RESTV: number of reads mapping to RESTV; EBOV: number of reads mapping to EBOV genome; total (%): percentage of reads mapping to the input genome; rRNA %: percentage of reads mapping to rRNA; MT (%): percentage of reads mapping to mitochondria;

infection	time point	replicate	reads	RESTV	EBOV	total (%)	rRNA (%)	MT (%)
Mock	3h	1	12 558 971	3	2	97.7	5.69	2.26
Mock	3h	2	13 778 743	1	1	97.5	5.21	2.16
Mock	3h	3	10 479 240	2	4	97.2	6.88	2.16
Mock	24h	1	12 095 333	1	11	97.1	3.36	1.56
Mock	24h	2	10 206 814	3	2	97.3	3.45	1.52
Mock	24h	3	13 178 371	5	2	97.2	3.32	1.05
RESTV	3h	1	12 777 540	2252	13	97.2	5.55	2.02
RESTV	3h	2	15 532 080	3192	21	97.4	3.95	1.52
RESTV	3h	3	7 805 396	1566	13	97	5.62	1.89
RESTV	24h	1	9 217 424	8855	83	98.6	4.18	1.57
RESTV	24h	2	9 113 946	9338	89	98.6	3.06	1.41
RESTV	24h	3	10 876 048	9622	65	98.7	3.38	1.25
EBOV	3h	1	14 937 502	13	72	98.6	5.53	2.73
EBOV	3h	2	14 004 962	7	50	98.8	13.77	1.98
EBOV	3h	3	10 731 754	7	73	98.6	5.1	1.70
EBOV	24h	1	9 774 072	66	31833	98.3	3.27	1.52
EBOV	24h	2	11 894 504	73	36664	96	4.13	1.15
EBOV	24h	3	9 360 129	39	21681	98.6	3.82	1.28

re-infect as fast as EBOV. This effect is stronger in THP1 than in HuH7 cells, suggesting that the cell lines have different attributes which affect RESTV life cycle. A few number of reads were found to map to the viral genomes in the Mock treatment as well. Since these numbers do not change between time points this might be an effect of the multimapping parameter or background.

*The small RNA-Seq data shows EBOV and RESTV cause a different cellular response at early infection in both cell lines*

In order to understand the cellular response a *de novo* annotation of ncRNAs based on the sequencing data was performed. This was necessary since the current publicly available human annotation (referred to as *public annotation*) only explained 50% of the mapped reads. To assess the importance of the newly annotated molecules, principal component analysis (PCA) was performed with the *public annotation* and the *full annotation* (containing also the

*de novo* annotated ncRNAs), using the 500 genes with the highest expression variance (see fig. 4.1A–D). For both annotations, the replicates of each treatment (EBOV, RESTV and Mock) cluster together independently of the cell line. At 3 h.p.i. in HuH7 cells RESTV and EBOV treatments cluster together (see fig. 4.1A). In THP1 cells, at 3 h.p.i. RESTV clusters together with Mock (see fig. 4.1B). With the *full annotation* it is possible to discriminate better between RESTV and EBOV treatments in HuH7 cells at 24 h.p.i. as the PC1 range is broader, but not at 3 h.p.i. (see fig. 4.1C). In THP1 cells, RESTV differs clearly from Mock at 3 h.p.i. (see fig. 4.1D). Since the *full annotation* helps to differentiate better between treatments and to get a more comprehensive overview of the expression signal from each treatment, this annotation was used for the rest of the analysis.

The PCA results suggest that there is a different cellular response against EBOV and RESTV already at an early time point of infection. In THP1 cells, this difference is observable already at 3 h.p.i., where RESTV treatment is not clustering with any other treatment. In HuH7 RESTV treated cells the difference starts at 3 h.p.i., but is more distinguishable at 24 h.p.i.. However, it is interesting to note the increased variance observed in THP1 cells after the *full annotation*, which currently can not be explained.

#### 4.1.2 THP1 and HuH7 cell lines share ncRNAs triggered by RESTV and EBOV infection

HuH7 and THP1 cells were chosen on the basis of their different nature, hepatome and macrophage-like respectively, which have been reported to be first infection targets of EBOV [14–16]. Here the aim was to look for genes which were responding in a similar way against either EBOV or RESTV infection (compared to Mock) in both cell lines, as this would point to a common pathway independent of cell type, and only being virus dependent. After *de novo* ncRNA annotation, ncRNAs which were triggered by either RESTV or EBOV infection in both cell lines were identified. Most of these genes were up-regulated in RESTV infection at 24 h.p.i. in both cell lines, some already at 3 h.p.i. (see fig. 4.2, and supplementary table. 7.1 for an extended list). Interestingly these genes show little or no differential expression in EBOV infected cells (compared to Mock). Also, at 3 h.p.i., the FC of RESTV treatment (compared to Mock) is higher in THP1 cells than in HuH7. All the above mentioned results suggest an early cellular response against RESTV infection.

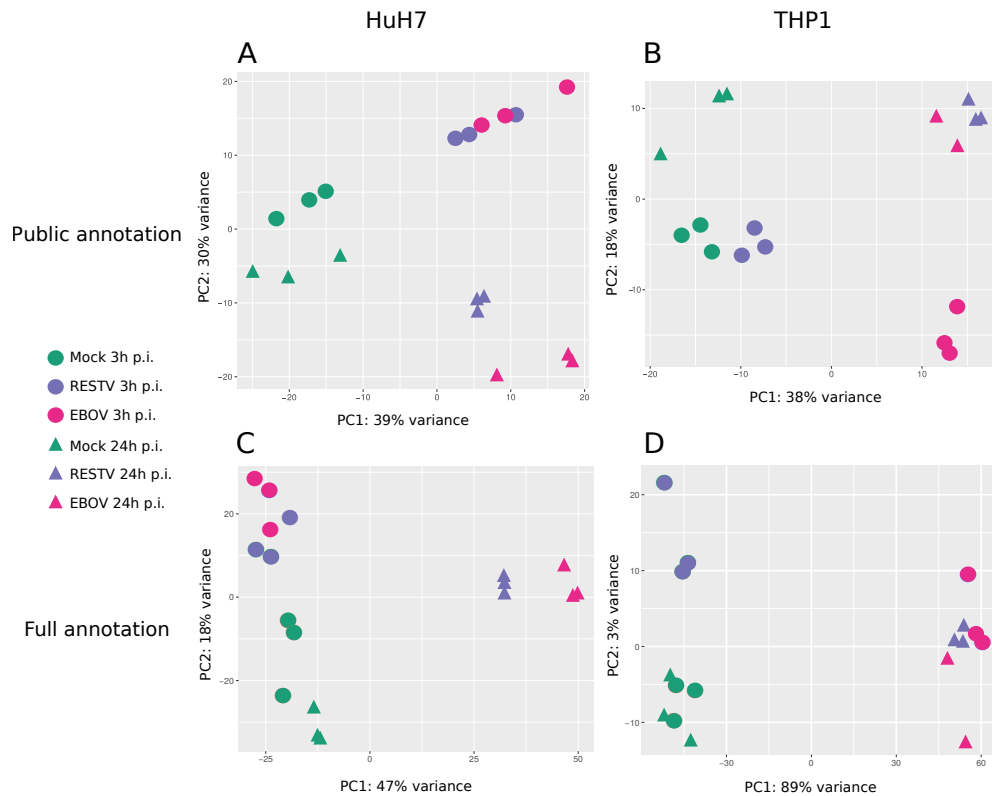


Figure 4.1: Principal Component Analysis (PCA) based on the 500 genes with the highest variance of the small RNA-Seq data based on the publicly available human annotation (A,B) and our full annotation (C,D). While comparing both annotations it is possible to discern better between treatments in HuH7 (A,C) and THP1 cells with the full annotation (B,D).

#### *snoRNAs expression discriminates better between RESTV and EBOV treatments*

It was explored whether a specific family of ncRNAs is causing the different cellular response to RESTV and EBOV infection by performing PCAs for snoRNAs and miRNAs (see fig. 4.3). In HuH7 cells, the snoRNA expression seems to be sufficient to discriminate between time points after infection in general, and between RESTV and EBOV infected cells at 3 h p.i. (fig. 4.3A). At 3 h p.i. RESTV and Mock treatments seem to be clustered together in PC1, and differentiate better at PC2, and EBOV treatment clearly separates in both components. At 24 h p.i. snoRNAs expression does not seem to vary between RESTV and EBOV treatment, and Mock treatment clearly differs from the infections at this time point. In THP1 cells, there was a similar effect as in HuH7 cells, but less pronounced because the components values are smaller (see fig. 4.3B). These results suggest that snoRNAs play a role in the differential cellular response caused by RESTV and EBOV infections, and mark a difference already at an early time point post infection. However,

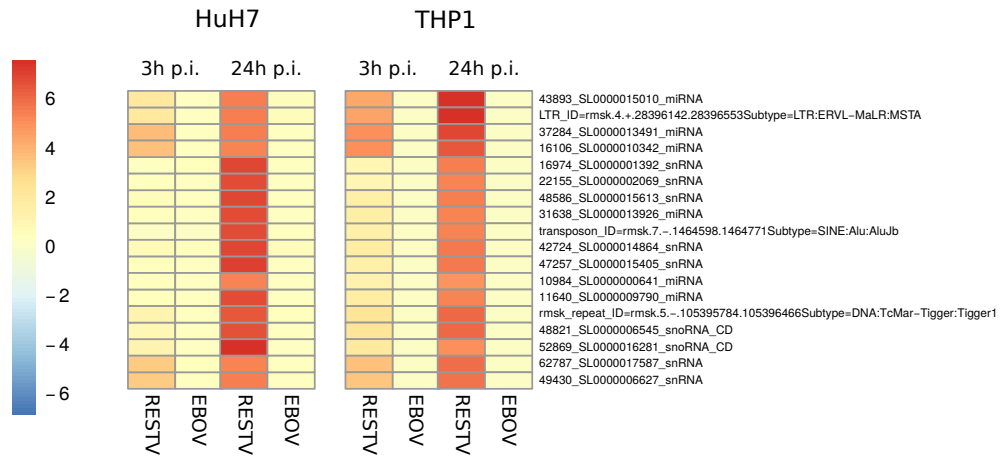


Figure 4.2: Heatmap of ncRNAs with the highest FC in both HuH7 and THP1 cells.

the variance in the PCA components is really small, suggesting that there are more genes which do not show any variance than the ones that cluster together. This can be of use for narrowing down the candidate genes which differentiate both viruses.

#### *Specific miRNAs are only triggered by RESTV*

In contrast, miRNA expression cannot discriminate between treatments at 3 h p.i. (neither in THP1 nor in HUH7 cells), but discriminates time points in HuH7 cells (see fig. 4.3C and D). At 24 h p.i. miRNAs show a difference between RESTV and EBOV treatment in HuH7 cells, but the samples are widely spread making it difficult to affirm this statement. However, the half-life of miRNAs varies depending on location, function, condition, form, etc. in a controlled and robust manner. Hence miRNA expression can vary between 1 h to days [64]. The presence of differentially expressed miRNAs (only considering the ca. 2400 miRNAs annotated in miRBase [58]) was explored. This was done only with the known miRNAs to understand the possible implications of their differential expression. In total 31 known miRNAs were found to be differentially expressed among all treatment comparisons. From these, 4 miRNAs had a different expression profile between viral treatments in HuH7 cells and 7 in THP1 cells (see fig. 4.4). In HuH7 cells hsa-miR-27a-5p, hsa-miR-4443, hsa-miR-1275 and hsa-miR-23-5p are up-regulated in EBOV treated cells at 24 h p.i. (see fig. 4.4 HuH7). The miRNAs hsa-miR-204-5p (miR-204) and hsa-miR-10b-5p (miR-10b) are up-regulated in RESTV infected THP1 cells since 3 h p.i., pointing towards candidates of early cellular

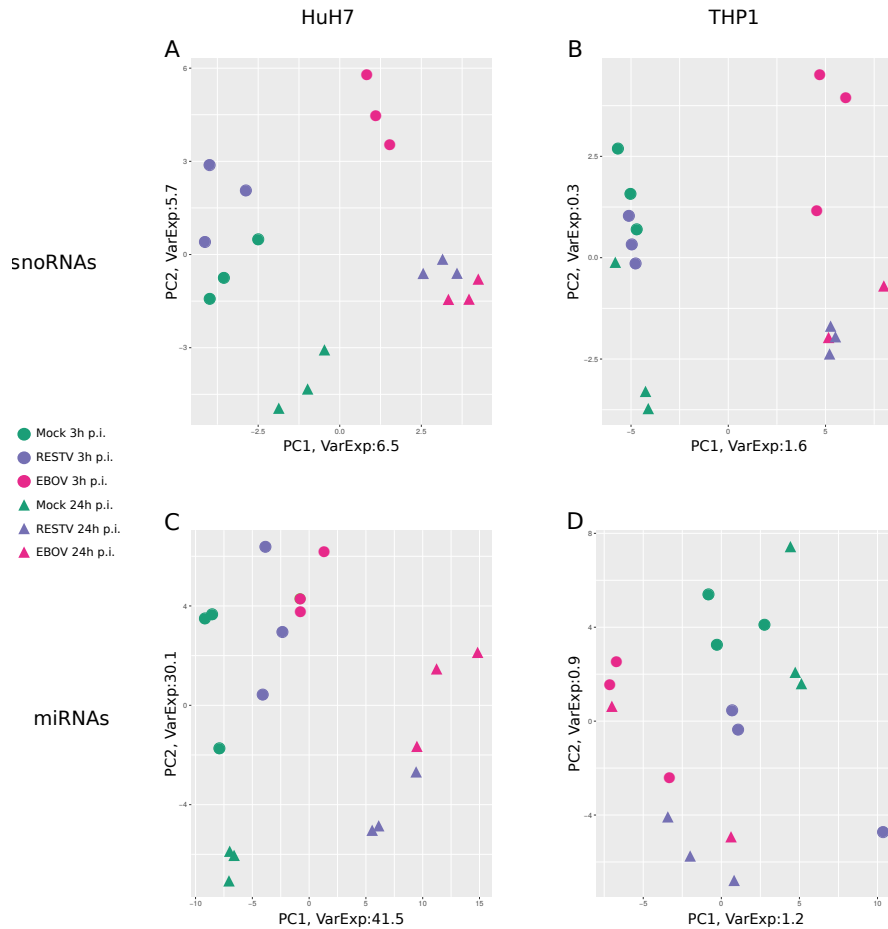


Figure 4.3: PCA of snoRNAs (A,B) and miRNAs (C,D) of HuH7 (A,C) and THP1(B,D) cells. (A) HuH7's snoRNAs can discriminate between time points of infection, and between RESTV and EBOV at early time points post infection. (B) THP1's snoRNAs values indicate that this difference is not as marked as for HuH7. (C) HuH7's miRNAs are not clustering nicely within the treatments, but between components it is possible to discern time points and treatments. However, (D) THP1 miRNAs seem to show no pattern due to the little variance.

response which could make a difference in the viral outcome. hsa-miR-33b-5p and hsa-miR-3916 expression differs between RESTV and EBOV 24 h p.i. infected THP1 cells (see fig. 4.4 THP1). Also, hsa-miR-1291, hsa-miR-3607-5p and hsa-miR-3653-5p miRNAs seem to be triggered faster in EBOV treated cells, because they are up-regulated after 3 h p.i. but in RESTV treated cells after 24 h p.i.. These results suggest either RESTV and EBOV cell response varies with speed, or RESTV is slower in triggering the response compared to EBOV. The miRNAs, due to their broad range of effects, are good candidates for exploring further their role in RESTV and EBOV differences.

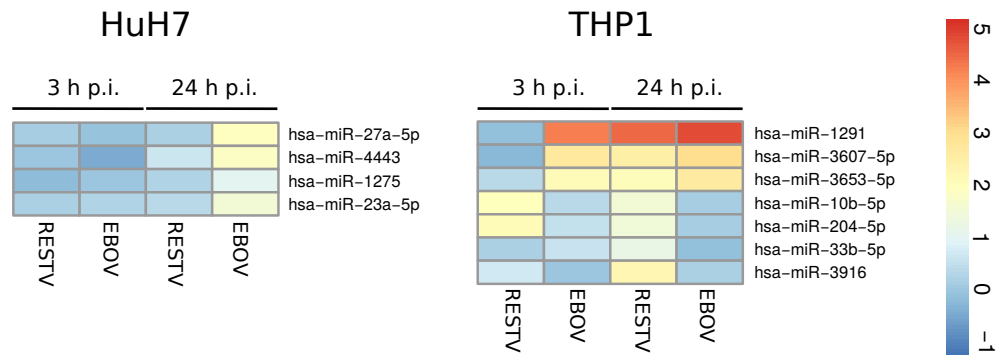


Figure 4.4: Heatmap of differentially expressed miRNAs. Here only miRNAs present in miRBase database [58], and with a different expression profile between RESTV and EBOV treatment are listed.

#### 4.1.3 THP1 cells show that RESTV triggers a ncRNA-immune response pathway

Since macrophages are one of the first targets of EBOV, THP1 transcriptome response to the infection was particularly interesting. The expression profile of the 80 genes with the highest differential expression against Mock in THP1 cells was analyzed. Most of these genes are *de novo* annotated genes (for genomic locations, please refer to the supplementary table .7.2 and .7.3). In addition, there were three protein coding genes, namely CD28, IFIT2 and CXCL10. This is unexpected because of the library preparation and counting restrictions (for details refer to Methods). The library preparation favors only small RNA fragments (below 200 nt). CD28 and IFIT2 are above the restricted size. Also, the library filters out mRNA degradation products, because it only recognizes ncRNA-like 3' modifications, which no mRNA should have (TruSeq Small RNA kit from Illumina). These signals, then, do not represent CD28 and IFIT2 transcripts. On a closer look, CD28 has a well-defined block of reads mapping in Mock, which is up-regulated with a log<sub>2</sub> fold change of ca. 3 in RESTV treatment 3 h p.i. compared to Mock. The read distribution of CXCL10 and IFIT2 is more spread (see fig. 4.5), suggesting the small reads being a product of degradation but from an ncRNA process. CD28, CXCL10 and IFIT2 are immune related genes, and RESTV induces an attenuated immune response compared to EBOV [30]. Along with our other findings, RESTV might trigger an immune response mechanism which is ncRNA regulated after early infection.

Based on the microarray analysis, CXCL10 and IFIT2 are downregulated in EBOV treated samples compared to RESTV treatment at 3 h p.i., with a fold change of -4,49 and -3,88 respectively, but with p-value of 0.2, meaning



the difference is not significant. The microarray probing for quantification (probes are 60 nt), might correspond to the degradation products observed via small RNA-Seq, which would not be exactly the same between replicates. Thus, the microarray data was analyzed for a better understanding of these values.

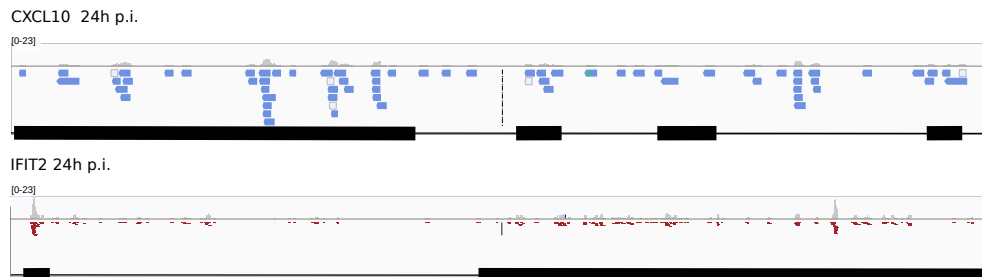


Figure 4.5: Visualization of reads from RESTV treatment mapping on IFIT2 and CXCL10 in THP1 cells (based on IGV [65]). Draw bottom black line and boxes represent exons/UTR based on the human annotation.

The presence of degraded products from immune genes in the smallRNAseq data only for RESTV infected cells would imply that RESTV is triggering an ncRNA related pathway which is controlling the immune response of the host. It was already shown that EBOV over stimulation of the immune response is one of the reasons for its fatality effect [66]. It is possible that ncRNAs could control this effect due to all their functions. This observation would imply that ncRNAs could be determinant regulators for RESTV outcome, and a possible tool to control EBOV symptoms. However, there is not a previous report which could help to understand these results.

#### 4.1.4 Microarray data shows early time point of infection as a common feature between cell lines against a pathogenic virus

Here all coding transcripts were investigated and also long ncRNAs that are significantly differentially expressed between treatments (EBOV vs. Mock, RESTV vs. Mock, and EBOV vs. RESTV) and filtered based on signal strength (for details see Methods). As a result, no gene was found that was in both cell lines significantly differentially expressed between treatments. For each cell line there were in total 14 genes to be significantly differentially expressed between treatments (see fig. 4.6). In THP1 cells most of the DEG show the major difference between RESTV and EBOV treatments at 3h p.i. (see fig. 4.6). In HuH7 cells half of the significantly DEG showed that RESTV and EBOV treatments differ at 3h p.i. (see fig. 4.6 HuH7), but little

is known about them. In THP1, KLK8 was found up-regulated in RESTV; ZG16, ANKRD2 and SCN10A were found up-regulated in EBOV infected cells at 3 h p.i. (see fig. 4.6 THP1.). These could be related to an entry process, based on their function.

The ncRNAs and coding genes results indicate that the main difference between EBOV and RESTV cellular response is at an early stage after 3 h p.i. . This time point has not been previously studied for the comparison of these viruses.

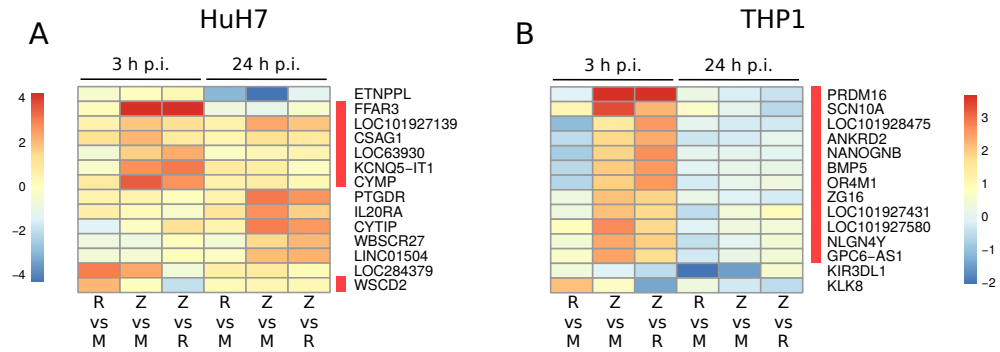


Figure 4.6: Microarray heatmap shows at 3 h p.i. a consistent point of difference between cell lines with a  $\log_2FC > 2$ . (A) HuH7 shows different groups of genes based on expression; next to the red bar are the genes which clustered with the main difference at 3 h p.i. (B) THP1 shows most of its highly differentiated genes at 3 h p.i., marked with the red bar.

## 4.2 RESTV vs EBOV: from assay establishment to evaluation of viral compatibility

In order to produce the viral proteins directly in cells, and evaluate them, one has to express them. The protein production and the system were already established for EBOV in the Virology Institute working group from Marburg. The genome sequence of RESTV strain used in the infections for this study was also available in the Institute. With RESTV sequence and the constructs from EBOV it was possible to design the approach for the cloning of the RESTV proteins inside mammalian expression vectors. Because SUDV is phylogenetically closer to RESTV than EBOV [67], consumables available for SUDV study were tested on RESTV (for details refer to the Material or Methods section).

A first hint of EBOV and RESTV differences could be explored by the comparison of both virus proteins. Size, expression, abundance and sequence, are the first hints of intrinsic traits that could be linked to pathogenicity.

Compatibility between both viruses and components exchange, in different study systems could give a hint of the properties of RESTV and EBOV proteins.

In this section: First, the aim is to develop a standard procedure for RESTV and EBOV comparison outside BSL4 conditions; second, to identify protein differences between RESTV and EBOV while exchanging each viral component and measuring the effect on different viral process; third, to evaluate if the aa sequence of EBOV and RESTV proteins could explain virus incompatibilities observed in the first and second points.

#### 4.2.1 Antibody selection for RESTV studies

There are different techniques for protein quantification, such as western-blot (WB) and silver gel, and for direct visualization, such as immunofluorescence (IF). These techniques give insight into the protein levels present in the environment studied, which may be cellular lysate, compartment or supernatant. The use of antibodies increases the specificity of the quantification and it can also be the only approach for some conditions, such as cellular protein measurement. Therefore, a proper analysis demanded antibody standardization for RESTV.

RESTV commercially available antibodies are against GP, hence the need of testing SUDV and EBOV available antibodies for all other viral proteins. Cells infected with RESTV were lysate and loaded in a 10% SDS gel for stripe WB (details in Methods). Three monoclonal antibodies and four serums were tested: 2C4, from mouse against EBOV mayinga VP40; B6C5, from mouse against EBOV mayinga NP; 3B11, from mouse against EBOV mayinga GP; Sudan, serum obtained from SUDV infected goat; Zaire, serum obtained from EBOV mayinga infected goat; Ch-NP, serum obtained from chicken vaccinated against EBOV mayinga NP; and Ch-VP40, serum obtained from chicken vaccinated against EBOV mayinga VP40. 2C4, Sudan, Ch-NP and Ch-VP40 were the only cross-reactive species with RESTV proteins, showing the expected band size between 100 - 130 KDa for NP, and the *ca* 40 KDa band for VP40 and lower bands for its other forms (see fig. 4.7). With these results four antibodies were determined for testing the newly produced expression plasmids for RESTV NP and VP40. RESTV GP and VP35 expected bands size were also observed with Sudan, and identified as the additional bands not observed with monoclonal antibodies (see fig. 4.7 line 4). Changing the gel percentage did not improve the detection of RESTV VP30 or VP24 over-expression in HEK293 cells with none of the serums (data not shown).

In conclusion, it is possible to detect RESTV proteins with EBOV and SUDV antibodies, SUDV being the most cross-reactive with RESTV. This will help to identify specifically the RESTV protein expression and evaluate them in further studies.

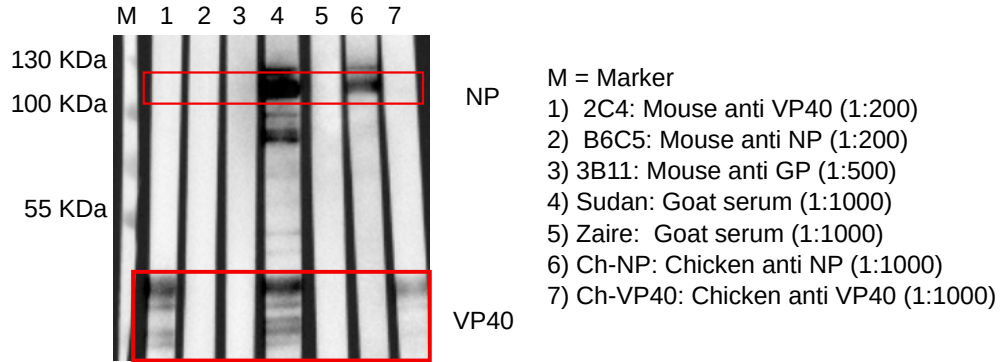


Figure 4.7: Stripe WB of RESTV with different available antibodies. Six antibodies commonly used for EBOV and one for SUDV were tested. The stripe blot shows in red rectangles the specific band for NP, VP40 and VP40 phosphorylated forms at the expected sizes. The numbers correspond to "Name:Species anti protein (concentration)". 2C4, Sudan, Ch-NP and Ch-VP40 were the only cross-reactive species with RESTV. The complete protocol can be found in Methods.

#### 4.2.2 Minigenome: viral transcription/replication shows minor differences between RESTV and EBOV

The minigenome assay was used to evaluate MARV and EBOV transcription/replication, and it was established with different protein concentration. Then, it was necessary to test if EBOV established system and conditions would also provoke an optimal result in RESTV developed system, and also VP24 and VP40 decrease transcription/replication activity of EBOV transcription/replication. This has not been tested for RESTV, but it would be expected that other intrinsic protein effects are similar between both viruses.

Here is studied: First, the amount of viral constructs needed to produce the highest signal for RESTV minigenome; and second, the effect of exchanging different viral components on transcription/replication in the minigenome context. The reporter activity signal of native components only, based on the minigenome origin, was considered as 100%, and used to calculate the relative reporter signal of each plasmid combination in each independent replicate. The lack of the polymerase (L) was used to determine

the background signal. Each protein plasmids combination's effect was compared to the viral based component mix and their significance calculated with Anova.

*RESTV minigenome establishment: EBOV unaltered minigenome protocol works the best with RESTV*

Different plasmid amounts from RESTV viral components were tested around EBOV established protocol. This was done to determine the functionality of the system for RESTV, and to establish the method for studying and comparing EBOV and RESTV transcription/replication. EBOV plasmids concentrations were used as reference for all minigenome assay. Only the plasmid concentrations of RESTV proteins NP, VP35 and VP30 were varied below and above the reference concentration values. The polymerase plasmid amount used for the assay was 1 ug in EBOV and MARV systems, so it is expected to be the same for RESTV, and it was not tested. The MG reporter activity will be used as point of comparison between RESTV and EBOV in further experiments. Then the concentration of this construct was left as originally to avoid the introduction of more variables. To prevent the influence of the amount of foreign DNA affecting the cell, an empty DNA vector was also transfected to compensate the concentration changes here tested.

EBOV established minigenome setup seemed to work with RESTV components. None of the plasmids' concentrations tested improved RESTV MG reporter activity significantly compared to the plasmids' concentrations used for EBOV MG assay. However, a reduction from 125 ng to 100 ng of RESTV NP construct did reduce the reporter activity in *ca.* 20% (see fig. 4.8 and supplementary table 7.4). An increase of RESTV VP30 from 100 ng to 200 ng also reduced RESTV MG reporter activity in *ca.* 20%. It is possible that more than one of the proteins needs to be adjusted to see a significant positive effect. For example, in fig. 4.8 NP increase and VP30 reduction could improve the reporter activity. Therefore, also tested was an increase of RESTV NP construct (250 ng) and a reduction of VP30 (70 ng), but there was not a significant change observed on RESTV MG reporter activity (data not shown with n=2).

These results show that it is possible to use EBOV MG assay setup to study RESTV transcription/replication. Also, the changes on the amount of construct here tested do not improve RESTV reporter activity, suggesting RESTV and EBOV need a relatively similar amount of proteins for transcription/replication. However, it is worth mentioning that the base level of 100% for RESTV was lower than EBOV.

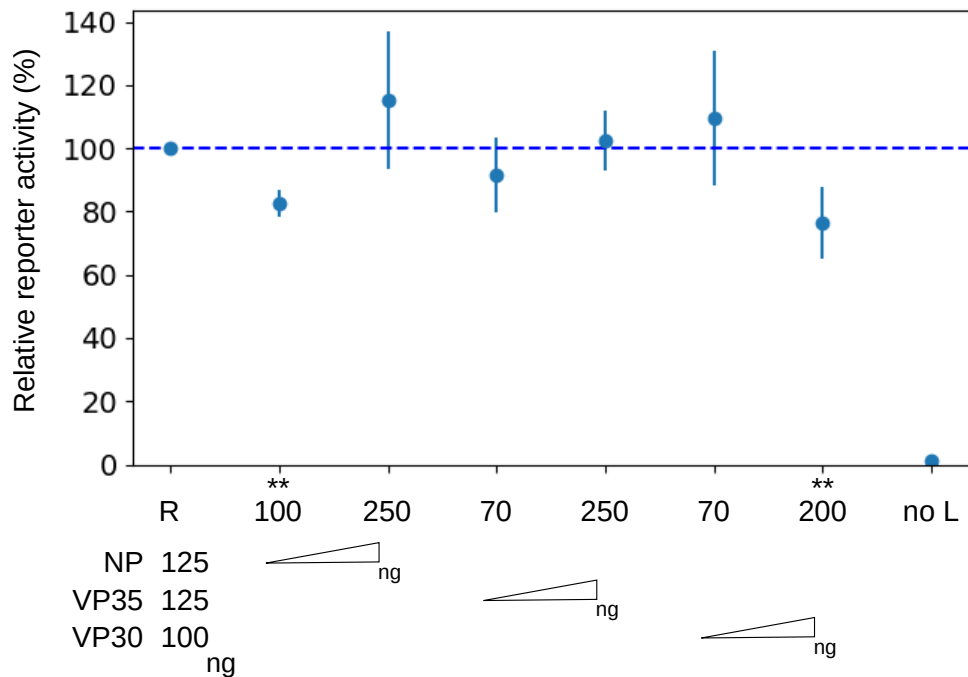


Figure 4.8: RESTV minigenome relative reporter activity comparison with different RESTV components concentrations. EBOV established concentrations of minigenome components were used as reference for RESTV MG (R: first column to 100%). NP, VP35 and VP30 concentrations were varied below and above EBOV optimized concentrations and minigenome reporter activity was measured and calculated relative to R. The graph shows the average(dot) and variance (line) for n=3-4 replicates measured relative to 100% activity of the ratio from MG reporter activity and FF luciferase. The significance of the values measured differing from the 100% based on EBOV plasmids quantities was calculated with Anova where \*\* =  $p$ val < 0.01. Only RESTV NP concentration reduction and RESTV VP30 concentration increase affected negatively RESTV minigenome activity. The values plotted come from supplementary table 7.4.

*Transcription/replication components evaluation: RESTV NP does not interact properly with EBOV VP35*

The classic minigenome assay was used to evaluate transcription/replication activity on different RESTV and EBOV protein combinations. EBOV MG reporter activity does not get affected when exchanging EBOV VP30 or VP35 for RESTV VP30 or VP35, but seems dead when exchanging EBOV NP or L for RESTV NP or L accordingly. However, RESTV VP35 together with RESTV L and EBOV NP, VP30, and MG, recover the reporter activity (see fig. 4.9 A), suggesting RESTV L is not able to interact properly with EBOV VP35, but EBOV L is able to interact properly with RESTV VP35. RESTV NP negative effect on EBOV MG reporter activity was counteracted when

RESTV VP35 and L were also included in the system (see fig. 4.9 A). These results suggest RESTV NP and EBOV NP differ in more than one protein domain affecting some interaction. RESTV MG reporter activity does not seem affected by exchanging RESTV NP or VP30 for EBOV NP or VP30 accordingly, but it gets reduced with EBOV VP35 instead of RESTV VP35, and is almost dead when RESTV L is exchanged for EBOV L (see fig. 4.9 B). EBOV L and EBOV VP35's negative effect on RESTV MG reporter activity seems to be compensated when EBOV NP is also present (see fig. 4.9 B).

Altogether, it seems RESTV NP does not interact with EBOV L in the absence of RESTV VP35. This suggest RESTV NP needs RESTV VP35 for a proper interaction with the polymerase. Also, VP35 interaction with NP differs between both viruses. However, EBOV NP seems to interact with RESTV L and VP35 without affecting transcription/replication. Furthermore, VP30 can be exchanged between both viruses without affecting the reporter activity in the transcription/replication context (see fig. 4.9).

*Minigenome inhibitors: VP24 is the only viral protein impairing transcription/replication consistently*

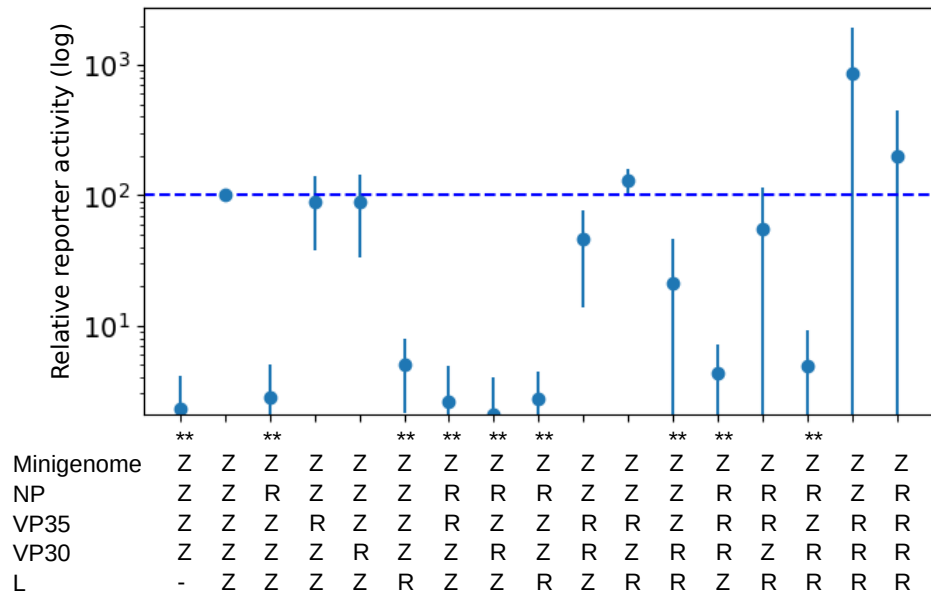
The minigenome assay was adapted to study the effect of ebolavirus proteins GP, VP40 and VP24, which include the reported transcription/replication inhibitors VP24 and VP40 [23, 68]. HuH7 cells were transfected with each of the different plasmids codifying for the viral proteins. The minigenome refers to the components necessary for transcription/replication from only one virus. An empty plasmid was added to compensate the cell stress on the 100% optimized plasmid combination which had no extra viral component included.

It was observed that VP24 significantly inhibits transcription/replication activity independently of the viral protein origin or target (see fig. 4.10). VP40's effect on transcription/replication is not significant in RESTV and EBOV, independently of the source or target of the VP40 construct used. Moreover, GP seems to increase the reporter activity of both viruses, but the high variance makes only RESTV GP on RESTV minigenome context significant. GP effect could be related to its capability to form vesicles and transport cellular material, in this case viral components.

Because there was to be expected a reduction of the MG reporter activity on the presence of VP40, the amount of NP and VP40 of the transfected cells was measured. The sample where there is a positive reporter activity in EBOV has a stronger band for NP than VP40, suggesting the result could be



A



B

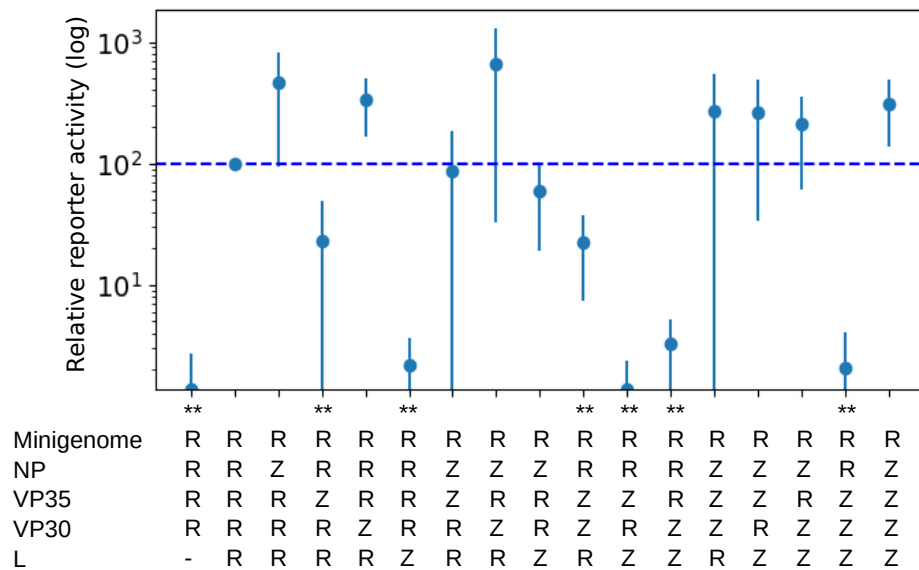


Figure 4.9: Minigenome reporter activity measurement after exchanging protein components between EBOV(Z) and RESTV (R). The graph shows the average(dot) and variance (line) for n=3 replicates measured relative to 100% activity of only Z (A) or only R (B). The significance of the values measured differing from the 100% optimized plasmid combination was calculated with Anova where \*\* = pval < 0.01. (A) EBOV minigenome reporter activity under the influence of different protein combinations of Z and R in the Minigenome assay context. The polymerase from RESTV seems not to recognize EBOV minigenome without RESTV VP35. RESTV NP seems to interact poorly or less efficiently with EBOV VP35 and L. The values plotted come from supplementary table 7.5 (B) RESTV minigenome reporter activity under the influence of different protein combinations of Z and R in the Minigenome assay context. The polymerase (L) from EBOV seems to not recognize RESTV minigenome without EBOV NP. Also, it seems EBOV VP35 does not interact efficiently with RESTV components. The values plotted come from supplementary table 7.6.



dependent on the ratio NP/VP40 (results not shown) . It seems there is a direct effect on NP/VP40 ratio which determines transcription/replication for EBOV, and not for RESTV minigenome. This would suggest that the interaction NP/VP40 from RESTV could be different. Also, the previous reports, where the effect of VP40 on transcription/replication were observed, were mainly done in HEK293 cells [23], suggesting this effect could also be cell line dependent. The difference between viral GPs might be related to the higher cytotoxicity of EBOV GP compared to RESTV GP ([31]).

#### 4.2.3 Major difference between EBOV and RESTV found on protein incorporation into filamentous particles

A viral infection and a transfection do not produce the same amount of infectious particles. A cellular transfection for iVLP production results with the release of a variety of particle forms, not all infectious. To produce iVLPs it is not necessary to have all seven viral proteins, mainly GP, for infecting new cells, and VP40 for forming the matrix, but NP determines what it is included into the particle. Therefore, the ratio between the proteins which form the iVLPs is of relevance for an optimal infection.

##### *Virus filamentous particles composition of RESTV and EBOV*

The protein ratio of EBOV and RESTV filamentous particles was not previously compared. The use of antibodies to compare them can lead to bias due to the sensitivity or specificity to the different species. Silver gel protein staining is a sensitive unspecific technique which allows the visualization of proteins from a sample. Silver gel quantification was performed to determine the protein composition of EBOV and RESTV produced particles (collected from supernatant). EBOV Mayinga, used in all the present study, has a higher fatality rate than the recent strain, and causative of the 2014 outbreak, EBOV Makona strain [69]. Therefore, it is expected that comparing the ratios of both EBOV strains with RESTV could highlight differences related strictly to the species' pathogenicity.

Supernatant from cells infected with EBOV strain Mayinga, EBOV strain Makona, and RESTV were concentrated and boiled for SDS gel run. The bands observed in the SDS gel after the silver staining correspond to the viral specific sizes of GP, NP, VP40 and VP24 proteins (see fig. 4.11). After determining the proteins' correspondent band, they were quantified and the protein ratios were calculated.

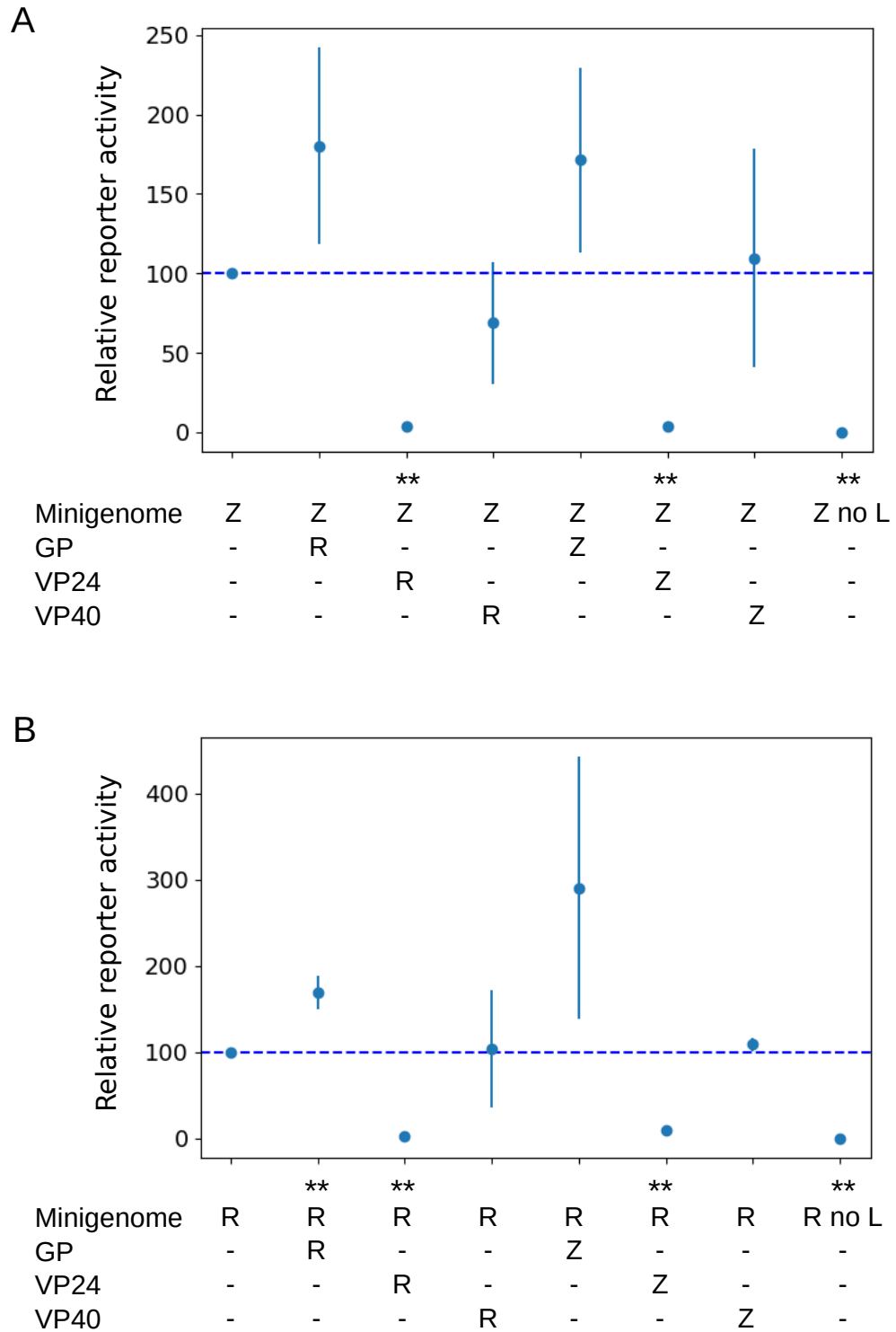


Figure 4.10: Minigenome reporter activity measurement after the addition of viral transcription/replication inhibitors between EBOV(Z) and RESTV (R). The graph shows the average(dot) and variance (line) for n=3 replicates measured relative to 100% activity of only Z (A) or only R (B). The significance of the values measured differing from the 100% optimized plasmid combination was done with Anova where \*\* = pval < 0.01. (A) EBOV minigenome reporter activity under the influence of different protein inhibitors of Z and R in the minigenome assay context. The values plotted come from supplementary table 7.7 (B) RESTV minigenome reporter activity under the influence of different protein inhibitors of Z and R in the Minigenome assay context. The values plotted come from supplementary table 7.8.

Table 4.3: Protein ratio calculation from RESTV and EBOV strains Makona and Mayinga. The values are based on the silver gel from figure 4.11.

	RESTV	EBOV Makona	EBOV Mayinga
GP/NP	1.16	1.95	0.56
GP/VP24	0.352	4.6	0.55
VP40/VP24	3.712	8.57	2.71
GP/VP40	0.09	0.54	0.2
VP24/NP	3.29	0.42	1.008
NP/VP40	0.08	0.27	0.205

It was observed that the amount of GP in reference to NP protein (GP/NP) is relatively more similar between RESTV and EBOV Makona (more GP than NP) compared to EBOV Mayinga (more NP than GP). Interestingly, RESTV and EBOV Mayinga share a relatively similar ratio between GP and VP24 proteins (GP/VP24), with more VP24 than GP, compared to EBOV Makona, with more GP than VP24. In RESTV, and both EBOV strains there is more VP40 than VP24 (VP40/VP24) incorporated into the filamentous particles, but the values go in the direction EBOV Mayinga < RESTV < EBOV Makona, showing RESTV and EBOV Mayinga with relatively more similar values. Also, in RESTV, EBOV Mayinga and Makona there is more VP40 than GP incorporated inside the filamentous particles, although the values do discern having RESTV the lowest amount of GP compared to VP40 incorporated in filamentous particles. EBOV Mayinga seems to have the same amount of VP24 and NP proteins incorporated into the filamentous particles, but RESTV has much more VP24 than NP, and EBOV Makona has more NP than VP24. NP/VP40 ratio is the only value where both EBOV strains are relative similar and RESTV differ the most (see table 4.3).

These results suggest the relative amount of viral proteins incorporated into the filamentous particles could play a role in pathogenicity. The proteins which seem to determine the pathogenicity or infectivity are the viral proteins NP, VP40 and GP, being the only ratio NP/VP40 where both EBOV strains are really similar. Also, with the viral relative amount of protein incorporated into the filamentous particles, it is possible to investigate if the iVLP assay system is properly developed for RESTV. However, these values have to be taken carefully, because the Silver gel sensitivity changes depend on the amino acid composition.

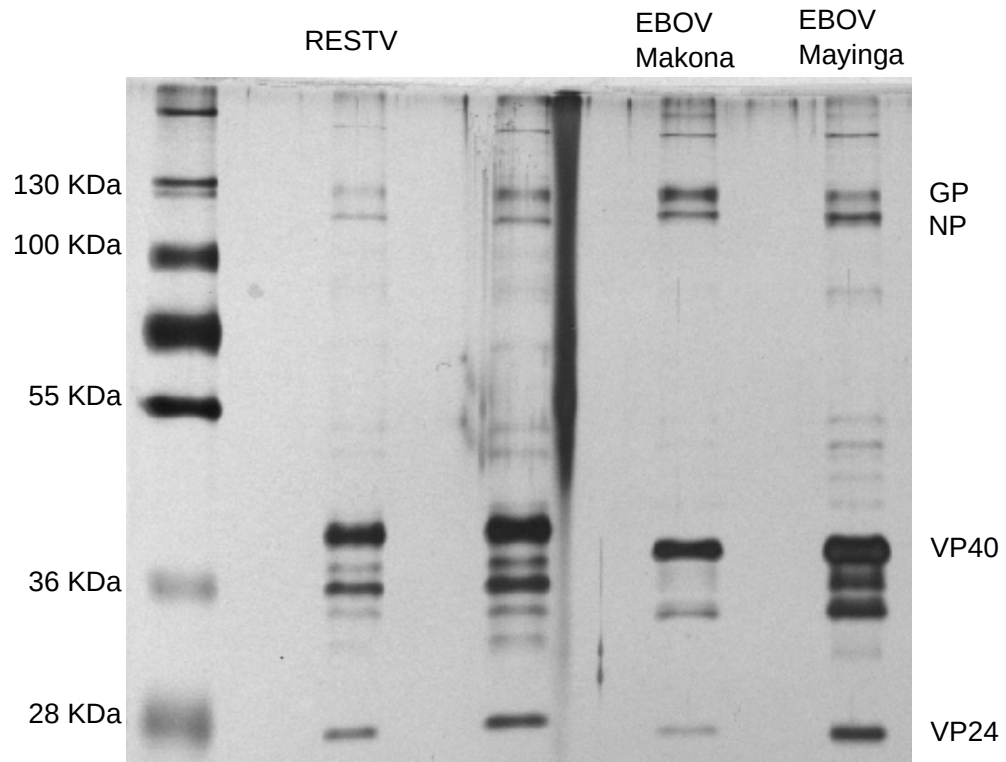


Figure 4.11: Silver gel of collected supernatant from cells infected with RESTV, EBOV (Makona and Mayinga). The gel observed is representative of 3 different runs

*Filamentous particle release: RESTV NP is found in low amounts in filamentous particles*

As mentioned above, there is a reduced incorporation of NP into RESTV produced viral particles, compared to EBOV. This would imply RESTV forms more empty particles than EBOV. Explored here is if the involved proteins on the particle formation can interact properly and if there is a protein limitation for the deficient assembly. This is addressed by the production of filamentous particles formed by GP, VP40 and NP in HuH7 cells. It is also investigated if the exchange of proteins between both viruses affects the incorporation of NP in the infectious particles. The filamentous particles were run in a 10% SDS gel and stained with silver. This was done to compare the protein amounts without introducing a sensitivity and specificity bias.

Both virus form VLPs which fall into the infectious category, because they are found in the fractions 4 to 6 of the supernatant purification (see fig. 4.12 A first two columns). GP is visible in fractions 4 to 6 from the tested protein combinations. It seems EBOV GP is recurrently more abundant, because the signal is stronger. NP band is faint compared to GP band. RESTV NP seems

smaller and less abundant. These traits suggest RESTV NP might be less incorporated into the VLPs. Yet, RESTV NP seems more abundant when EBOV VP40 is also present (see fig. 4.12 A). Moreover, RESTV VP40 band runs above EBOV VP40 band. This difference represents on average 3 KDa more in RESTV VP40 (could be due to the extra 5 aa in the C terminus). To corroborate the specific bands, the same samples were run and stained with different antibodies. It was possible to confirm the size of VP40 and to show RESTV NP is more prominent when also EBOV VP40 is present (see fig. 4.12 B). The cells used for producing VLPs were also collected and analyzed to confirm NP presence in the experiments. NP is visible in every combination in the cell lysates, and shows the slight size difference mentioned above (see fig. 4.12 C). RESTV NP was present in low amounts in fractions 4 to 6, but was clearly visible in fractions 1 to 3 (see fig. 4.12 C), where smaller filaments, most not infectious are present.

Altogether, it was possible to form and collect filamentous particles from RESTV. As with the virus filamentous particles, there is more VP40 than NP, implying the composition of the filamentous particles of the iVLP system is similar to the filamentous particles formed by the virus. These results suggest RESTV NP is able to go to the supernatant, but it does not assemble with VP40 in an efficient manner. However, there are more components involved in the formation of a virus infectious particle which could also contribute to the observed differences.

#### *Transcription and replication in iVLP context: NP exchange affects both viruses*

The incorporation of RESTV NP into the filamentous particles could be improved with another viral protein from RESTV or EBOV, such as VP24 and VP35 which transport the nucleocapsid (NC) around the cell [22]. Therefore iVLPs were produced with the minigenome, VP30, L, and VP35 from the same species, and GP, NP, VP24, and VP40 were exchanged between RESTV and EBOV. The relative reporter activity was measured, the ratio of minigenome activity signal and firefly signal, and it was compared to 100% EBOV or RESTV alone. The significance of the differences between protein combinations was tested with Anova. As observed previously, NP from RESTV combined with EBOV components does not show a reporter activity (see fig. 4.13 left). Also, EBOV NP seems to decrease the reporter activity of RESTV minigenome in a significant manner (see fig. 4.13 right). It would look as if RESTV VP24 affects EBOV minigenome, and EBOV VP24 and GP also affect RESTV minigenome activity, but this difference is not

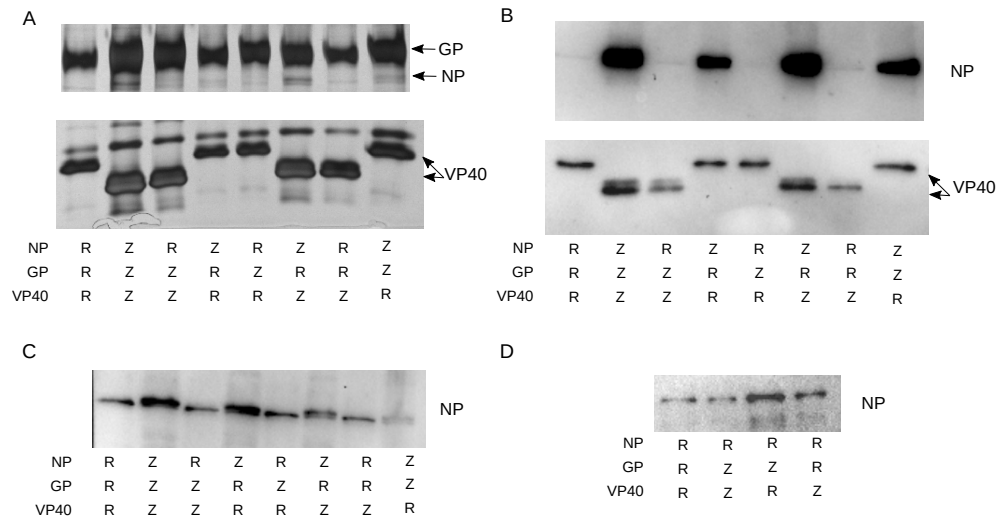


Figure 4.12: iVLP preparation with different combinations of NP, GP and VP40 from RESTV (R) and EBOV (Z) in HuH7 cells. (A) Silver staining of fractions 4 to 6 from VLPs supernatant: GP and VP40 are clearly visible independent of the combination. RESTV NP is not easy to identify. (B) Blot staining with Ch-NP and Sudan antibodies of fractions 4 to 6 from VLPs supernatant. EBOV NP is clearly visible, but RESTV has a faint signal. (C) Blot staining with Sudan antibody of cells transfected with the different protein combinations for VLP production. It is possible to identify RESTV and EBOV NP in every combination (D) Blot staining with Sudan antibody of fractions 1 to 3 of all the combinations containing RESTV NP. It is possible to clearly observe NP. \*All these images correspond to the same experiment.

significant. Already, VP24 has been shown as a strong inhibitor of the transcription/replication independently of the viral source combination. This can be explained by the relative amounts used of VP24 for each case. Also, the exchange of VP40 had no effect on the reporter activity of RESTV and EBOV MG.

Further, the iVLPs were purified and only the filamentous particles were used for infecting new cells; then, it was evaluated how functional the newly formed particles are. Knowing that the exchange between NPs reduces transcription/replication could give an indication of the process that is being affected by NP. It is expected to measure no minigenome reporter activity on the infected cells if there was no replication, or not a proper interaction between NC components. If the reporter activity in the producer cells is decreased and there is not a negative effect on the infectability of the particles, this would imply a transcription deficiency, based on a certain viral protein combination, but a proper replication.

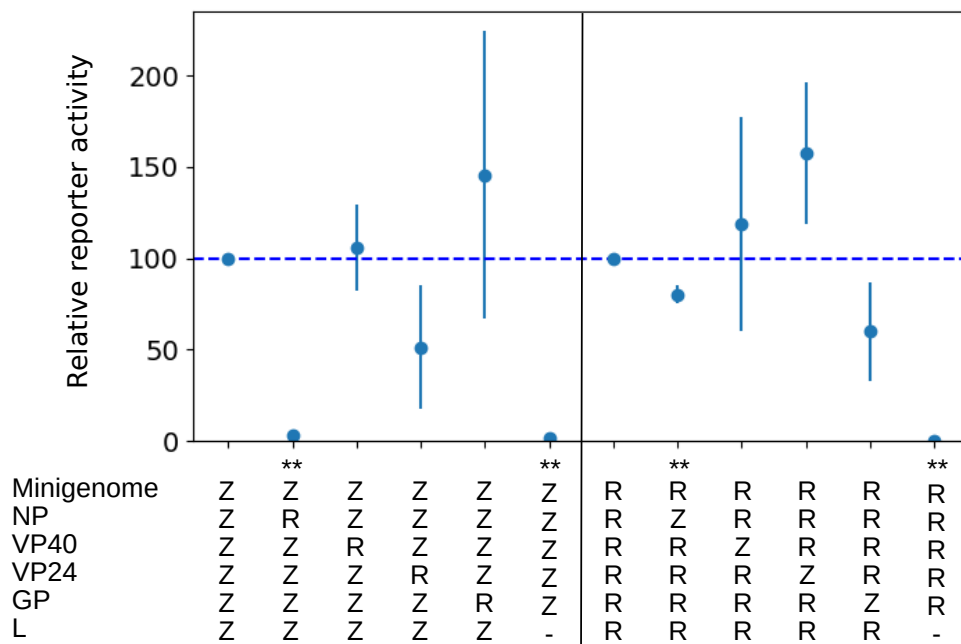


Figure 4.13: Relative reporter activity of minigenome during the production of iVLPs in HuH7 cells. All seven ebolavirus proteins were transfected into HuH7 cells and the minigenome reporter activity was measured. GP, VP40, VP24 and NP were exchanged between EBOV (Z) and RESTV (R) to evaluate the effect on transcription/replication when all viral components are included in the system. The graph shows the average(dot) and variance (line) for n=3 replicates measured relative to 100% activity of only Z (left) or only R (right). The significance of the values measured differing from the 100% optimized plasmid combination was done with Anova where \*\* = pval < 0.01. The values plotted come from supplementary table 7.9.

#### *iVLP infectivity: EBOV NP and VP40 can improve RESTV infection rate*

It was possible to collect iVLPs from every combination of EBOV and RESTV proteins. The amounts of the proteins inside the iVLPs changed, but the effect on the infection needs to be evaluated. The minigenome represents the viral RNA, which needs to be properly assembled into the NC in order to be incorporated into the viral particles. Without a proper inclusion of the viral RNA into the particles it is not possible to have a continuous infection. Therefore, it was checked to see if there were copies of the minigenome incorporated into the iVLPs by using them for infecting HuH7 cells which were actively producing EBOVs NP, VP35, VP30 and L. It was only tried with EBOV proteins on both RESTV and EBOV minigenome, because the outcome of the reporter is higher, suggesting less false negative results.

It was observed that the signal of EBOV minigenome was always found when combined with all EBOV proteins (see table.4.4). This did not change when RESTV VP40 or RESTV GP was used with EBOV remaining proteins. EBOV minigenome was not found in one of the four infections of VLPs formed with RESTV VP24. This could be due to a handling error, or the ability of VP24 to affect the transport of the NC to the membrane. Moreover, EBOV minigenome signal was not observed when RESTV NP was used for producing the EBOV iVLPs in any of the replicates. The NC (which transports the RNA) needs to interact with VP40 in order to introduce the RNA into the VLPs. In order to discard the interaction of RESTV NP with EBOV VP40 as a factor, it was also tested exchanging EBOV VP40 and NP for RESTV VP40 and NP in EBOV context. There was no reporter activity in the cells infected with the filamentous particles formed by RESTV NP and VP40 with EBOV remaining proteins in any of the replicates (see table 4.4 EBOV minigenome).

RESTV minigenome signal was observed only in half of the replicates where cells were infected with RESTV iVLPs. This value did not change with the exchange of NP, GP or VP24 from RESTV to EBOV (see Table 4.4 RESTV minigenome). However, the minigenome signal did decrease when EBOV VP40 was used instead of RESTV VP40, suggesting there is indeed not a proper interaction between RESTV NP and EBOV VP40. And the MG signal also increased when NP and VP40 from EBOV were used instead of RESTV's.

The NC surrounds and incorporates into the VLPs the negative strand of the minigenome, or viral RNA. The absence of reporter activity in the infected cells suggests the minigenome RNA was not properly incorporated into the NC. In the previously mentioned results it was possible to determine that RESTV NP in EBOV minigenome context decreases significantly the reporter activity. Both results (iVLP and minigenome) support a deficiency on minigenome replication or NC formation when RESTV NP is present. This reinforces the possibility that RESTV produces more empty particles. Further, live cell imaging (LCI) was used to evaluate the NC movement on the different viral protein combination, and it was checked to see if this is the limiting factor for the empty particle formation.



Table 4.4: iVLP infection ratio in HuH7 pre-transfected cells with EBOV NP, VP35, VP30 and L. Different combinations of RESTV (R) and EBOV (Z) proteins were used for iVLP production. These were used for infecting pre-transfected cells and to measure the reporter activity. The rate of infection was calculated from at least three replicates, the numbers represents the proportion of replicates which was positive.

EBOV minigenome							
protein	species source						
NP	Z	R	Z	Z	Z	R	Z
VP40	Z	Z	R	Z	Z	R	Z
GP	Z	Z	Z	R	Z	Z	Z
VP24	Z	Z	Z	Z	R	Z	Z
noL							Z
Infection rate	1.00	0.00	1.00	1.00	0.75	0.00	0.00

RESTV minigenome							
protein	species source						
NP	R	Z	R	R	R	Z	R
VP40	R	R	Z	R	R	Z	R
GP	R	R	R	Z	R	R	R
VP24	R	R	R	R	Z	R	R
noL							R
Infection rate	0.50	0.50	0.30	0.50	0.50	1.00	0.25

#### 4.2.4 RESTV NP and EBOV VP35 do not form a stable NC

RESTV NP incorporation into the filamentous particles could also be limited by the NC movement. The transport of the NC around the cell would determine the amount of particles which get to reach the membrane. LCI was used to address the effect of RESTV NC movement in the incorporation of NP into the filamentous particles. Also NC protein components from EBOV and RESTV were combined to see if RESTV NP and EBOV VP35 failed to interact not only for transcription and replication but also for transport.

It was possible to observe in almost every viral protein combination that the NC was following long trajectories which, depending on the setup, were varying with length, speed and cell location (see fig. 4.14). Based on the Maximum intensity projection (MIP), most protein combinations between RESTV and EBOV are able to form long NC trajectories, but not RESTV NP and EBOV VP35 (see fig. 4.14). In fig. 4.14 there is an example of NC track or movement for each protein combination which was followed with a red line. However, it was not possible to identify any trajectory in the combination of RESTV NP with EBOV VP35 and VP24, but the particles

had a "wobbling" movement. Also the combination of RESTV NP, VP24 and EBOV VP35 showed short trajectories, suggesting RESTV VP24 is able to compensate in some degree for the lack of interaction between RESTV NP and EBOV VP35.

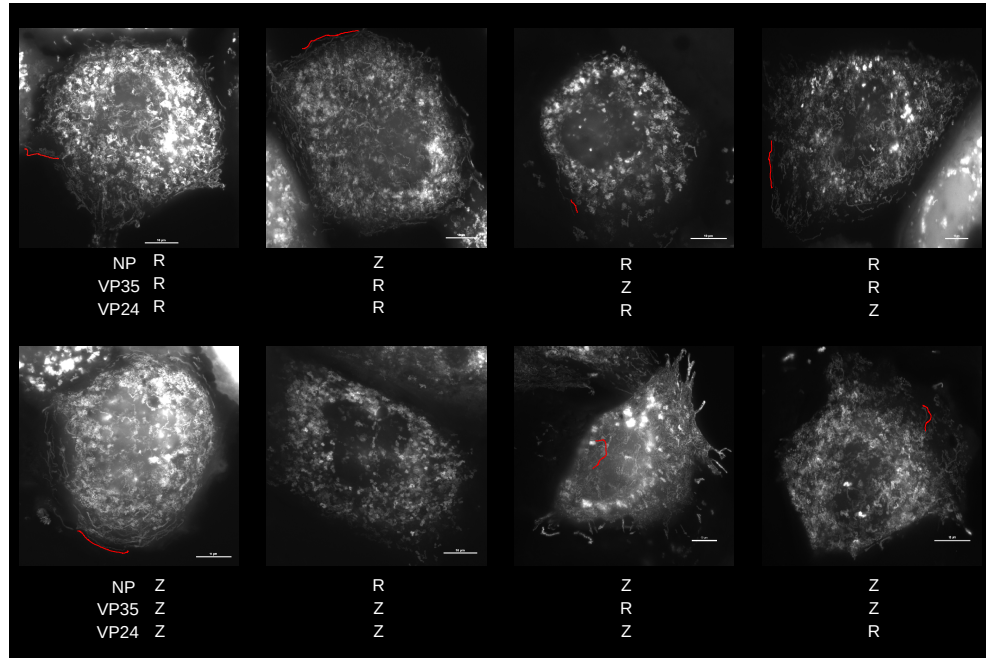


Figure 4.14: Maximum intensity projection of moving nucleocapsids (NC) formed with different combinations of NP, VP35 and VP24 from RESTV (R) and EBOV (Z). The red lines show an individual trajectory. The white bar below each cell represents 10  $\mu$ m. RESTV NP and EBOV VP35 do not form trajectories.

For a more objective and detailed evaluation of the particles' movements, the programs from Andreas Rausch were used. With the programs it was possible to evaluate, for most particles, the distance they move in total (Distance), the speed of most of the particles (Velocity), and an estimate of the displacement from the origin of travel, and to plot the values with their mean and media (see fig. 4.15). Also, three additional setups, with no NP, no VP35 and no VP24 are included as negative controls. Without the addition of NP it is not possible to form a NC, but because VP30 (reporter gene) can interact with VP35, and VP35 with VP24, it would be possible to observe the movement of particles. A signal showing movement from VP35, VP30 and VP24 combination might show an intermediate state of the viral assembly or the proteins effect/interactions in/with the host cellular components. With these three negative controls the parameters were selected for filtering out static particles to reduce noise and also for computer requirements. Previous

reports suggest positive NCs travel at a speed of at least 85 nm/s [22], but it was observed that long trajectories were filtered out with this parameter. A lower speed of 65 nm/s and a displacement movement of 4 were chosen for filtering the particles (see fig. 4.15 A). The speed filter is confusing, and can be controversial and therefore a second filter based on the displacement alone (above 4) was also applied (see fig. 4.15 B).

With the double filter (speed and displacement) there were no observed particles moving in the absence of VP35. However, with the absence of NP or VP24 one can observe a wobbling movement, suggesting either the need of VP35 for the direct contact with the actin filaments for the NC movement, and NP and VP24 for the stabilization of the NC, or that VP30 needs VP35 for coupling to the NC and to move with it around the cell. With only the displacement filter it is possible to find particles which moved at a speed of a reported positive NC (above 85 nm/s [22]) on all the negative controls. This would imply that the use of the speed is indeed unreliable to discriminate positive NC movement because of the intrinsic membrane movement, cell activity and cytosol crowding. Moreover, it was interesting to observe that the distance of the overall number of particles does not seem to be a good indicator for NC positive movement, independent of the filter. This could be explained because of the inclusion of every particle movement and not because of the displacement from the initial position. Nevertheless, there is a clear difference in the distribution of values between the expected control negatives and all other combinations. Also, the constant production of viral proteins inside the cell causes during the LCI the observation of different steps or stages of the NC assembly and transport at the same time. It is possible to restrict the values even more, but this would depend on what one is looking for and the aim of the study.

Based on the MIP long trajectories were not observable where RESTV NP and EBOV VP35 were combined. Also, with the overall analysis of the particles it is possible to say that there is movement and displacement of particles where RESTV NP and EBOV VP35 were combined. This would suggest RESTV NP and EBOV VP35 do not hold a stable structure, but are able to interact in a less efficient manner and fulfill their function in the NC context. However, the LCI method needs an over-expression of all the proteins, saturating them in the cell, probably "forcing" contacts. Moreover, the values of the plasmid combinations which include RESTV NP and EBOV VP35 are really similar to the combination EBOV NP and VP35 and RESTV VP24. This is interesting because based on the MPI there are clear long trajectories. The MPI is done with the software accompanying the microscope used for

acquiring the data, directly on the analyzed pictures. LCI is based on picture acquisition taken every set amount of time, in this case every two seconds for three minutes, and really fast molecules are traced as dots in a row instead of a line. The numbers come from an independent software written by collaborators. A hand evaluation of each experiment shows there is still a need for improving the scanning of the pictures to automatize the process. It is also necessary to reduce the time between acquisitions to avoid the dot-like trajectories, that are considered by the collaborator's software as interrupted or individual sequences, and now only able to be recognized during the manual scanning. Therefore, the difference between MPI and the numbers could correspond to a software difference.

In summary, the LCI results are in accordance with the minigenome and iVLP results, where RESTV NP is the limiting factor for RESTV processes. There could be compensatory mutations in RESTV proteins to maintain their interactions but it is interesting to find that RESTV can improve different functions with EBOV NP.

#### 4.2.5 Cell entry: EBOV releases its content into the cytosol faster than RESTV

The small RNA-Seq data consistently showed that the leading difference between EBOV and RESTV infection is the robust response against RESTV since 3 h p.i. which seems to be progressive. In contrast, EBOV shows a more clear difference between the time points than against Mock at 3 h p.i. The microarray data supports the observation that the biggest difference in cellular response against RESTV vs. EBOV is at 3 h p.i. Few processes are expected at such an early time point of infection, which would go from plasma membrane contact to viral content release into the cytosol. Due to the differences until now observed it is hypothesized that both viruses differ on their entry to the cell. In the previous sections almost every viral component which affects different stages of infection was evaluated but not GP, the component directly responsible for infection and entry. To test if there is a distinction at the early stage of infection between both viruses, an entry assay adapted from [50] (see fig. 4.16 A) was used. This measures the time the virus needs for releasing its content into the cytosol. Briefly, filamentous iVLPs containing EBOV NP, VP40, VP30 fused to a luciferase (VP30-FF) and EBOV GP or RESTV GP (see fig. 4.16 B) were purified and used for infecting HEK293 in suspension. At the indicated time point the cells were put on ice and luciferase signal was measured. If the content of the filamentous particles

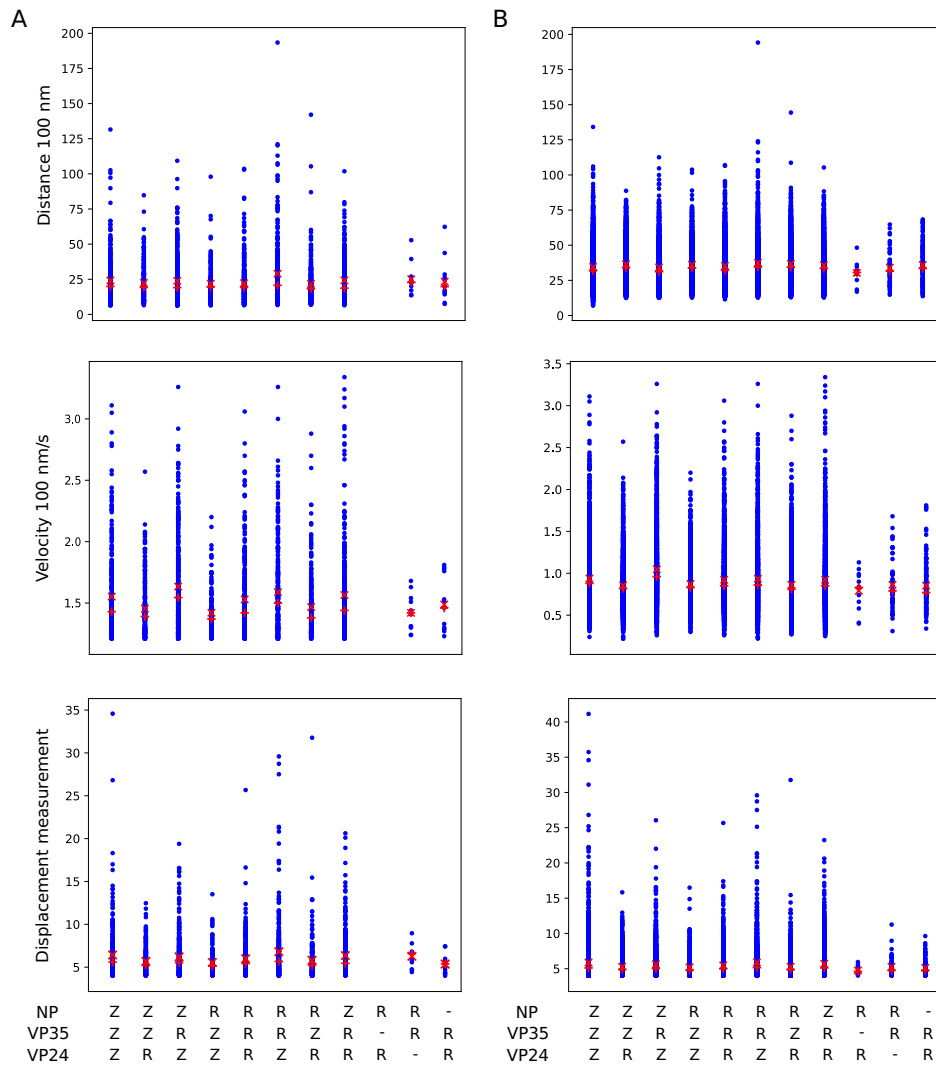


Figure 4.15: Detailed evaluation of chimeric RESTV (R) and EBOV (Z) NCs. Every blue dot represents a NC, the red X represents the mean of all particles and the + the median. (A) NC with a Velocity below 65 nm/s and Displacement measurement below 4 were filtered out. (B) Particles with a displacement below 4 were filtered out. The values were chosen based on the negative controls (missing one of NP, VP35 or VP24).

is released into the cell the luciferase signal can be measured. First, it was checked to see if the filamentous particles formed with RESTV GP and EBOV GP differed in GP or VP30-FF content. The VLP production was similar for the different virus GPs, which was measured using silver gel. Also the luciferase signal of the VLPs lysates of the different VLPs was measured with a luminometer and showed similar values (data not shown).

EBOV released its content into the cytosol almost two times faster than RESTV (see fig. 4.16 C). Both viruses seemed to enter between the first and

second hour after infection. In summary, EBOV GP promotes a faster entry into the cell than RESTV GP.

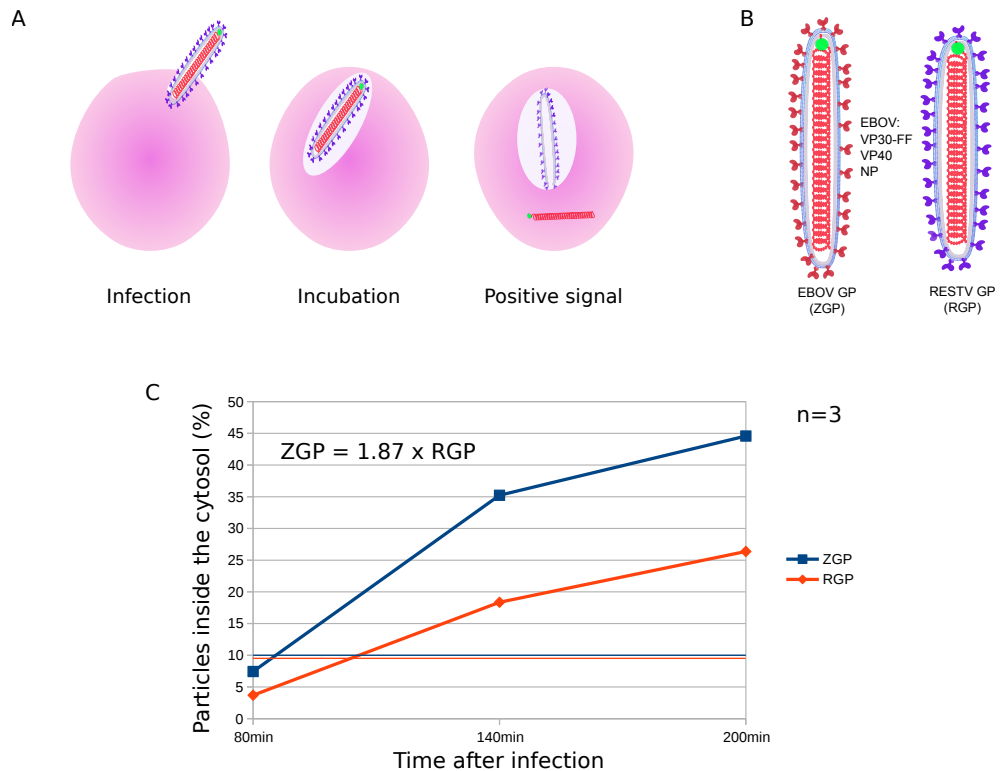


Figure 4.16: Entry assay result summary. The entry assay shows EBOV that releases its content faster than RESTV. A: Graphical overview of the assay. B: VLPs composition used for the comparison of RESTV and EBOV. C: Result based on three replicates shows consistently that based on GP the viral release is faster only in EBOV containing GP VLPs (ZGP) than RESTV (RGP). The colored lines show the background, which was similar for ZGP and RGP.

### 4.3 Ebolavirus intrinsic differences

#### 4.3.1 Bioinformatic protein comparison: Conserved amino acids in ebolaviruses are not entirely shared with RESTV

In the previous section EBOV and RESTV proteins were identified whose interactions might affect different viral processes. The differences were pinpointed based on RESTV and EBOV compatibility, and were narrowed down to NP, VP35, L and VP40 protein interactions. The protein aa sequence could give a hint of the differences between the Ebola viruses. Here the aa are evaluated which differ between RESTV and all other ebolaviruses for the

proteins of interest (NP, VP35, L and VP40). For this analysis more than one sequence of each species was considered (see Materials and Methods) except for TAFV which had only one sequence available.

RESTV NP aa sequence differs in 18 positions which are conserved in all other ebolaviruses; RESTV VP35 has 14 positions; and RESTV VP40 has 8 positions and has additional 5 aa in the C-terminus that do not exist in EBOV VP40. Based on the differences observed in the aa sequence of NP, the C-termini could be less acidic in RESTV. It contains in this region two glutamic acids which are less acidic than aspartic acid, which is contained in all the other ebolavirus species (see Table 4.5). Also, based on the analysis of NP residues 439-492 and 589-739 EBOV NP has a stronger charge than RESTV. The RESTV VP40 additional aa would partially explain the running behavior in the SDS page gel, which shows RESTV VP40 band size above EBOV VP40 band.

The polymerase L is the biggest protein of ebolaviruses with 2212 aa. The amount of differences between RESTV and EBOV was not limited to single aa exchange, but also contained insertions/deletions. From all the single aa exchanges in the whole protein, Alanine (A) to Serine (S) and S to A were the most abundant changes in RESTV, but conserved in all other ebolaviruses (see Table.4.6). The region between the residues 280-370 was also evaluated, because of its role in L function [70]. Seven residues were conserved among all ebolaviruses, but not shared with RESTV (EBOVpositionRESTV): L289V, L290I, Y318F, A332S, T336, E356D and T367S. The specific differences could explain the impaired EBOV and RESTV protein interactions and are further addressed in the discussion.

#### 4.3.2 Ebolavirus non-coding regions comparison: RESTV and EBOV contain putative functional ncRNAs

The smallRNAseq data set comprised not only host RNA, but also viral RNA. The multimapping parameter also allowed the identification of homologous regions between RESTV and EBOV viruses. These regions overlap with transcription start sites (TSS), which are located in intergenic secondary structures already reported to be conserved among ebolaviruses [71] So far there is not a complete understanding of these regions, but some are considered "helpers" of genomic replication [19]. The library preparation used for sequencing would imply that the TSS covered by reads are processed and would have an ncRNA function. With this data it was possible to confirm the presence of viral particles from RESTV and EBOV inside the cells since

Table 4.5: NP, VP35 and VP40 amino acids which are conserved among different ebolavirus species but differ only in RESTV

	RESTV	EbolaviruSerine (S)	Position
NP	Threonine (T)	Serine (S)	30
	Lysine (K)	Arginine (R)	39
	Serine (S)	Proline (P)	42
	Valine (V)	Isoleucine (I)	56;570
	Isoleucine (I)	Valine (V)	64
	Leucine (L)	Methionine (M)	137
	Tyrosine (Y)	Phenylalanine (F)	212
	Alanine (A)	Serine (S)	279
	Asparagine (N)	Lysine (K)	416
	Glutamine (Q)	Tyrosine (Y)	421
	Glutamic acid (E)	Aspartic acid (D)	426;446
	Isoleucine (I)	Threonine (T)	454
	Glutamic acid (E)	Glycine (G)	517
	Serine (S)	Threonine (T)	568
	Threonine (T)	Proline (P)	607
	Asparagine (N)	Glycine (G)	729
VP35	Serine (S)	Glutamine (Q)	50
	Glutamic acid (E)	Aspartic acid (D)	54
	Asparagine (N)	Threonine (T)	79
	Alanine (A)	Serine (S)	84;15
	Isoleucine (I)	Valine (V)	85
	Serine (S)	Alanine (A)	86
	Valine (V)	Threonine (T)	87
	Aspartic acid (D)	Glutamic acid (E)	88;243
	Lysine (K)	Glycine (G)	89
	Valine (V)	Alanine (A)	90
	Alanine (A)	Valine (V)	91
	Lysine (K)	Glutamine (Q)	92
VP40	Valine (V)	Threonine (T)	45
	Threonine (T)	Proline (P)	85
	Isoleucine (I)	Threonine (T)	105
	Valine (V)	Isoleucine (I)	122
	Asparagine (N)	Glycine (G)	201
	Proline (P)	Glutamine (Q)	247
	Glutamine (Q)	Histidine (H)	271
	DKQXXYQ	EK	C terminus



Table 4.6: Polymerase L most abundant aminoacid substitution in RESTV compared to all other Ebolavirus species.

RESTV	Ebolavirus	position
A	S	853;874;1115;1525;1585
S	A	332;980;1242;1567

3 h p.i. . Also, was explored the possibility of ncRNAs being transcribed by the virus, and the differences between EBOV and RESTV were looked for at this level.

*Transcription start sites suggest common regulation with other ebolaviruses*

Based on the ebolavirus genome sequence it was possible to obtain a conserved secondary structure for each TSS (see fig. 4.17), which also shared a nucleotide sequence between the five species of ebolaviruses. It is interesting to notice that the 5' side of each hairpin is more conserved, nucleotide base, than the 3'. Also, the bottom of each hairpin is nucleotide conserved, but the upper part of the hairpin, although not sequence conserved, is structure conserved. However, it is worth mentioning that SUDV and RESTV contained most of the nucleotide insertions, therefore deforming the hairpin in the secondary structure. This can be pointed out clearly in VP30's hairpin, where are "-" observed because SUDV and RESTV had two extra nucleotides there. This indicates the presence of two factors for the recognition of the TSS which is conserved between the Ebolavirus species, first sequence based recognition, and the second structure based. While evaluating the individual alignments RESTV and SUDV differ the most from the other Ebolaviruses SUDV has more differences than RESTV, and SUDV is considered the second (after EBOV) most aggressive ebolavirus for humans. Therefore, the TSS might not mark a pathogenic relevant feature.

*Viral putative small ncRNAs could represent a new factor for host response*

At 24h p.i. the reads covered almost all the virus, but hot spots of reads could be marked. The Trailer region is the most covered by sequencing reads in both viruses. Then, VP40 TSS and GP TSS are also well covered in their 5' prime region, after 3 h p.i. (see fig. 4.18). It is interesting to notice that GP and VP40 are the envelope and matrix, respectively, forming the outer structure of the filamentous particle. VP40 TSS was already suggested as the ncRNA EBOV-pre-miRNA-T2 [72]. However, it is in the conserved region between

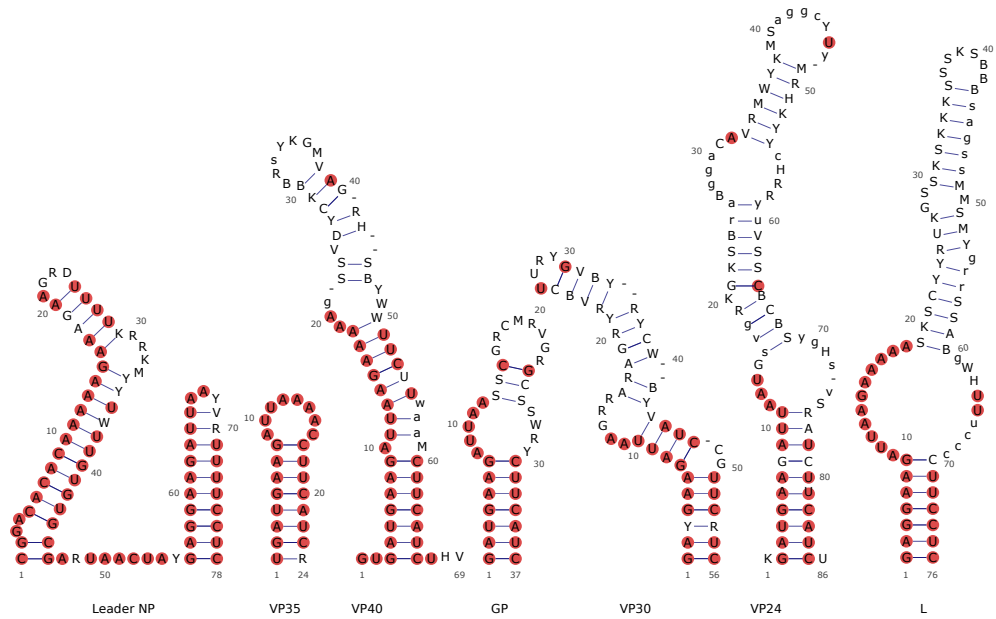


Figure 4.17: Predicted common secondary structure of the transcription starting site of each mRNA codified in ebolaviruses. The structures were predicted in Locarna using the UTRs of the five ebolavirus species (TAFV, BEVOV, SUDV, RESTV, EBOV). In red color are the bases entirely conserved between the ebolavirus. The uncolored shows the most conserved nucleotide (s). The base pairing is indicated with lines, and shows the consensus secondary structure. This was done for every upstream mRNA and presented in the genome order (NP, VP35, VP40, GP, VP30, VP24, L).

RESTV and EBOV. Therefore this might not be a difference for pathogenesis, but fulfills a function as a ncRNA in addition to TSS.

Further, the read strand holds the information of genome and transcriptome, and for RESTV the genome is also well covered, while in EBOV it is the transcriptome. This could suggest that the RESTV switch between transcription and replication is impaired in humans, and/or the release of the genome into the cytosol, to be further processed, is slower. The sequencing data would support previously mentioned results, where RESTV iVLPs are not infecting in the same ratio as EBOV (see fig. 4.4), and would support a relationship with the incorporation of the genome into the newly formed viral filamentous particles.

#### 4.4 Cellular candidates and their influence in viral fitness

The sequencing data showed that THP1 cells infected with RESTV increased the expression of different miRNAs, in comparison with Mock and EBOV which did not show an increase on these miRNAs. Two of these miRNAs

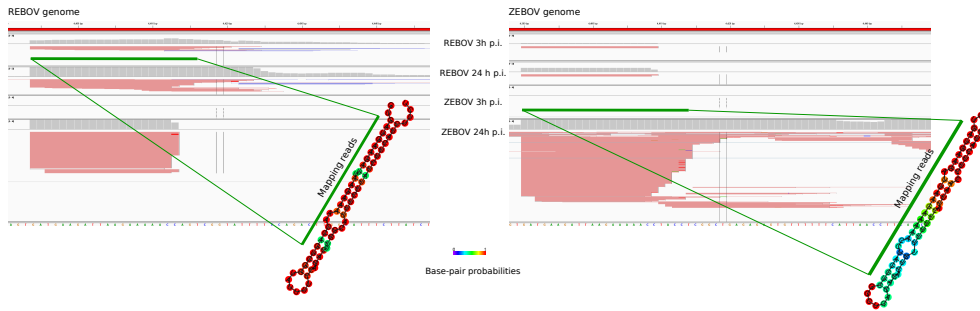


Figure 4.18: Viral sequence coverage by reads and predicted structure based on the sequence. VP40-TSS has reads covering a specific region which would correspond to a putative ncRNA

which were up-regulated after 3 h p.i. were hsa-mir204-5p (miR-204) and hsa-mir10b-5p (miR-10b). Because the effect was not observed in HuH7 cell line and the established system of study is in this cell line, hsa-miR10a-5p (miR-10a) was also included in the study. This was done because both miR-10 have different tissue abundance. miR-204 has been found to interfere with HBV virus replication/viral production [73], and because it is present in the liver, it was still chosen for the further studies.

MiR-204, miR-10a and miR-10b were studied with the use of the Agomir molecules. Agomir are synthesized miRNAs which contain a cholesterol modification to improve cellular transfection. The protocol for the use of these molecules is detailed in Methods section. Additionally, as a negative control a scramble sequence was acquired which does not target human genes and here is referred to as miR-NC.

In summary, HuH7 cells were transfected with 50 nM of each Agomir, and after 3 h p.t. the cells were re-transfected with the components necessary for iVLP formation. After three days p.t. the supernatant was collected for filamentous particle purification, and the cell lysate divided for luciferase and protein quantification and RNA extraction. The iVLP system has three points of study: transcription/replication, iVLP production, and the infectivity of the newly formed particles. Only the filamentous particles were considered for the evaluation of the iVLPs infectivity. With this approach it was expected to elucidate the possible role of the miRNAs candidates on the viral life cycle. These steps will help to select one molecule for viral evaluation.

#### 4.4.1 Mir-204 and miR-10a affect viral transcription/replication

The transcription/replication activity of RESTV, based on the MG reporter activity, does not seem affected by the addition of the specific miRNAs compared to the miR-NC (see fig. 4.19). This was expected because RESTV increases the presence of these molecules, according to the sequencing results. However, EBOV seems to be significantly affected by miR-204 and miR-10a (see fig. 4.19). MiR-10a presence seems to increase EBOV relative reporter activity in an average of 43%. MiR-204 over-expression reduces EBOV reporter activity by 42%. These results would suggest miR-204 is a cellular candidate which decreases the viral fitness affecting transcription/replication of EBOV, and most probably of RESTV. The other miRNAs Agomirs did not significantly affect the reporter activity.

It is fascinating to find that one of the candidates selected, based on RESTV cell's response, could partially explain the differences between both viruses. This implies that miR-204 could be one cellular component controlling RESTV's natural replication, and could be used to control EBOV. Moreover, the presence of these molecules decreases the minigenome reporter activity, most probably because of the extra stress which caused a higher cell death in the Agomir transfected cells.

#### 4.4.2 miR-204 affects NP/VP40 ratio on filamentous particles

Based on section 4.2.3 it was observed that RESTV NP does not incorporate into the viral filamentous particles as efficiently as EBOV NP. To assess if miR-204 could be affecting EBOV NP/VP40 ratio, filamentous particles were purified and NP/VP40 ratio was quantified via WB. This step was performed with exactly the same samples as for transcription/replication studies above. The ratio of NP and VP40 was first calculated inside the cells, and the value was normalized by tubulin. It was observed that miR-204 does not affect significantly the amount of NP/VP40 inside the cells (based on tubulin) compared to miR-NC (see fig. 4.20 A). It seems that the ratio is above the other treatments suggesting NP might be getting trapped inside the cells, but the variance is too high to affirm this statement. Nevertheless, EBOV ratio NP/VP40 in the filamentous particles did vary significantly on miR-204 transfected cells compared to miR-NC (see fig. 4.20 B). The ratio of EBOV NP/VP40 was lower, suggesting there is less NP incorporated into the iVLPs.

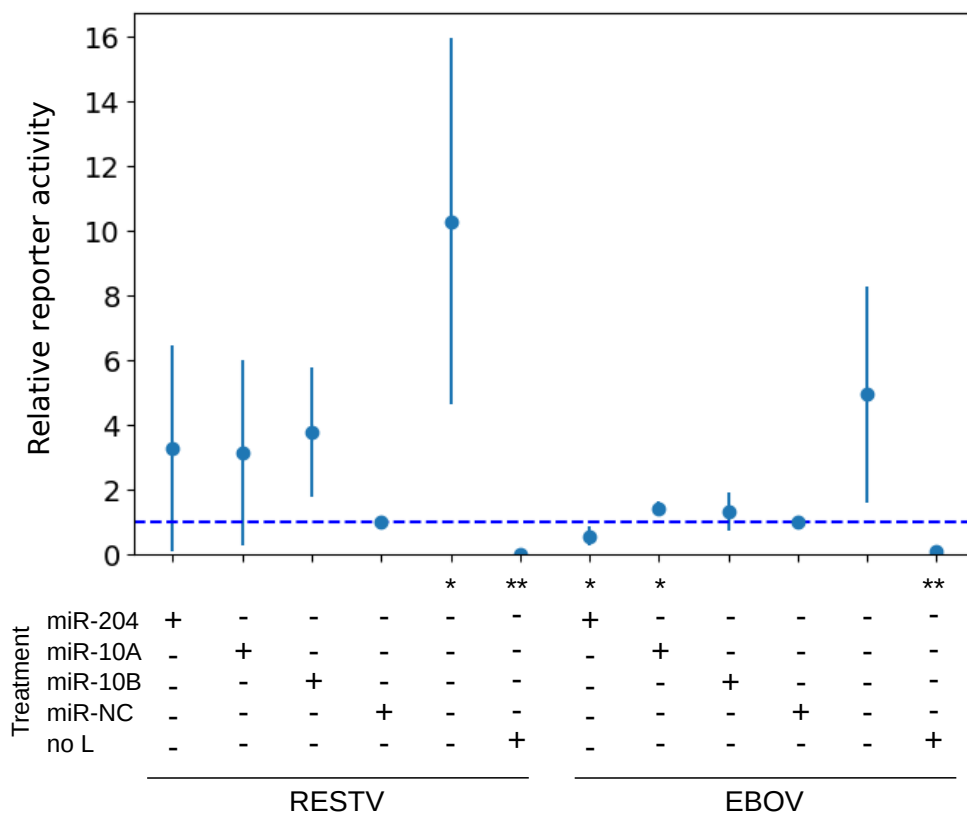


Figure 4.19: Effect of different miRNAs on the minigenome reporter activity of RESTV and EBOV. The graph shows the average(dot) and variance (line) for n=>3 replicates measured relative to miR-NC. The significance was calculated with Anova where \* = pval <0.05, and \*\* = pval < 0.01. RESTV minigenome reporter activity does not vary specifically with the addition of the molecules. EBOV minigenome reporter activity seems reduced when treated with miR-204 and increased with miR-10a compared to miR-NC. The values plotted come from supplementary table 7.10.

MiR-204 negatively affects EBOV transcription/replication and NP iVLP incorporation. These two traits were observed as a normal feature for RESTV. The sequencing data showed RESTV infection triggers an over-expression of miR-204 (see section 4.1) and the effect of this miRNA could be related to a less efficient NP incorporation into the filamentous particles, trapping NP inside the cells.

#### 4.4.3 miR-204 effect in the viral proteins cellular distribution

At 24 h p.t. viral transcription/replication and NC movement are mainly observed inside the cell. At 48 h p.t. it is possible to collect viral particles, and

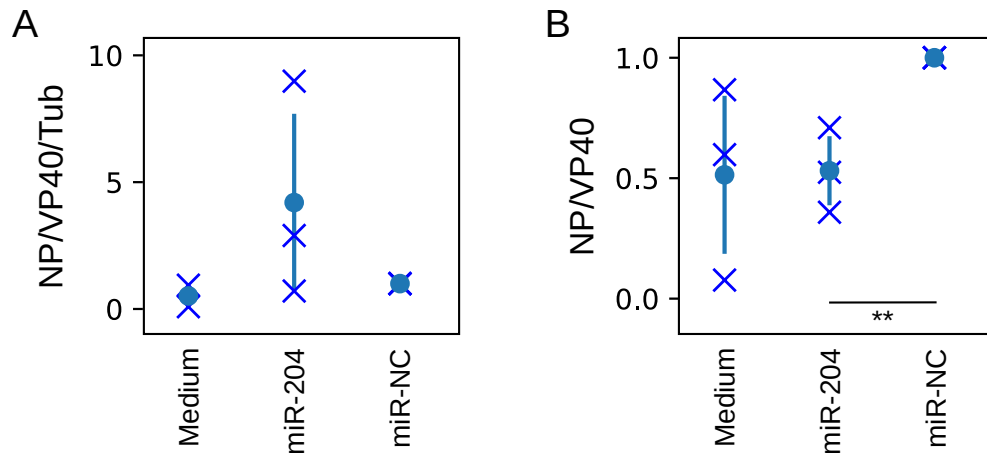


Figure 4.20: Effect of miR-204 on EBOV's protein ratio NP/VP40 measured by WB (A) Inside the cells normalized by tubulin (NP/VP40/Tub). (B) In the filamentous particles (fraction 4-6) The graph shows the average(dot) and variance (line) for  $n \geq 3$  replicates measured relative to miR-NC. The significance was calculated with Anova where \*\* =  $p$ val < 0.01. One can observe miR-204 affects the protein ratio of EBOV proteins inside the filamentous particles. The values plotted come from supplementary table 7.11.

then it is expected to also find new-infections. As observed above, viral transcription/replication and particle formation can be affected by miR-204, and these were observed to be related to NP in RESTV. Therefore the effect of miR-204 was studied on NP distribution inside the cells, specifically NP inclusion bodies, transcription/replication loci inside the cell. NP inclusion bodies were analyzed via IF. These bodies form a clear aggregated signal of NP (big dots) around the cellular cytoplasm.

For the IF study HuH7 cells were pre-transfected with 100nM miR-204 (or miR-NC) and then transfected with the components necessary for iVLP production of RESTV or EBOV. The cells were collected at 24 h p.t. and 48 h p.t. to assess the overall effect of miR-204 on RESTV and EBOV. There was no visible effect on RESTV protein distribution between Agomir transfections (see fig. 4.21 RESTV). This was expected because, based on the small RNA-Seq results, in the cells infected with RESTV there is an up-regulation of miR-204, and so it could be present in each experiment where RESTV components were expressed, but in different quantities. EBOV NP does show a new phenotype when miR-204 is present in the cells. EBOV inclusion bodies were reduced or even not present (no observable NP aggregations) on miR-204 pre-treated cells (see fig. 4.21 EBOV). It is possible to see the EBOV NP signal inside the cell, but it does not form a clear bright, big, distinguishable signal in miR-204 pre-treated cells compared to Medium and miR-NC (see

fig. 4.21 EBOV). The disruption of EBOV NP inclusion bodies would correlate with a reduction on transcription/replication. Hence this would imply that miR-204 targets a cell component which is involved in the inclusion bodies' integrity.

*Aggregates formed by EBOV NP alone and with minigenome components do not get affected by miR-204*

NP can form big aggregates without the need of other viral component (see fig. 4.22 A medium). The inclusion bodies can be observed with the minigenome components only (see fig. 4.22 B medium). MiR-204 could be disturbing NP aggregations or the inclusion bodies, or promoting NC disassociation from the inclusion bodies. As in the previous section, this was addressed with IF analysis of cells transfected with EBOV's NP plasmid or minigenome components and treated with the different Agomir miRNAs. It seems EBOV's NP aggregations are not disturbed in any of the treatments (see fig. 4.22 A). Also, the inclusion bodies formed in the minigenome context look similar between treatments (see fig. 4.22 B). These results adduce that miR-204 regulates a cellular protein which affects EBOV's transition from the inclusion body to the NC, but also disrupts the incorporation of the NC into the filamentous particles. This would explain the transcription/replication and NP/VP40 particles' reduction.

#### 4.4.4 EBOV infection and inclusion bodies are affected by miR-204

The iVLP system is used as a representation of the virus, but it is necessary to prove the effect of miR-204 on the viral context. Therefore HuH7 cells were pre-transfected with 100nM of miR-204 or miR-NC and then infected with RESTV or EBOV for IF analysis (details in Methods). miR-NC and miR-204 transfection reduced the number of infected cells compared to Medium for RESTV and EBOV infected cells, suggesting the transfection affects negatively the infection. RESTV Medium and miR-204 NP distributions look similar. The different cells observed and analyzed do not show differences between the treatments, as compared with the iVLP system. Moreover, miR-204 reduced the inclusion bodies' size in EBOV infected cells (see fig. 4.23 B), which is in accordance with the iVLP observations. The EBOV NP signal was distributed in the whole cell, forming only one aggregation, and mostly spread in the cytosol in the miR-204 treated cells.

Additionally, miR-NC transfection provoked a reduced infection and small and fewer inclusion bodies, compared to the Medium treatment for



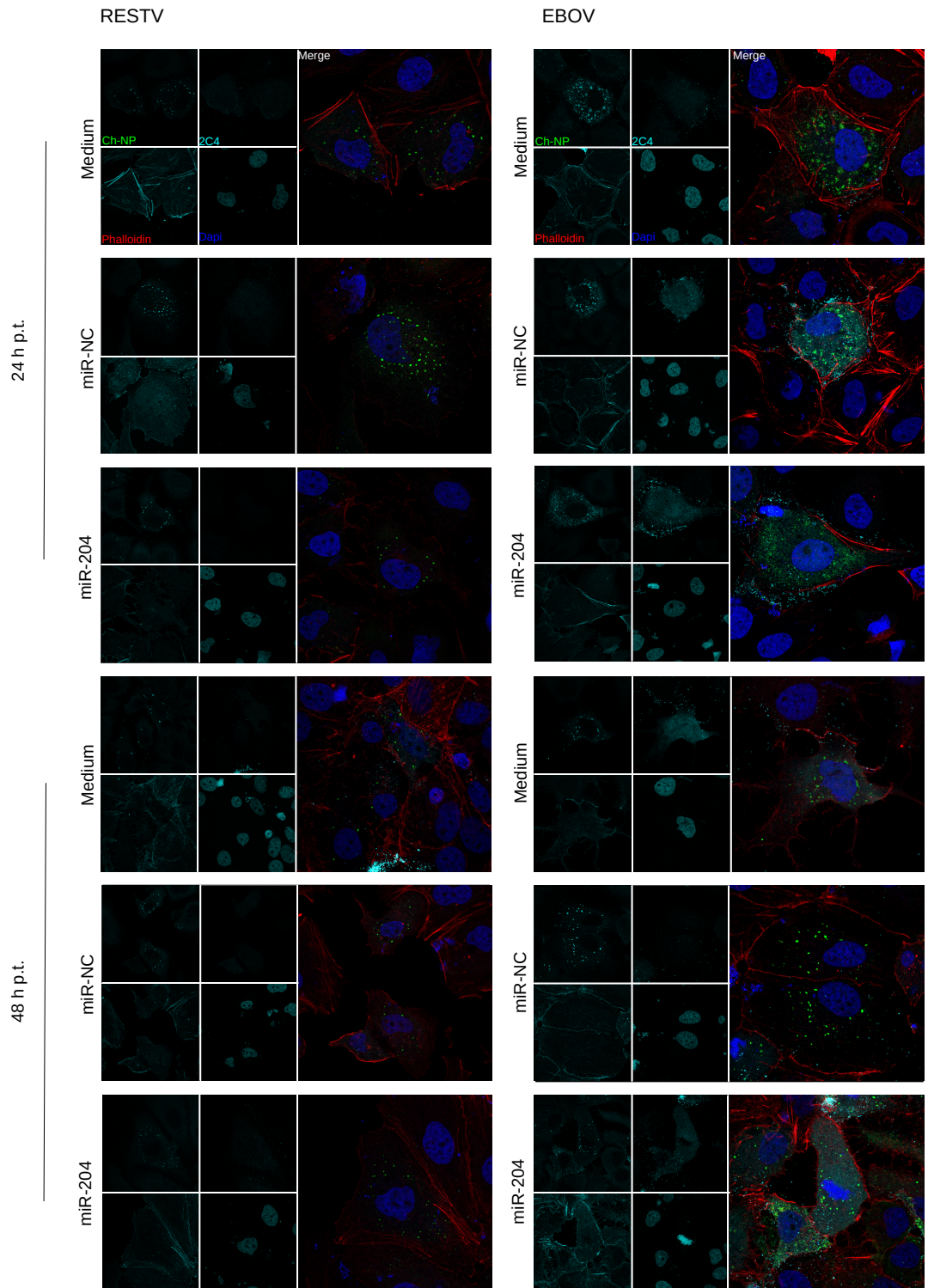


Figure 4.21: Immunofluorescence of HuH7 cells treated with miR-204 and transfected with iVLP components from RESTV and EBOV collected at 24 h p. t. and 48 h p. t. . NP was stained with Ch-NP (green), VP40 with 2C4 (light blue), Actin with Phalloidin (red) and the nuclei with Dapi (blue). The individual signals for each antibody are on the left side of each merged picture. RESTV protein distribution does not seem to be altered by the presence of miR-204. EBOV does not present NP inclusion bodies in miR-204 treated cells.



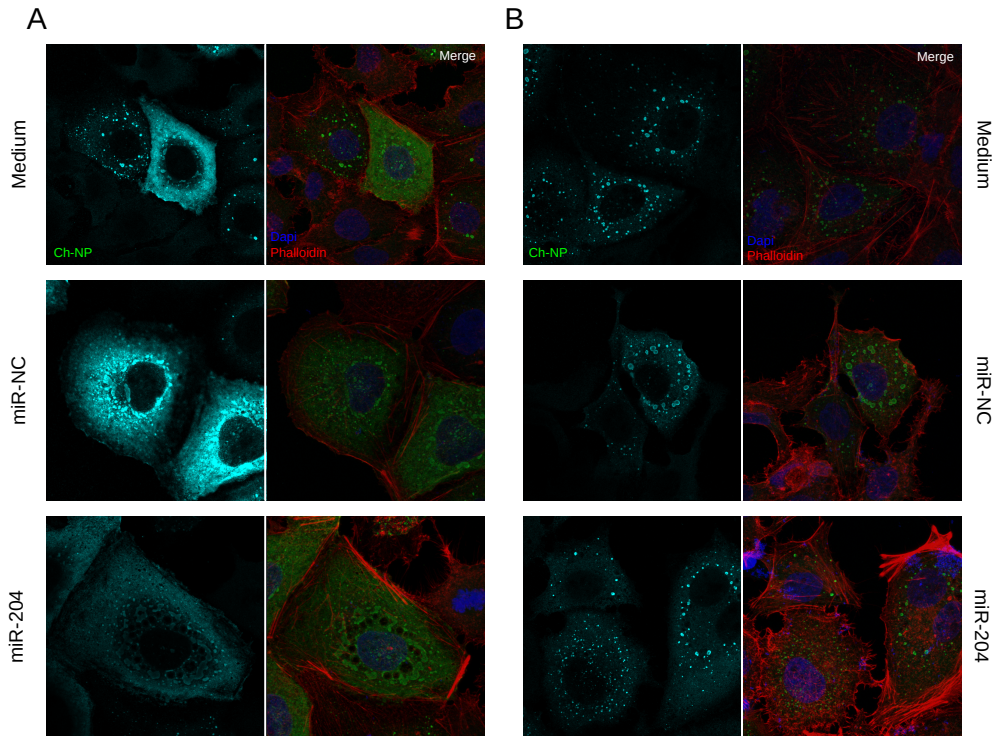


Figure 4.22: Immunofluorescence of HuH7 cells treated with miR-204 and transfected with NP (A) and minigenome components (B) from EBOV collected at 40 h p. t. . NP was stained with Ch-NP (green), Actin with Phalloidin (red) and the nuclei with Dapi (blue). NP signal is on the left side of the merge picture. EBOV NP signal does not seem affected by miR-204 treatment in this context.

RESTV and EBOV viruses (see fig. 4.23 miR-NC treated cells). miR-NC was used as a control of Agomir treatment because it does not target any cellular component, but has the chemical composition and form of the specific miR-204 (not sequence). However, miR-NC has a more similar sequence than the untranslated region of VP24 (VP24-TSS), making it possible for miR-NC to target the viral genome directly. A successful genome targeting would truncate replication and reduce transcription. This effect was not previously observed because in the iVLP system only the coding sequences were used for the protein production.

However, there were three NP phenotypes clearly distinguishable in the different treatments. Therefore NP distribution was used to discern between the pre-transfection with miR-204, miR-NC and medium. The number of cells showing these phenotypes was used to determine the specificity of the Agomirs. miR-NC causes a clear NP distribution, suggesting the cells without this phenotype are cells which were infected but not transfected. miR-NC transfection effect facilitates the discrimination of transfected vs

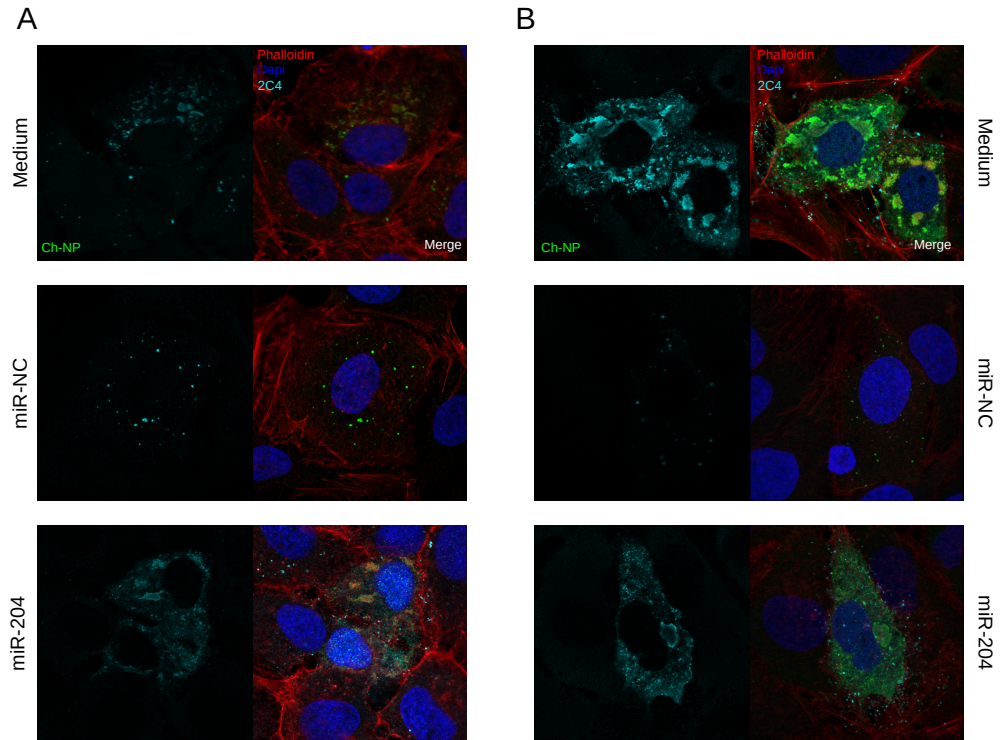


Figure 4.23: Immunofluorescence of HuH7 cells treated with miR-204 and infected with RESTV (A) and EBOV (B) at 18 h p. t. . NP was stained with Ch-NP (green), VP40 with 2C4 (light blue), Actin with Phalloidin (red) and the nuclei with Dapi (blue). NP signal is on the left side of the merged picture.

non-transfected cells, supporting a high efficient transfection and that the results are specific. miR-204 transfection shows a higher ratio of cells with EBOV NP spread in the cytosol without clear blocks, but also shows tiny aggregates around the nucleus-like miR-NC in a smaller proportion of the cells (see table 4.7) At 18 and 42 h.p.i. different types of EBOV NP aggregates were observed in the Medium treatment (see table 4.7, suggesting that the phenotype observed with miR-NC and miR-204 transfection represents a stage of NP distribution. These results further confirm that miR-204 affects negatively EBOV NP distribution inside the cells, which would cause a lower transcription/replication and NC interaction with the membrane, with the production of more empty particles.

Table 4.7: Ratio of EBOV infected cells with different NP distribution observed in miR-NC and miR-204 treated samples after 18 and 42 h p.i..

18 hrs			
Treatment\Phenotype	Medium	MiR-NC	MiR-204
Medium	0.6	0.3	0.1
MiR-NC	0.1	0.9	0
MiR-204	0.1	0.3	0.6

42 hrs			
Treatment\Phenotype	Medium	MiR-NC	MiR-204
Medium	0.9	0.05	0.05
MiR-NC	0.2	0.8	0.0
MiR-204	0	0.4	0.6

## 4.5 Results' graphical summary

This study analyzed the human cellular response against RESTV and EBOV infection, differences in the life cycle of EBOV and RESTV and the effect of specific miRNAs in EBOV life cycle (see fig. 4.24). Firstly, it was observed that independent of the human cell type (HuH7 and THP1) and study method (microarray or RNA sequencing) RESTV and EBOV cellular responses differentiate at early infection. This was partially explained with an entry assay which showed RESTV releases its content into the cytosol slower than EBOV (see fig. 4.24 A). Secondly, it was found that RESTV and EBOV do not differ significantly in transcription/replication, inclusion bodies formation and NC transport (see fig. 4.24 B,C). Thirdly, the protein interaction between both viruses shows there is an incompatibility which points towards RESTV NP being one of the main limiting factors for RESTV success. This was supported by a reduced RESTV NP incorporation in the filamentous particles, more likely in the NC, which explains the lower ratios of infection and implies that the process which seems to be strongly affected could be the replication of the viral genome (see fig. 4.24 B,C). Fourthly, based on all the above mentioned results, several of RESTV traits which correspond to differences with EBOV were also observed in the presence of miR-204 in EBOV context. This was further analyzed and a clear reduction of NP inclusion bodies, and NP incorporation in the filamentous particles was observed when EBOV infected cells were also over-expressing miR-204.

This is the first time these viral processes are analyzed as a whole for the comparison of EBOV and RESTV. With such a comprehensive study it is possible to say NP protein is a limiting factor for RESTV success in humans infection and is a potential target protein for EBOV treatments.

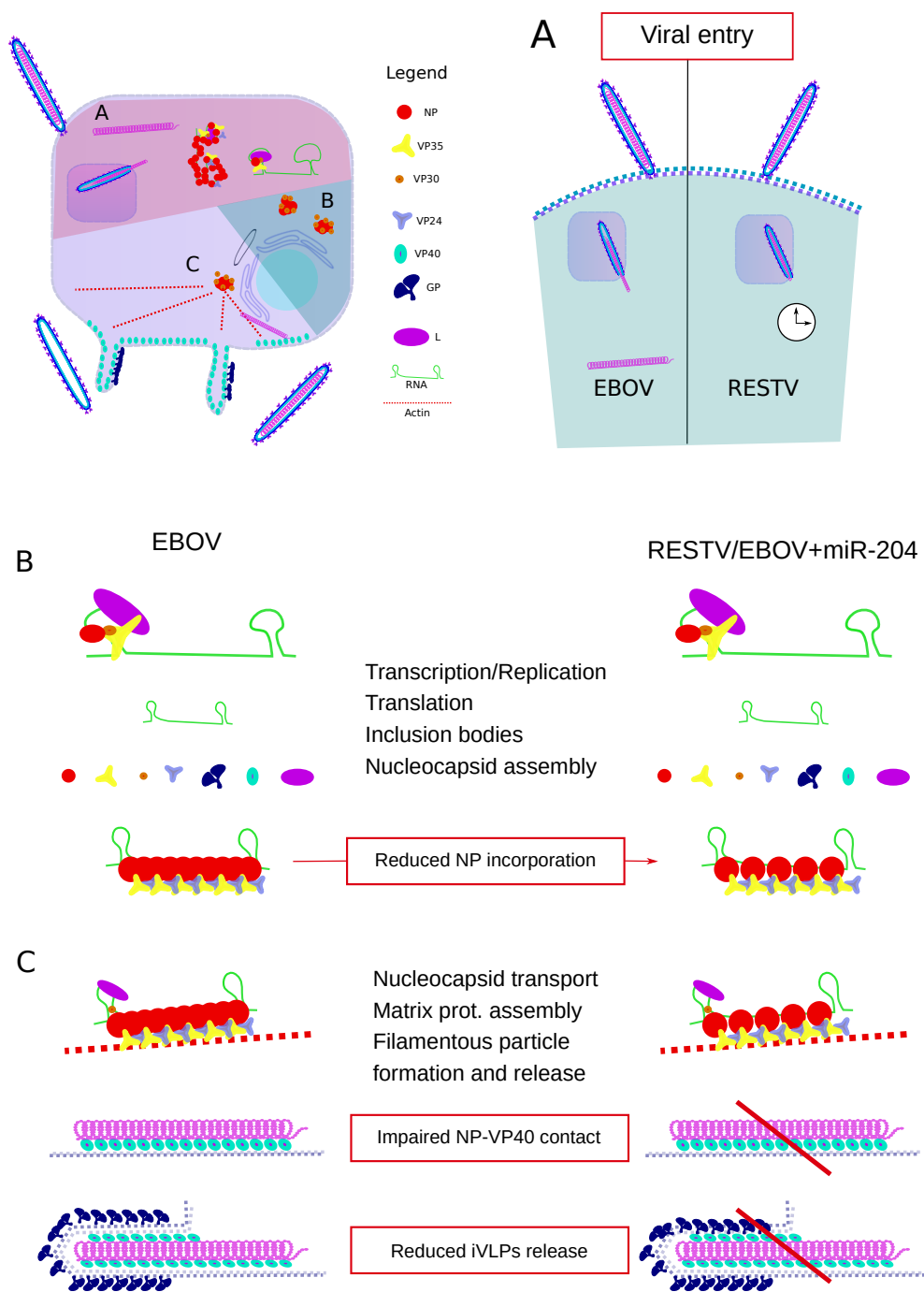


Figure 4.24: RESTV and EBOV observed summarized life cycle. (A) Entry from first contact to cytosol genome release is slower in RESTV than in EBOV (B) Transcription, replication and translation with protein modifications, shows NP fails to interact properly with components which reduces its incorporation in the NC (C) Viral particle assembly and release. The reduced NP amount seems to limit points of contact with VP40, impairing further the assembly of the particles and diminishing the effective iVLPs release.



## DISCUSSION

---

The aim of this study was to determine differences and similarities between RESTV and EBOV infection, cellular response and life cycle in order to pinpoint the traits which make these two viruses different for humans.

Based on the transcriptomic data of RESTV and EBOV infected cells, both viruses seem to differentiate the most at 3 h p.i. (see figs. 4.1 and 4.6). At this early time point, only a few events could have influenced the differential expression. Namely, these are the direct contact with the cell surface, macropinocytosis, endosomal to lysosomal passage [74] and release of viral content into the cytosol. Here it was observed that RESTV and EBOV differ in triggering entry related genes which would support the early contrast between RESTV and EBOV cellular response. In THP1 RESTV infected cells KLK8 was found up-regulated; KLK8 is a serine protease identified for the entry of papilloma virus [75]. It was also reported that serine proteases are needed for coronavirus's cellular entry, but cysteine proteases for EBOV entry [76]. KLK8 interacts with Rab-39A which among its functions are phagosome regulation and phagosome-lysosomes fusions [77, 78], supporting the hypothesis that RESTV might go into the cell with a mechanism other than EBOV, or that this gene is cell specific. In THP1 EBOV infected cells there were multiple up-regulated genes such as ZG16, ANKRD2 and SCN10A, which imply an EBOV effect after entry. ZG16 is proposed to form a glycosaminoglycan-binding site [79]. Filoviruses seem to require glycosaminoglycans for attachment to the target cell [80]. This suggests that the triggering of ZG16 promotes the re-infection of the cell favoring EBOV spreading. This indicates that EBOV increase dissemination could be determined after early infection, which was not observed in RESTV infected cells. ANKRD2 does not have a determined function. However, ANKRD2 is a paralogue of ANKRD1 which was found to be up-regulated in HCV and which modulates the viral entry [81]. This would indicate ANKRD2 could be also related to EBOV entry. SCN10A is a voltage-gated sodium channel subunit. Voltage channels have been reported as necessary for the entry of EBOV, but mainly TPC1 two pore channels which are also voltage-gated sodium channels [82]. It is possible that in THP1 cells SCN10A becomes active and



promotes viral entry. In HuH7 cells half of the significantly differentially expressed genes show that RESTV and EBOV differ at 3 h p.i. (see fig. 4.6). One of these genes is the potassium channel KCNQ5 which is up-regulated in RESTV infected cells. EBOV has been shown to depend on ion channels for its entry, whereas Bunyavirus, another negative-sense single-stranded RNA virus, is explicitly reported to need potassium channels for the entry of the virus [83]. As in THP1 cells, RESTV seems to promote another set of genes than EBOV for cellular entry. These results support the fact that RESTV triggers a different entry mechanism than EBOV, which disfavors RESTV further cellular transmission and gives a disadvantage against the cell. It seems the effect is not cell dependent, and the entry process could affect the viral cycle downstream, like dissemination.

To explore further the first stage of infection, an entry assay performed here, showed that RESTV-like particles take longer than EBOV to release their content into the cytosol (see fig. 4.16). This difference was determined by GP. These results are in accordance with previous reports which show RESTV GP cleavage is deficient [84, 85], and GP cleavage is determinant for the release of viral content into the cytosol [86, 87]. Furthermore, the results imply that the cell has more time to react to RESTV infection compared to EBOV, backing the observed different cellular response. Moreover, the assay was performed in HEK293 cells, which are known to be less prone to infection than THP1 and HuH7 cell lines. Therefore, in THP1 and HuH7 cell lines the entry or infection is expected to be faster with similar results. However, GP was shown to not be the only determinant factor for the different outcome of RESTV and EBOV infection [31]. Therefore it was necessary to explore the next steps of the viral life cycle and other viral components, to understand the whole context.

SnoRNAs play an important role in the cellular transcription and translation machinery [41–43]. It is not known if EBOV transcription and/or replication might start at 3 h p.i., but after this time point snoRNAs' expression differed in EBOV treated cells (see fig. 4.3). An up-regulation of snoRNAs suggests that EBOV promotes an rRNA and mRNA cellular regulation after early infection, indicating that EBOV activates transcription/replication already after 3 h p.i. (or even earlier). This finding correlates with the small RNA-Seq results, where there is a higher increase of viral signal from 3 h p.i. to 24 h p.i. in EBOV infected cells compared to RESTV infection (see Tab. 4.1). There are three possible explanations for the increased number of transcribed reads of EBOV and not RESTV: firstly, the cell is able to respond



to RESTV and stop it; secondly, the viral proteins are not properly recognized and therefore modified to fulfill their function, which could include the triggering of the snoRNA ; thirdly, EBOV's demand on the cell makes it necessary to regulate the snoRNAs for improving general transcription and replication from the cell itself. However, it is not possible to say if the snoRNAs triggered are required by EBOV, as in Vaccinia virus [48]. Nevertheless, these results suggest snoRNAs as target molecules for controlling EBOV replication.

In the scope of this thesis it was observed that NP, VP35 and L viral components differ between RESTV and EBOV, because there is a reduced reporter activity if these components are exchanged between both viruses systems (see fig. 4.9 ). An incompatibility of RESTV NP with VP35 affects other viral processes, including the NC transport, which could also directly affect the incorporation of NC in the viral particles. Previously, bioinformatic analysis showed aa comparison between EBOV and RESTV which would confer different protein interactions. NP residues Y21 and H22 and positions 375-381 form the NP oligomers which will compact the viral RNA into the NC, killing transcription/replication [20, 21]. This region does not differ between RESTV and EBOV (see table. 4.5), indicating that the reduced transcription/replication with RESTV NP in EBOV context is not due to RESTV NP oligomerization. Further, there are two interactions between VP35 and NP, the first one necessary for transcription/replication and the second one for the NC movement. VP35 residues 240-252 are part of the NC assembly (disrupt transcription/replication) [20]. VP35 residues 1-80 (sputnik region) bind to NP [21], are conserved among ebolaviruses and are necessary for transcription/replication but not for IFN inhibition [88]. Specifically, VP35 residues 20-52 are closely related to transcription/replication with two interacting regions with NP [20]. A previous comparison between EBOV and RESTV proteins showed different residues in the NP-VP35 binding site in RESTV [89], but was not evaluated if the substitutions were compensatory. Based on the comparison performed here of all ebolaviruses against RESTV, there are three residues differing in the sputnik region. On the other hand, based on the minigenome assay and NC movement (see figs. 4.9, 4.8 and 4.14) RESTV NP and RESTV VP35 interact and have efficient transcription/replication activity. This suggests that VP35 and NP residues reported aa substitutions might be compensatory and not directly related to the viral outcome. Although, the residue modification is an indication that indeed RESTV NP and EBOV VP35 have a reduced contact impairing proper assembly or interaction of both particles, it is not known if there are more interactions related

to other viral functions, but in this study RESTV components are able of transcription/replication in human cells. EBOV and RESTV differ in several positions along the whole polymerase L. Here it was observed that RESTV VP35 does function properly with EBOV L and RESTV L, but RESTV L does not seem to interact properly with EBOV VP35. Furthermore, it was reported that the highest residue exchange in L was shared between all ebolaviruses and not RESTV. Exchange from Alanines (A) to Serines (S) and vice versa are found mostly between residues 853 and 1585 of L (see table 4.6 ). This is an interesting aa change, because S allows protein modifications, while A does not. An important region for EBOV L is in the N-terminus (aa 280-370), as it interacts directly with VP35 and its recruited to NP inclusions [70]. In this study it was found RESTV differs from all Ebolaviruses in 7 positions between 280-370 L residues. These residue changes suggest either a reduced post-translational modification in this area due to the nature of the aa exchanged, or to an impaired interaction between L and VP35 of RESTV. Based on these results it is difficult to say that RESTV VP35 has compensatory modifications for RESTV L binding, because it would be expected to reduce its interaction with EBOV L, which was not observed. Therefore, it is more likely that either RESTV L has different modifications which translate into another kind of interaction with VP35, or the whole complex which involves NP-VP35-L for transcription/replication is the one compensated and the function sustained in RESTV. Altogether, it seems that the observed increase of transcription/replication of EBOV in the sequencing data is due to both a cellular factor and protein modifications/interactions.

EBOV Mayinga and EBOV Makona differ in the ratio of several of their proteins (see fig. 4.3). Both EBOV strains differ also in pathogenicity, as Makona is slightly less pathogenic than Mayinga [69]. However, the strain of EBOV Mayinga studied here also has varied its protein ratio compared to the first report from the virus. The first report where EBOV protein properties, such as size, were studied showed the amount of protein inside a filamentous particle to be 2% L, 4.7% GP, 17% NP, 37.7% VP40, 24.5% VP35, 6.6% VP30 and 7.5% VP24 [10]. The ratios based on VP24 have changed. Interestingly the original values are similar to Makona's current ratios, indicating that VP24 reduction might be an effect of the laboratory conditions or cellular effect, but not necessarily of pathogenicity. This could be due to viral passage or adaptation to laboratory conditions. It was also observed that there was a reduced amount of EBOV Mayinga NP in the supernatant compared to the first EBOV report, but after this reduction there was a relatively similar amount to that in EBOV Makona. Furthermore, it was interesting

to observe that NP/VP40 ratio is the most similar between both strains of EBOV and differs the most with RESTV, where the main difference of both species is the human pathogenicity. NP/VP40 ratio in the supernatant is an indicator of complete viral particles. The reduced NP/VP40 ratio observed in RESTV would suggest the release of more empty particles, which would lead to a lower infection rate than EBOV (also observed in this study) and which would be explained by the reduced NP incorporation in the iVLPs. A previous report shows little difference regarding the filamentous particle formation between EBOV and RESTV (based on electron microscope imaging). The filamentous particles of RESTV were smaller in every cell line tested. This could be because of some of their observations of missing tips of NC in the newly formed filamentous particles of RESTV [9]. Although, in Geisbert et.al's study there was no measurement of the percentage of damaged particles lacking NC tips, the observations in this thesis support RESTV might have them. These results support the fact that RESTV reduced pathogenicity could be directly related to NP incorporation in the filamentous particles. This effect seems to be directly related to RESTV NP, but as discussed above not to its transcription/replication role, or its NC transport role. Moreover, for a proper iVLP formation and function the NC needs to be incorporated into the filamentous particles, and VP40 is the viral protein which mediates this step with the NC protein VP35 [90].

EBOV NP C-terminus positions 439-492 aa and 589-739 aa are necessary for the NC assembly into the filamentous particles, and are particularly distinguished by their acidic character and increased charge, which is disordered [91]. While comparing NP residues 439-492 aa and 589-739 aa between RESTV and EBOV it was observed that RESTV has a lower charge than EBOV. This can explain NP's different SDS gel migration and RESTV NP band below EBOV's NP band, and suggests RESTV NP has less affinity, in cellular conditions, with other proteins or NC assembly into the filamentous particles. Therefore the RESTV property of forming more empty viral particles could be directly related to the intrinsic sequence of RESTV NP. However, VP40 is another major protein involved in the particle formation and efficient NC incorporation into the filamentous particles. Previous reports show VP40 (EBOVpositionRESTV) Q245P breaks an alpha helix, P85T located in the octamer interface [89]. This is interesting, because here it was found that RESTV VP40 can efficiently form iVLPs, but does not reduce transcription/replication, and could even increase iVLP efficient transcription/replication in infected cells (data not shown) without affecting the infection rate. VP40 octamer binds RNA and the most important residues are

F125 and R134 [92], but it is not known which kind of RNA binds. Based on EBOV and RESTV differences on VP40, it is possible that the P85T which would decrease post-translation modification, or that I122V, due to its closeness to F125 residue, reduces RESTV VP40 interaction with RNA, decreasing the negative effect on transcription/replication, but also shortens a point of contact with the NC. This also suggests that VP40 is binding viral RNA, specifically the hairpins of the virus genome, because in this study only the Leader and Trailer (3' and 5') sequences of the virus were used in the minigenome assay. Moreover, EBOV NP N- (aa 2-150) and C-termini (aa 601-739) interact with VP40, but only the C-terminus was shown to be necessary for transport and VLP incorporation, while the N-terminus is much more conserved among Mononegavirales [93]. In this study the aa difference of RESTV NP against all other Ebolavirus species was investigated. It was observed that RESTV NP differs from EBOV NP in two residues in this region, T607P and N729G. NP positions 607 and 729 could be then interaction residues to VP40 which reduced the NC incorporation to the filamentous particles. It is not possible to say if it is because the residue is not properly modified for VP40 interaction, or if it is another kind of interaction. These results reinforce the observation that RESTV NP and VP40 proteins do have different modifications inside human cells which could reduce the efficient viral particle formation in this host. Advocating that RESTV NP is not recognized properly in human cells, and therefore any required modification needed for NP's several functions is impaired. These results have to be further explored to understand the real implication of the above mentioned modifications, which with the current data are promising target viral proteins against EBOV.

It was possible to narrow down the viral proteins which seem to determine the pathogenicity of EBOV and RESTV. Yet it was also elucidated that cellular factors do play a role in the difference between the two viruses. Based on the sequencing data, RESTV infected cells have an up-regulation of miR-204 miRNA since 3 h.p.i. (see fig. 4.4). This suggests that the effect of this miRNA could affect further steps in the viral life cycle, and not necessarily the entry. miR-204 was already proposed to decrease the fitness (transcription and replication and release) of Hepatitis B virus (HBV). However the mechanism is still not understood [73]. Therefore it was interesting to test the effect of this miRNA in EBOV life cycle. Here, it was observed that miR-204 over-expression in the cells reduced EBOV transcription/replication (see fig. 4.19) and also reduced NP incorporation into the filamentous particles significantly in the minigenome and iVLP system (see fig. 4.20), as it was

observed for HBV [73]. Cells infected with EBOV also showed a reduced NP in supernatant when treated with foreign miR-204, but there were un-specific effects from the negative control which made the interpretation of the outcome difficult, as discussed below. A more detailed look at the cells showed miR-204 disrupts NP inclusion bodies in EBOV infected cells and in the iVLP system (see fig. 4.21 and 4.23). The observed dispersal of EBOV NP in the cell would explain the reduced transcription/replication in the iVLP system, a disruption of NC assembly which would lead to a reduced NP release in the filamentous particles. All of these effects were observed when miR-204 was present. These results suggests that miR-204 affects NP protein interactions, and hinting to miR-204 being one of the cellular components which diminishes RESTV propagation in human cells. It is not possible to say how miR-204 is working, but the up-regulation of this miRNA has been observed accompanied with the inhibition of IL6R, blocking the recognition of Il6, and then also blocking phosphorylation of STAT3 (pSTAT3) [94]. Moreover, EBOV is able to activate IL6 in human macrophages but not RESTV [30]. Although there was not a study of the sRNA population it is possible to speculate there was an up-regulation of miR-204 in RESTV infected cells. MARV also seems to inhibit IL6 and STAT3 phosphorylation via VP40 [33]. It has not been explored if RESTV VP40 causes the same effect, but it is possible to suggest VP40 could be the protein activating miR-204 upon entry. This could be supported by the host gene of miR-204, the Transient Receptor Potential Cation Channel Subfamily M Member 3 (TRPM3), which shares with miR-204 the promotor. TRPM3 is a membrane protein which controls the Ca (2+) and Zn (2+) flux and can be regulated by miR-204 [95]. EBOV VP40 was suggested to need the activation of Ca<sup>+</sup> exchange for binding to the membrane and egressing the cell [96]. If miR-204 reduces the Ca<sup>+</sup> flux via TRPM3, it would cause a reduced release of viral particles, but not necessarily of less NC incorporation. Then another target of miR-204 should be involved in the NC incorporation into the iVLPs and the formation of NP inclusion bodies. There are more proposed targets for miR-204 which could be involved in different cellular processes, therefore affecting more than one component of the virus life cycle. For example, the adaptor-related protein complex 1 sigma 3 subunit (AP1S3) gene is targeted by miR-204 [97]. AP1S3 is part of the clathrin-associated adaptor protein complex 1, which mediates vesicular protein trafficking from the Golgi and endosomes [78], and AP1S3 seems to be involved in HCV cycle, protecting the virus from

ubiquitin-degradation pathway [98]. Therefore this miRNA should be further explored to determine the link to ebolavirus NP, because this could be used as a target molecule for ebolavirus treatment.

Currently, this is the first study attempting to compare RESTV and EBOV human cellular response in the ncRNA context and at such an early time point after infection. Although HuH7 is broadly used for EBOV study, it is necessary to extend the number of cell lines for further validating the differences observed between RESTV and EBOV. THP1 cells are not standardized for EBOV study, and it was not possible to establish a protocol for transfecting them. Thus it was not feasible to validate the results on them. In summary, it is possible to state that RESTV and EBOV differ in the entry to the target cell causing a different cellular response which affects further steps in the viral life cycle. Cellular factors combined with viral NP and VP40 properties can determine the main difference between RESTV and EBOV. NcRNAs are part of the differences of the cell response against both viruses, and are possible targets for controlling EBOV infection. However, more studies are needed to understand the implications of the snoRNAs and the specific effect on EBOV life cycle. It seems miR-204 impairs viral molecule modifications/interactions which affect NP, the major player in the viral life cycle. It is possible that the mechanism of miR-204 could be used for EVD treatment. Nonetheless, miR-204 has to be explored further to confirm the observations here stated, specifically with an inhibitory molecule like Antagomirs to confirm the effects and another negative control in the viral infections. In addition, targeting specifically and directly the TSS of VP24, as presumed with miR-NC, was observed to reduce viral fitness. This could be used as another tool to target the virus, but due to the unexpected behavior it was not deeply investigated in this thesis.

## CONCLUSION

---

In the present study, it was possible to determine there is a clear difference between RESTV and EBOV cellular response since 3 h.p.i.: There are entry related genes and different ncRNAs which support this statement. The observed DEG in cells infected with RESTV and EBOV suggest a different entry mechanism for RESTV and that EBOV is even stimulating further infections since the first hours after infection. Also, RESTV is slower for going into the cell, and triggers a cascade which would negatively control the viral transcription, replication and release. In contrast EBOV seems faster in every infection step and snoRNAs could be the molecules facilitating the transcription/replication of EBOV. Where RESTV NP seems to make most of the difference between RESTV and EBOV performance inside the cell.

Also, RESTV seems to trigger the expression of miR-204, which when expressed in EBOV "context" could compromise its fitness as observed "naturally" for RESTV. Here are proposed snoRNAs, and miR-204 as potential targets against EBOV fast transcription/replication and viral particle assembly control, respectively.





SUPPLEMENTARY DATA

---

## 7.1 Cellular response

HuH7 and THP1 top differentially expressed genes are:

Top 80 genes differentially expressed in THP1 cells

Top 80 differentially expressed genes in HuH7

## 7.2 Minigenome

EBOV MG with RESTV components

RESTV MG with EBOV components

RESTV transcription/replication with inhibitors

## 7.3 iVLP

## 7.4 miR-204

Table 7.1: Top 80 commonly differentially expressed genes in HuH7 and THP1 cells genomic location

GeneName	Chr	Start	End	Strand
rmsk_repeat_Simple_repeat(TA)n	1	80958369	80958468	+
02374_SL0000012417_snRNA	1	80958425	80958441	+
02391_SL0000003563_snRNA	1	81773955	81773972	-
31638_SL0000013926_miRNA	2	77599518	77599534	+
39294_SL0000005263_snRNA	3	10702593	10702610	-
42724_SL0000014864_snRNA	3	180933308	180933325	+
LTR_Subtype=LTR:ERV1-MaLR:MSTA	4	28396142	28396553	+
43893_SL0000015010_miRNA	4	28396230	28396252	+
46230_SL0000006196_snRNA	4	160041045	160041060	-
46617_SL0000015089_scRNA	4	182156093	182156111	+
47116_SL0000015147_snRNA	5	11306916	11306933	+
47257_SL0000015405_snRNA	5	18148842	18148859	+
47835_SL0000015520_snRNA	5	52709260	52709276	+
48586_SL0000015613_snRNA	5	92447078	92447095	+
transposon_Subtype=LINE:L1:L1M2	5	97240361	97241284	+
48688_SL0000015631_snoRNA_CD	5	97240940	97240959	+
rmsk_repeat_Subtype=DNA:TcMar-Tigger:Tigger1	5	105395784	105396466	-
48821_SL0000006545_snoRNA_CD	5	105395871	105395889	-
49429_SL0000015733_snRNA	5	135945446	135945464	+
49430_SL0000006627_snRNA	5	135945446	135945465	-
52869_SL0000016281_snoRNA_CD	6	102969995	102970013	+
transposon_Subtype=SINE:Alu:AluJb	7	1464598	1464771	-
55273_SL0000016315_scRNA	7	36890207	36890225	+
56828_SL0000016533_scRNA	7	113617221	113617237	+
59768_SL0000008042_snRNA	8	89972584	89972601	-
60528_SL0000017015_scRNA	8	128594872	128594888	+
transposon_Subtype=SINE:Alu:AluJo	8	128594874	128595150	+
transposon_Subtype=SINE:MIR:MIR3	9	19465880	19466088	-
ncRNA_exon_Parent=uc010msx.3	9	102668915	102668988	+
ncRNA_exon_Parent=uc010msx.3	9	102677460	102677644	+
ncRNA_exon_Parent=uc011lvd.2	9	102677460	102677644	+
ncRNA_exon_Parent=uc010msx.3	9	102678331	102678450	+
ncRNA_exon_Parent=uc010msx.3	9	102691060	102691125	+
ncRNA_exon_Parent=uc011lvd.2	9	102691060	102691125	+
ncRNA_exon_Parent=uc010msx.3	9	102713342	102713567	+
ncRNA_exon_Parent=uc011lvd.2	9	102713342	102713567	+
ncRNA_exon_Parent=uc010msx.3	9	102722387	102722437	+
ncRNA_exon_Parent=uc011lvd.2	9	102722387	102722437	+
62787_SL0000017587_snRNA	9	102722400	102722419	+
62788_SL0000008314_snRNA	9	102722400	102722419	-
ncRNA_exon_Parent=uc010msx.3	9	102729935	102730021	+
ncRNA_exon_Parent=uc011lvd.2	9	102729935	102730021	+
ncRNA_exon_Parent=uc010msx.3	9	102730716	102736818	+
ncRNA_exon_Parent=uc011lvd.2	9	102730716	102736818	+
62845_SL0000017304_snRNA	9	105711885	105711901	+
transposon_Subtype=SINE:Alu:AluSc	10	85039242	85039540	+
08032_SL0000000226_snRNA	10	85039351	85039368	-
08033_SL0000009247_snRNA	10	85039351	85039368	+
10984_SL0000000641_miRNA	11	71938750	71938766	-
11640_SL0000009790_miRNA	11	105441935	105441952	+
11798_SL0000000749_scRNA	11	112614773	112614788	-
12320_SL0000009881_snRNA	11	131999198	131999215	+
14338_SL000001062_scRNA	12	95560323	95560338	-
16106_SL0000010342_miRNA	13	53870398	53870420	+
16974_SL0000001392_snRNA	13	104381441	104381458	-
22155_SL0000002069_snRNA	16	22801178	22801195	-
29301_SL0000012134_snRNA	19	45133077	45133094	+
transposon_Subtype=LINE:L2:L2b	20	45834165	45834427	+
36733_SL0000004248_snRNA	20	61248236	61248253	-
37284_SL0000013491_miRNA	21	22247839	22247861	+
rmsk_repeat_ISimple_repeat(CG)n	21	40032708	40032861	+
37659_SL0000013547_snRNA	21	40032853	40032871	+

Table 7.2: Top 80 differentially expressed genes in THP1 cells genomic location

GeneName	Chr	Start	End	Strand
rmsk_repeat_Simple_repeat(TA)n	1	80958369	80958468	+
02374_SL0000012417_snRNA	1	80958425	80958441	+
02391_SL0000003563_snRNA	1	81773955	81773972	-
31638_SL0000013926_miRNA	2	77599518	77599534	+
39294_SL0000005263_snRNA	3	10702593	10702610	-
42724_SL0000014864_snRNA	3	180933308	180933325	+
LTR_Subtype=LTR:ERV1-MaLR:MSTA	4	28396142	28396553	+
43893_SL0000015010_miRNA	4	28396230	28396252	+
46230_SL0000006196_snRNA	4	160041045	160041060	-
46617_SL0000015089_scRNA	4	182156093	182156111	+
47116_SL0000015147_snRNA	5	11306916	11306933	+
47257_SL0000015405_snRNA	5	18148842	18148859	+
47835_SL0000015520_snRNA	5	52709260	52709276	+
48586_SL0000015613_snRNA	5	92447078	92447095	+
transposon_Subtype=LINE:L1:L1M2	5	97240361	97241284	+
48688_SL0000015631_snoRNA_CD	5	97240940	97240959	+
rmsk_repeat_Subtype=DNA:TcMar-Tigger:Tigger1	5	105395784	105396466	-
48821_SL0000006545_snoRNA_CD	5	105395871	105395889	-
49429_SL0000015733_snRNA	5	135945446	135945464	+
49430_SL0000006627_snRNA	5	135945446	135945465	-
52869_SL0000016281_snoRNA_CD	6	102969995	102970013	+
transposon_Subtype=SINE:Alu:AluJb	7	1464598	1464771	-
55273_SL0000016315_scRNA	7	36890207	36890225	+
56828_SL0000016533_scRNA	7	113617221	113617237	+
59768_SL0000008042_snRNA	8	89972584	89972601	-
60528_SL0000017015_scRNA	8	128594872	128594888	+
transposon_Subtype=SINE:Alu:AluJo	8	128594874	128595150	+
transposon_Subtype=SINE:MIR:MIR3	9	19465880	19466088	-
ncRNA_exon_Parent=uc010msx.3	9	102668915	102668988	+
ncRNA_exon_Parent=uc010msx.3	9	102677460	102677644	+
ncRNA_exon_Parent=uc011lvd.2	9	102677460	102677644	+
ncRNA_exon_Parent=uc010msx.3	9	102678331	102678450	+
ncRNA_exon_Parent=uc010msx.3	9	102691060	102691125	+
ncRNA_exon_Parent=uc011lvd.2	9	102691060	102691125	+
ncRNA_exon_Parent=uc010msx.3	9	102713342	102713567	+
ncRNA_exon_Parent=uc011lvd.2	9	102713342	102713567	+
ncRNA_exon_Parent=uc010msx.3	9	102722387	102722437	+
ncRNA_exon_Parent=uc011lvd.2	9	102722387	102722437	+
62787_SL0000017587_snRNA	9	102722400	102722419	+
62788_SL0000008314_snRNA	9	102722400	102722419	-
ncRNA_exon_Parent=uc010msx.3	9	102729935	102730021	+
ncRNA_exon_Parent=uc011lvd.2	9	102729935	102730021	+
ncRNA_exon_Parent=uc010msx.3	9	102730716	102736818	+
ncRNA_exon_Parent=uc011lvd.2	9	102730716	102736818	+
62845_SL0000017304_snRNA	9	105711885	105711901	+
transposon_Subtype=SINE:Alu:AluSc	10	85039242	85039540	+
08032_SL0000000226_snRNA	10	85039351	85039368	-
08033_SL0000009247_snRNA	10	85039351	85039368	+
10984_SL0000000641_miRNA	11	71938750	71938766	-
11640_SL0000009790_miRNA	11	105441935	105441952	+
11798_SL0000000749_scRNA	11	112614773	112614788	-
12320_SL0000009881_snRNA	11	131999198	131999215	+
14338_SL0000001062_scRNA	12	95560323	95560338	-
16106_SL0000010342_miRNA	13	53870398	53870420	+
16974_SL0000001392_snRNA	13	104381441	104381458	-
22155_SL0000002069_snRNA	16	22801178	22801195	-
29301_SL0000012134_snRNA	19	45133077	45133094	+
transposon_Subtype=LINE:L2:L2b	20	45834165	45834427	+
36733_SL0000004248_snRNA	20	61248236	61248253	-
37284_SL0000013491_miRNA	21	22247839	22247861	+
rmsk_repeat_Simple_repeat(CG)n	21	40032708	40032861	+
37659_SL0000013547_snRNA	21	40032853	40032871	+

Table 7.3: Top 80 differentially expressed genes in HuH7 cells genomic location

GeneName	Chr	Start	End	Strand
rmsk_repeat_Simple_repeat:(TA)n	1	80958369	80958468	+
02374_SL0000012417_snRNA	1	80958425	80958441	+
02391_SL0000003563_snRNA	1	81773955	81773972	-
31638_SL0000013926_miRNA	2	77599518	77599534	+
39294_SL0000005263_snRNA	3	10702593	10702610	-
42724_SL0000014864_snRNA	3	180933308	180933325	+
LTR_Subtype=LTR:ERV1-MaLR:MSTA	4	28396142	28396553	+
43893_SL0000015010_miRNA	4	28396230	28396252	+
46230_SL0000006196_snRNA	4	160041045	160041060	-
46617_SL0000015089_scRNA	4	182156093	182156111	+
47116_SL0000015147_snRNA	5	11306916	11306933	+
47257_SL0000015405_snRNA	5	18148842	18148859	+
47835_SL0000015520_snRNA	5	52709260	52709276	+
48586_SL0000015613_snRNA	5	92447078	92447095	+
transposon_Subtype=LINE:L1:L1M2	5	97240361	97241284	+
48688_SL0000015631_snoRNA_CD	5	97240940	97240959	+
rmsk_repeat_Subtype=DNA:TcMar-Tigger:Tigger1	5	105395784	105396466	-
48821_SL0000006545_snoRNA_CD	5	105395871	105395889	-
49429_SL0000015733_snRNA	5	135945446	135945464	+
49430_SL0000006627_snRNA	5	135945446	135945465	-
52869_SL0000016281_snoRNA_CD	6	102969995	102970013	+
transposon_Subtype=SINE:Alu:AluJb	7	1464598	1464771	-
55273_SL0000016315_scRNA	7	36890207	36890225	+
56828_SL0000016533_scRNA	7	113617221	113617237	+
59768_SL0000008042_snRNA	8	89972584	89972601	-
60528_SL0000017015_scRNA	8	128594872	128594888	+
transposon_Subtype=SINE:Alu:AluJo	8	128594874	128595150	+
transposon_Subtype=SINE:MIR:MIR3	9	19465880	19466088	-
ncRNA_exon_Parent=uc010msx.3	9	102668915	102668988	+
ncRNA_exon_Parent=uc010msx.3	9	102677460	102677644	+
ncRNA_exon_Parent=uc011lvd.2	9	102677460	102677644	+
ncRNA_exon_Parent=uc010msx.3	9	102678331	102678450	+
ncRNA_exon_Parent=uc010msx.3	9	102691060	102691125	+
ncRNA_exon_Parent=uc011lvd.2	9	102691060	102691125	+
ncRNA_exon_Parent=uc010msx.3	9	102713342	102713567	+
ncRNA_exon_Parent=uc011lvd.2	9	102713342	102713567	+
ncRNA_exon_Parent=uc010msx.3	9	102722387	102722437	+
ncRNA_exon_Parent=uc011lvd.2	9	102722387	102722437	+
62787_SL0000017587_snRNA	9	102722400	102722419	+
62788_SL0000008314_snRNA	9	102722400	102722419	-
ncRNA_exon_Parent=uc010msx.3	9	102729935	102730021	+
ncRNA_exon_Parent=uc011lvd.2	9	102729935	102730021	+
ncRNA_exon_Parent=uc010msx.3	9	102730716	102736818	+
ncRNA_exon_Parent=uc011lvd.2	9	102730716	102736818	+
62845_SL0000017304_snRNA	9	105711885	105711901	+
transposon_Subtype=SINE:Alu:AluSc	10	85039242	85039540	+
08032_SL0000000226_snRNA	10	85039351	85039368	-
08033_SL0000009247_snRNA	10	85039351	85039368	+
10984_SL0000000641_miRNA	11	71938750	71938766	-
11640_SL0000009790_miRNA	11	105441935	105441952	+
11798_SL0000000749_scRNA	11	112614773	112614788	-
12320_SL0000009881_snRNA	11	131999198	131999215	+
14338_SL000001062_scRNA	12	95560323	95560338	-
16106_SL0000010342_miRNA	13	53870398	53870420	+
16974_SL0000001392_snRNA	13	104381441	104381458	-
22155_SL0000002069_snRNA	16	22801178	22801195	-
29301_SL0000012134_snRNA	19	45133077	45133094	+
transposon_Subtype=LINE:L2:L2b	20	45834165	45834427	+
36733_SL0000004248_snRNA	20	61248236	61248253	-
37284_SL0000013491_miRNA	21	22247839	22247861	+
rmsk_repeat_Simple_repeat:(CG)n	21	40032708	40032861	+
37659_SL0000013547_snRNA	21	40032853	40032871	+

Table 7.4: RESTV MG reporter activity standardization

Concentration	Relative values of luciferase activity per replicate			
Standard	99.99	100.00	100.00	100.00
NP [100ng]	77.72	80.36	88.76	83.38
NP [250ng]	145.39	88.55	101.85	125.07
VP35 [70ng]	88.04	100.10	73.82	103.97
VP35 [250ng]	90.78	108.01	96.20	114.76
VP30 [70ng]	135.21	110.55	83.28	
VP30 [200ng]	92.56	68.71	67.81	
No L	0.10	0.37	3.03	

Table 7.5: Relative EBOV MG reporter activity in the combination of RESTV and EBOV components

Exchanged component	Relative luciferase per replicate		
no L	0.06	2.38	4.53
EBOV	100.00	100.00	100.01
RESTV_NP	0.24	5.58	2.55
RESTV_VP35	35.09	157.37	74.76
RESTV_VP30	27.79	75.96	160.69
RESTV_L	1.64	4.71	8.66
RESTV_NP,VP35	0.92	5.85	1.09
RESTV_NP,VP30	0.28	4.74	1.16
RESTV_NP,L	0.67	4.88	2.64
RESTV_VP35,VP30	33.35	14.47	89.23
RESTV_VP35,L	96.43	123.20	170.61
RESTV_VP30,L	1.62	5.92	56.34
RESTV_NP,VP30,VP35	0.83	4.56	7.66
RESTV_NP,VP35,L	8.96	15.60	141.05
RESTV_NP,VP30,L	0.28	3.53	10.76
RESTV_VP35,VP30,L	87.73	143.85	2370.73
RESTV_NP,VP35,VP30,L	11.79	39.32	549.89

Table 7.6: Relative RESTV MG reporter activity in the combination of RESTV and EBOV components

Exchanged component	Relative reporter activity per replicate		
no L	0.09	0.80	3.22
RESTV	100.00	100.00	100.01
EBOV_NP	148.77	255.77	975.76
EBOV_VP35	7.38	2.09	60.22
EBOV_VP30	372.39	113.10	520.46
EBOV_L	1.48	0.81	4.27
EBOV_NP,VP35	38.14	1.46	222.71
EBOV_NP,VP30	282.46	153.96	1545.88
EBOV_NP,L	37.86	25.03	117.29
EBOV_VP35,VP30	23.96	3.42	40.58
EBOV_VP35,L	0.61	0.77	2.79
EBOV_VP30,L	2.68	1.22	5.93
EBOV_NP,VP30,VP35	135.17	15.86	649.86
EBOV_NP,VP35,L	194.33	23.28	571.94
EBOV_NP,VP30,L	120.33	89.47	417.01
EBOV_VP35,VP30,L	0.47	0.77	4.93
EBOV_NP,VP35,VP30,L	304.91	100.46	532.38

Table 7.7: Relative EBOV MG reporter activity in the presence of viral inhibitors

Added component	Relative reporter activity per replicate		
EBOV MG	100.01	100	100
RESTV GP	94.57	237.13	209.17
RESTV VP24	0.73	7.97	2.66
RESTV VP40	44.33	122.82	38.91
EBOV GP	93.98	185.99	233.91
EBOV VP24	1.26	4.51	4.67
EBOV VP40	54.52	67.53	206.24
EBOV no L	0.04	0.69	0.17

Table 7.8: Relative RESTV MG reporter activity in the presence of viral inhibitors

Added component	Relative reporter activity per replicate		
RESTV	100	100	100.01
RESTV GP	159.79	196.33	151.73
RESTV VP24	1.46	2.64	2.61
RESTV VP40	48.48	199.61	63.80
EBOV GP	140.24	497.92	232.50
EBOV VP24	12.16	13.44	4.32
EBOV VP40	98.87	117.24	109.87
RESTV no L	0.10	0.72	0.14

Table 7.9: Relative MG reporter activity of EBOV and RESTV iVLPs after protein exchange

Exchanged component	Relative reporter activity per replicate		
EBOV	100	100	100
RESTV NP	0.33	4.46	5.30
RESTV VP40	85.10	138.61	93.70
RESTV VP24	5.98	86.00	62.30
RESTV GP	46.15	238.17	152.75
EBOV no L	1.67	2.67	1.44
RESTV	100.00	100.00	100.00
EBOV NP	86.09	74.18	79.95
EBOV VP40	35.69	155.30	165.17
EBOV VP24	180.02	189.77	102.70
EBOV GP	23.70	67.44	88.93
RESTV no L	0.11	0.19	0.36

Table 7.10: Relative reporter MG activity of RESTV and EBOV after AgoMiR treatments

	Added AgoMiR	Relative reporter activity per replicate			
RESTV MG	miR-204	0.77	0.92	2.88	8.60
	miR-10a	1.43	7.17	0.84	
	miR-10b	2.79	6.59	1.98	
	miR-NC	1.00	1.00	1.01	1.00
	no L	0.02	0.01	0.00	
EBOV MG	miR-204	0.83	0.29	0.30	0.90
	miR-10a	1.10	1.60	1.60	
	miR-10b	2.10	0.68	1.21	
	miR-NC	1.00	1.00	1.01	1.00
	no L	0.07	0.11	0.15	

Table 7.11: Effect of miR-204 on EBOV's protein amount inside the cells and filamentous particles measured by WB

Added component	Cellular quantification			Filamentous quantification	
	NP	VP40	Tubulin	NP	VP40
miR-204	1754896	46002	28842	1065614	18238
miR-NC	1939696	68728	61820	2157364	13244
Medium	3154184	566698	135806	4665958	371734
miR-204	1947114		272948	1493400	1138128
miR-NC	4159107		185463	2075616	829824
Medium	2201341		310496	2639160	1765152
miR-204	2940000	701250	1010252	4790520	4312252
miR-NC	1990000	2818842	1527821	6243375	3987975
Medium	1760000	2905176	1396721	3882552	2859912
miR-204	4756644	1016304	184250		
miR-NC	4384968	717678	170650		
Medium	5639193	507052	106750		



## BIBLIOGRAPHY

---

- [1] JG Breman, P Piot, KM Johnson, MK White, M Mbuyi, P Sureau, DL Heymann, S Van Nieuwenhove, JB McCormick, JP Ruppol, et al. “The epidemiology of Ebola hemorrhagic fever in Zaire, 1976”. In: *Ebola virus haemorrhagic fever* (1978), pp. 103–124.
- [2] Centers for disease control and prevention. *Years of ebola virus disease outbreaks*. 2018. URL: <https://www.cdc.gov/vhf/ebola/history/chronology.html> (visited on 11/09/2018).
- [3] Heinz Feldmann and Thomas W Geisbert. “Ebola haemorrhagic fever”. In: *The Lancet* 377.9768 (2011), pp. 849–862.
- [4] World Health Organization. *Ebola virus disease – Democratic Republic of the Congo*. 201. URL: <https://www.who.int/csr/don/14-february-2019-ebola-drc/en/> (visited on 02/14/2019).
- [5] Jean-Jacques Muyembe-Tamfum, S Mulangu, Justin Masumu, JM Kayembe, A Kemp, and Janusz T Paweska. “Ebola virus outbreaks in Africa: past and present”. In: *Onderstepoort Journal of Veterinary Research* 79.2 (2012), pp. 06–13.
- [6] Jens H Kuhn, Yímíng Bào, Sina Bavari, Stephan Becker, Steven Bradfute, Kristina Brauburger, J Rodney Brister, Alexander A Bukreyev, Yíngyún Cài, Kartik Chandran, et al. “Virus nomenclature below the species level: a standardized nomenclature for filovirus strains and variants rescued from cDNA”. In: *Archives of virology* 159.5 (2014), pp. 1229–1237.
- [7] Jens H Kuhn, Stephan Becker, Hideki Ebihara, Thomas W Geisbert, Karl M Johnson, Yoshihiro Kawaoka, W Ian Lipkin, Ana I Negredo, Sergey V Netesov, Stuart T Nichol, et al. “Proposal for a revised taxonomy of the family Filoviridae: classification, names of taxa and viruses, and virus abbreviations”. In: *Archives of virology* 155.12 (2010), pp. 2083–2103.
- [8] ME Miranda, TG Ksiazek, TJ Retuya, Ali S Khan, Anthony Sanchez, Charles F Fulhorst, Pierre E Rollin, AB Calaor, DL Manalo, MC Roces, et al. “Epidemiology of Ebola (subtype Reston) virus in the Philippines, 1996”. In: *The Journal of infectious diseases* 179.Supplement\_1 (1999), S115–S119.

- [9] TW Geisbert and PB Jahrling. "Differentiation of filoviruses by electron microscopy". In: *Virus research* 39.2-3 (1995), pp. 129–150.
- [10] Luanne H Elliott, Michael P Kiley, and Joseph B McCormick. "Descriptive analysis of Ebola virus proteins". In: *Virology* 147.1 (1985), pp. 169–176.
- [11] Ilhem Messaoudi, Gaya K Amarasinghe, and Christopher F Basler. "Filovirus pathogenesis and immune evasion: insights from Ebola virus and Marburg virus". In: *Nature Reviews Microbiology* 13.11 (2015), p. 663.
- [12] William Wan, Larissa Kolesnikova, Mairi Clarke, Alexander Koehler, Takeshi Noda, Stephan Becker, and John AG Briggs. "Structure and assembly of the Ebola virus nucleocapsid". In: *Nature* 551.7680 (2017), p. 394.
- [13] Diego Cantoni and Jeremy S Rossman. "Ebolaviruses: New roles for old proteins". In: *PLoS neglected tropical diseases* 12.5 (2018), e0006349.
- [14] Mike Bray and Thomas W Geisbert. "Ebola virus: the role of macrophages and dendritic cells in the pathogenesis of Ebola hemorrhagic fever". In: *The international journal of biochemistry & cell biology* 37.8 (2005), pp. 1560–1566.
- [15] Thomas W Geisbert, Lisa E Hensley, Tom Larsen, Howard A Young, Douglas S Reed, Joan B Geisbert, Dana P Scott, Elliott Kagan, Peter B Jahrling, and Kelly J Davis. "Pathogenesis of Ebola hemorrhagic fever in cynomolgus macaques: evidence that dendritic cells are early and sustained targets of infection". In: *The American journal of pathology* 163.6 (2003), pp. 2347–2370.
- [16] A Baskerville, SP Fisher-Hoch, GH Neild, and AB Dowsett. "Ultrastructural pathology of experimental Ebola haemorrhagic fever virus infection". In: *The Journal of pathology* 147.3 (1985), pp. 199–209.
- [17] Sven Moller-Tank and Wendy Maury. "Ebola virus entry: a curious and complex series of events". In: *PLoS pathogens* 11.4 (2015), e1004731.
- [18] Yohei Kurosaki, Mahoko Takahashi Ueda, Yusuke Nakano, Jiro Yasuda, Yoshio Koyanagi, Kei Sato, and So Nakagawa. "Different effects of two mutations on the infectivity of Ebola virus glycoprotein in nine mammalian species". In: *The Journal of general virology* 99.2 (2018), p. 181.
- [19] Elke Mühlberger. "Filovirus replication and transcription". In: (2007).

- [20] Daisy W Leung, Dominika Borek, Priya Luthra, Jennifer M Binning, Manu Anantpadma, Gai Liu, Ian B Harvey, Zhaoming Su, Ariel Endlich-Frazier, Juanli Pan, et al. "An intrinsically disordered peptide from Ebola virus VP35 controls viral RNA synthesis by modulating nucleoprotein-RNA interactions". In: *Cell reports* 11.3 (2015), pp. 376–389.
- [21] Robert N Kirchdoerfer, Dafna M Abelson, Sheng Li, Malcolm R Wood, and Erica Ollmann Saphire. "Assembly of the Ebola virus nucleoprotein from a chaperoned VP35 complex". In: *Cell reports* 12.1 (2015), pp. 140–149.
- [22] Yuki Takamatsu, Larissa Kolesnikova, and Stephan Becker. "Ebola virus proteins NP, VP35, and VP24 are essential and sufficient to mediate nucleocapsid transport". In: *Proceedings of the National Academy of Sciences* 115.5 (2018), pp. 1075–1080.
- [23] T Hoenen, N Biedenkopf, F Zielecki, S Jung, A Groseth, H Feldmann, and S Becker. "Oligomerization of Ebola virus VP40 is essential for particle morphogenesis and regulation of viral transcription". In: *Journal of virology* 84.14 (2010), pp. 7053–7063.
- [24] Rob WH Ruigrok, Guy Schoehn, Andréa Dessen, Eric Forest, Viktor Volchkov, Olga Dolnik, Hans-Dieter Klenk, and Winfried Weissenhorn. "Structural characterization and membrane binding properties of the matrix protein VP40 of Ebola virus". In: *Journal of molecular biology* 300.1 (2000), pp. 103–112.
- [25] Luke D Jasenosky, Gabriele Neumann, Igor Lukashevich, and Yoshihiro Kawaoka. "Ebola virus VP40-induced particle formation and association with the lipid bilayer". In: *Journal of virology* 75.11 (2001), pp. 5205–5214.
- [26] Qian Cong, Jimin Pei, and Nick V Grishin. "Predictive and comparative analysis of Ebolavirus proteins". In: *Cell Cycle* 14.17 (2015), pp. 2785–2797.
- [27] Daisy W Leung, Reed S Shabman, Mina Farahbakhsh, Kathleen C Prins, Dominika M Borek, Tianjiao Wang, Elke Mühlberger, Christopher F Basler, and Gaya K Amarasinghe. "Structural and functional characterization of Reston Ebola virus VP35 interferon inhibitory domain". In: *Journal of molecular biology* 399.3 (2010), pp. 347–357.

- [28] Daisy W Leung, Kathleen C Prins, Dominika M Borek, Mina Farahbakhsh, JoAnn M Tufariello, Parameshwaran Ramanan, Jay C Nix, Luke A Helgeson, Zbyszek Otwinowski, Richard B Honzatko, et al. "Structural basis for dsRNA recognition and interferon antagonism by Ebola VP35". In: *Nature structural & molecular biology* 17.2 (2010), pp. 165–172.
- [29] John C Kash, Elke Mühlberger, Victoria Carter, Melanie Grosch, Olivia Perwitasari, Sean C Proll, Matthew J Thomas, Friedemann Weber, Hans-Dieter Klenk, and Michael G Katze. "Global suppression of the host antiviral response by Ebola and Marburgviruses: increased antagonism of the type I interferon response is associated with enhanced virulence". In: *Journal of virology* 80.6 (2006), pp. 3009–3020.
- [30] Judith Olejnik, Adriana Forero, Laure R Deflubé, Adam J Hume, Whitney A Manhart, Andrew Nishida, Andrea Marzi, Michael G Katze, Hideki Ebihara, Angela L Rasmussen, et al. "Ebola viruses associated with differential pathogenicity induce distinct host responses in human macrophages". In: *Journal of virology* 91.11 (2017), e00179–17.
- [31] Allison Groseth, Andrea Marzi, Thomas Hoenen, Astrid Herwig, Don Gardner, Stephan Becker, Hideki Ebihara, and Heinz Feldmann. "The Ebola virus glycoprotein contributes to but is not sufficient for virulence in vivo". In: *PLoS pathogens* 8.8 (2012), e1002847.
- [32] Jessica R Spengler, Greg Saturday, Kerry J Lavender, Cynthia Martellaro, James G Keck, Stuart T Nichol, Christina F Spiropoulou, Heinz Feldmann, and Joseph Prescott. "Severity of Disease in Humanized Mice Infected with Ebola Virus or Reston Virus is Associated with Magnitude of Early Viral Replication in Liver". In: *The Journal of infectious diseases* 217.1 (2017), pp. 58–63.
- [33] Charalampos Valmas, Melanie N Grosch, Michael Schumann, Judith Olejnik, Osvaldo Martinez, Sonja M Best, Verena Kräling, Christopher F Basler, and Elke Mühlberger. "Marburg virus evades interferon responses by a mechanism distinct from ebola virus". In: *PLoS pathogens* 6.1 (2010), e1000721.
- [34] Thomas Hoenen, Allison Groseth, Fabian de Kok-Mercado, Jens H Kuhn, and Victoria Wahl-Jensen. "Minigenomes, transcription and replication competent virus-like particles and beyond: reverse genetics systems for filoviruses and other negative stranded hemorrhagic fever viruses". In: *Antiviral research* 91.2 (2011), pp. 195–208.

- [35] Allison Groseth, Heinz Feldmann, Steven Theriault, Gülsah Mehmetoglu, and Ramon Flick. “RNA polymerase I-driven minigenome system for Ebola viruses”. In: *Journal of virology* 79.7 (2005), pp. 4425–4433.
- [36] Martin Hölzer, Verena Krähling, Fabian Amman, Emanuel Barth, Stephan H Bernhart, Victor AO Carmelo, Maximilian Collatz, Gero Doose, Florian Eggenhofer, Jan Ewald, et al. “Differential transcriptional responses to Ebola and Marburg virus infection in bat and human cells”. In: *Scientific reports* 6 (2016), p. 34589.
- [37] Janice Duy, Jeffrey W Koehler, Anna N Honko, Randal J Schoepp, Nadia Wauquier, Jean-Paul Gonzalez, M Louise Pitt, Eric M Mucker, Joshua C Johnson, Aileen O’Hearn, et al. “Circulating microRNA profiles of Ebola virus infection”. In: *Scientific reports* 6 (2016), p. 24496.
- [38] Thomas R Cech and Joan A Steitz. “The noncoding RNA revolution—trashing old rules to forge new ones”. In: *Cell* 157.1 (2014), pp. 77–94.
- [39] Victor Ambros. “The functions of animal microRNAs”. In: *Nature* 431.7006 (2004), pp. 350–355.
- [40] Manel Esteller. “Non-coding RNAs in human disease”. In: *Nature Reviews Genetics* 12.12 (2011), pp. 861–874.
- [41] Gisela Storz, Shoshy Altuvia, and Karen M Wassarman. “An abundance of RNA regulators”. In: *Annu. Rev. Biochem.* 74 (2005), pp. 199–217.
- [42] Marina Falaleeva, Amadis Pages, Zaneta Matuszek, Sana Hidmi, Lily Agranat-Tamir, Konstantin Korotkov, Yuval Nevo, Eduardo Eyras, Ruth Sperling, and Stefan Stamm. “Dual function of C/D box small nucleolar RNAs in rRNA modification and alternative pre-mRNA splicing”. In: *Proceedings of the National Academy of Sciences* 113.12 (2016), E1625–E1634.
- [43] Marina Falaleeva, Justin R Welden, Marilyn J Duncan, and Stefan Stamm. “C/D-box snoRNAs form methylating and non-methylating ribonucleoprotein complexes: Old dogs show new tricks”. In: *Bioessays* 39.6 (2017).
- [44] Qisheng Li, Brianna Lowey, Catherine Sodroski, Siddharth Krishnamurthy, Hawwa Alao, Helen Cha, Stephan Chiu, Ramy El-Diwany, Marc G Ghany, and T Jake Liang. “Cellular microRNA networks regulate host dependency of hepatitis C virus infection”. In: *Nature communications* 8.1 (2017), p. 1789.

- [45] Iana H Haralambieva, Richard B Kennedy, Whitney L Simon, Krista M Goergen, Diane E Grill, Inna G Ovsyannikova, and Gregory A Poland. "Differential miRNA expression in B cells is associated with inter-individual differences in humoral immune response to measles vaccination". In: *PloS one* 13.1 (2018), e0191812.
- [46] Paul A Tambyah, Sugunavathi Sepramaniam, Jaminah Mohamed Ali, Siaw Ching Chai, Priyadharshini Swaminathan, Arunmozhiarasi Arumugam, and Kandiah Jeyaseelan. "microRNAs in circulation are altered in response to influenza A virus infection in humans". In: *PloS one* 8.10 (2013), e76811.
- [47] Michael Niepmann, Lyudmila A Shalamova, Gesche K Gerresheim, and Oliver Rossbach. "Signals Involved in Regulation of Hepatitis C Virus RNA Genome Translation and Replication". In: *Frontiers in microbiology* 9 (2018), p. 395.
- [48] Clement A Meseda, Kumar Srinivasan, Jasen Wise, Jennifer Catalano, Kenneth M Yamada, and Subhash Dhawan. "Non-coding RNAs and heme oxygenase-1 in vaccinia virus infection". In: *Biochemical and biophysical research communications* 454.1 (2014), pp. 84–88.
- [49] Alexander Koehler. "The species-specific effects of guinea pig-adaptive mutations in Marburg virus VP40 and L on the protein's functions and viral fitness". Institut für Virologie. PhD thesis. Philipps-Universität Marburg, Mar. 2017.
- [50] Eva Mittler, Larissa Kolesnikova, Bettina Hartlieb, Robert Davey, and Stephan Becker. "The cytoplasmic domain of Marburg virus GP modulates early steps of viral infection". In: *Journal of virology* 85.16 (2011), pp. 8188–8196.
- [51] Marcel Martin. "Cutadapt removes adapter sequences from high-throughput sequencing reads". In: *EMBnet. journal* 17.1 (2011), pp–10.
- [52] Robert Schmieder and Robert Edwards. "Quality control and pre-processing of metagenomic datasets". In: *Bioinformatics* 27.6 (2011), pp. 863–864.
- [53] Simon Andrews et al. "FastQC: a quality control tool for high throughput sequence data". In: (2010).
- [54] Cole Trapnell, Lior Pachter, and Steven L Salzberg. "TopHat: discovering splice junctions with RNA-Seq". In: *Bioinformatics* 25.9 (2009), pp. 1105–1111.

- [55] Pavankumar Videm, Dominic Rose, Fabrizio Costa, and Rolf Backofen. “BlockClust: efficient clustering and classification of non-coding RNAs from short read RNA-seq profiles”. In: *Bioinformatics* 30.12 (2014), pp. i274–i282.
- [56] Marc R Friedländer, Sebastian D Mackowiak, Na Li, Wei Chen, and Nikolaus Rajewsky. “miRDeep2 accurately identifies known and hundreds of novel microRNA genes in seven animal clades”. In: *Nucleic acids research* 40.1 (2011), pp. 37–52.
- [57] Yuk Yee Leung, Paul Ryvkin, Lyle H Ungar, Brian D Gregory, and Li-San Wang. “CoRAL: predicting non-coding RNAs from small RNA-sequencing data”. In: *Nucleic acids research* 41.14 (2013), e137–e137.
- [58] Sam Griffiths-Jones, Russell J Grocock, Stijn Van Dongen, Alex Bateman, and Anton J Enright. “miRBase: microRNA sequences, targets and gene nomenclature”. In: *Nucleic acids research* 34.suppl\_1 (2006), pp. D140–D144.
- [59] Yang Liao, Gordon K Smyth, and Wei Shi. “featureCounts: an efficient general purpose program for assigning sequence reads to genomic features”. In: *Bioinformatics* 30.7 (2013), pp. 923–930.
- [60] Michael I Love, Wolfgang Huber, and Simon Anders. “Moderated estimation of fold change and dispersion for RNA-seq data with DESeq2”. In: *Genome biology* 15.12 (2014), p. 550.
- [61] Ross Ihaka and Robert Gentleman. “R: a language for data analysis and graphics”. In: *Journal of computational and graphical statistics* 5.3 (1996), pp. 299–314.
- [62] Sebastian Will, Tejal Joshi, Ivo L Hofacker, Peter F Stadler, and Rolf Backofen. “LocARNA-P: accurate boundary prediction and improved detection of structural RNAs”. In: *Rna* 18.5 (2012), pp. 900–914.
- [63] Martin Hölzer and Manja Marz. “PoSeiDon: a web server for the detection of evolutionary recombination events and positive selection”. unpublished. N.D.
- [64] Stefan Rügger and Helge Großhans. “MicroRNA turnover: when, how, and why”. In: *Trends in biochemical sciences* 37.10 (2012), pp. 436–446.
- [65] James T Robinson, Helga Thorvaldsdóttir, Wendy Winckler, Mitchell Guttman, Eric S Lander, Gad Getz, and Jill P Mesirov. “Integrative genomics viewer”. In: *Nature biotechnology* 29.1 (2011), p. 24.

- [66] S Baize, EM Leroy, AJ Georges, M-C GEORGES-COURBOT, M Capron, I Bedjabaga, J Lansoud-Soukate, and E Mavoungou. "Inflammatory responses in Ebola virus-infected patients". In: *Clinical & Experimental Immunology* 128.1 (2002), pp. 163–168.
- [67] Serena A Carroll, Jonathan S Towner, Tara K Sealy, Laura K McMullan, Marina L Khristova, Felicity J Burt, Robert Swanepoel, Pierre E Rollin, and Stuart T Nichol. "Molecular evolution of viruses of the family Filoviridae based on 97 whole-genome sequences". In: *Journal of virology* 87.5 (2013), pp. 2608–2616.
- [68] Shinji Watanabe, Takeshi Noda, Peter Halfmann, Luke Jasenosky, and Yoshihiro Kawaoka. "Ebola virus (EBOV) VP24 inhibits transcription and replication of the EBOV genome". In: *The Journal of infectious diseases* 196.Supplement\_2 (2007), S284–S290.
- [69] Andrea Marzi, Spencer Chadinah, Elaine Haddock, Friederike Feldmann, Nicolette Arndt, Cynthia Martellaro, Dana P Scott, Patrick W Hanley, Tolbert G Nyenswah, Samba Sow, et al. "Recently identified mutations in the Ebola Virus-Makona genome do not alter pathogenicity in animal models". In: *Cell reports* 23.6 (2018), pp. 1806–1816.
- [70] Martina Trunschke, Dominik Conrad, Sven Enterlein, Judith Olejnik, Kristina Brauburger, and Elke Mühlberger. "The L–VP35 and L–L interaction domains reside in the amino terminus of the Ebola virus L protein and are potential targets for antivirals". In: *Virology* 441.2 (2013), pp. 135–145.
- [71] Sven Enterlein, Kristina M Schmidt, Michael Schümann, Dominik Conrad, Verena Krähling, Judith Olejnik, and Elke Mühlberger. "The marburg virus 3' noncoding region structurally and functionally differs from that of ebola virus". In: *Journal of virology* 83.9 (2009), pp. 4508–4519.
- [72] Yue Teng, Yuzhuo Wang, Xianglilan Zhang, Wenli Liu, Hang Fan, Hongwu Yao, Baihan Lin, Ping Zhu, Wenjun Yuan, Yigang Tong, et al. "Systematic genome-wide screening and prediction of microRNAs in EBOV during the 2014 ebolavirus outbreak". In: *Scientific reports* 5 (2015).
- [73] Jyun-Yuan Huang, Hung-Lin Chen, and Chiaho Shih. "MicroRNA miR-204 and miR-1236 inhibit hepatitis B virus replication via two different mechanisms". In: *Scientific reports* 6 (2016), p. 34740.



- [74] Mohammad F Saeed, Andrey A Kolokoltsov, Thomas Albrecht, and Robert A Davey. "Cellular entry of ebola virus involves uptake by a macropinocytosis-like mechanism and subsequent trafficking through early and late endosomes". In: *PLoS pathogens* 6.9 (2010), e1001110.
- [75] Carla Cerqueira, Pilar Samperio Ventayol, Christian Vogeley, and Mario Schelhaas. "Kallikrein-8 proteolytically processes human papillomaviruses in the extracellular space to facilitate entry into host cells". In: *Journal of virology* (2015), JVI-00234.
- [76] Yanchen Zhou, Punitha Vedantham, Kai Lu, Juliet Agudelo, Ricardo Carrion Jr, Jerritt W Nunneley, Dale Barnard, Stefan Pöhlmann, James H McKerrow, Adam R Renslo, et al. "Protease inhibitors targeting coronavirus and filovirus entry". In: *Antiviral research* 116 (2015), pp. 76–84.
- [77] Damian Szklarczyk, Annika L Gable, David Lyon, Alexander Junge, Stefan Wyder, Jaime Huerta-Cepas, Milan Simonovic, Nadezhda T Doncheva, John H Morris, Peer Bork, et al. "STRING v11: protein-protein association networks with increased coverage, supporting functional discovery in genome-wide experimental datasets". In: *Nucleic acids research* 47.D1 (2019), pp. D607–D613.
- [78] Michael Rebhan, Vered Chalifa-Caspi, Jaime Prilusky, and Doron Lancet. "GeneCards: integrating information about genes, proteins and diseases". In: *Trends in Genetics* 13.4 (1997), p. 163.
- [79] Mayumi Kanagawa, Tadashi Satoh, Akemi Ikeda, Yukiko Nakano, Hirokazu Yagi, Koichi Kato, Kyoko Kojima-Aikawa, and Yoshiki Yamaguchi. "Crystal structures of human secretory proteins ZG16p and ZG16b reveal a Jacalin-related  $\beta$ -prism fold". In: *Biochemical and biophysical research communications* 404.1 (2011), pp. 201–205.
- [80] Beatriz Salvador, Nicole R Sexton, Ricardo Carrion, Jerritt Nunneley, Jean L Patterson, Imke Steffen, Kai Lu, Marcus O Muench, David Lembo, and Graham Simmons. "Filoviruses utilize glycosaminoglycans for their attachment to target cells." In: *Journal of virology* (2013), JVI-01621.
- [81] Thoa T Than, Giao VQ Tran, Kidong Son, Eun-Mee Park, Seungtaek Kim, Yun-Sook Lim, and Soon B Hwang. "Ankyrin repeat domain 1 is up-regulated during hepatitis C virus infection and regulates hepatitis C virus entry". In: *Scientific reports* 6 (2016), p. 20819.

- [82] Yasuteru Sakurai, Andrey A Kolokoltsov, Cheng-Chang Chen, Michael W Tidwell, William E Bauta, Norbert Klugbauer, Christian Grimm, Christian Wahl-Schott, Martin Biel, and Robert A Davey. "Two-pore channels control Ebola virus host cell entry and are drug targets for disease treatment". In: *Science* 347.6225 (2015), pp. 995–998.
- [83] Samantha Hover, Barnabas King, Bradley Hall, Eleni-Anna Loundras, Hussah Taqi, Janet Daly, Mark Dallas, Chris Peers, Esther Schnettler, Clive McKimmie, et al. "Modulation of potassium channels inhibits bunyavirus infection". In: *Journal of Biological Chemistry* 291.7 (2016), pp. 3411–3422.
- [84] Viktor E Volchkov, Heinz Feldmann, Valentina A Volchkova, and Hans-Dieter Klenk. "Processing of the Ebola virus glycoprotein by the proprotein convertase furin". In: *Proceedings of the National Academy of Sciences* 95.10 (1998), pp. 5762–5767.
- [85] Jeffrey E Lee and Erica Ollmann Saphire. "Ebola virus glycoprotein structure and mechanism of entry". In: *Future virology* 4.6 (2009), pp. 621–635.
- [86] Kartik Chandran, Nancy J Sullivan, Ute Felber, Sean P Whelan, and James M Cunningham. "Endosomal proteolysis of the Ebola virus glycoprotein is necessary for infection". In: *Science* 308.5728 (2005), pp. 1643–1645.
- [87] Chantelle L Hood, Jonathan Abraham, Jeffrey C Boyington, Kwanyee Leung, Peter D Kwong, and Gary J Nabel. "Biochemical and structural characterization of cathepsin L-processed Ebola virus glycoprotein: implications for viral entry and immunogenicity". In: *Journal of virology* 84.6 (2010), pp. 2972–2982.
- [88] David Karlin and Robert Belshaw. "Detecting remote sequence homology in disordered proteins: discovery of conserved motifs in the N-termini of Mononegavirales phosphoproteins". In: *PLoS One* 7.3 (2012), e31719.
- [89] Morena Pappalardo, Miguel Juliá, Mark J Howard, Jeremy S Rossman, Martin Michaelis, and Mark N Wass. "Conserved differences in protein sequence determine the human pathogenicity of Ebolaviruses". In: *Scientific reports* 6 (2016), p. 23743.
- [90] Reed F Johnson, Sarah E McCarthy, Peter J Godlewski, and Ronald N Harty. "Ebola virus VP35-VP40 interaction is sufficient for packaging

- 3E-5E minigenome RNA into virus-like particles". In: *Journal of virology* 80.11 (2006), pp. 5135–5144.
- [91] Wei Shi, Yue Huang, Mark Sutton-Smith, Berangere Tissot, Maria Panico, Howard R Morris, Anne Dell, Stuart M Haslam, Jeffrey Boyington, Barney S Graham, et al. "A filovirus-unique region of Ebola virus nucleoprotein confers aberrant migration and mediates its incorporation into virions". In: *Journal of virology* 82.13 (2008), pp. 6190–6199.
- [92] Thomas Hoenen, Viktor Volchkov, Larissa Kolesnikova, Eva Mittler, Joanna Timmins, Michelle Ottmann, Olivier Reynard, Stephan Becker, and Winfried Weissenhorn. "VP40 octamers are essential for Ebola virus replication". In: *Journal of virology* 79.3 (2005), pp. 1898–1905.
- [93] Takeshi Noda, Shinji Watanabe, Hiroshi Sagara, and Yoshihiro Kawaoka. "Mapping of the VP40-binding regions of the nucleoprotein of Ebola virus". In: *Journal of virology* 81.7 (2007), pp. 3554–3562.
- [94] Xiaolan Zhu, Huiling Shen, Xinming Yin, Lulu Long, Xiaofang Chen, Fan Feng, Yueqin Liu, Peiqing Zhao, Yue Xu, Mei Li, et al. "IL-6R/STAT3/miR-204 feedback loop contributes to cisplatin resistance of epithelial ovarian cancer cells". In: *Oncotarget* 8.24 (2017), p. 39154.
- [95] Daniel P Hall, Nicholas G Cost, Shailaja Hegde, Emily Kellner, Olga Mikhaylova, Yiwen Stratton, Birgit Ehmer, William A Abplanalp, Raghav Pandey, Jacek Biesiada, et al. "TRPM3 and miR-204 establish a regulatory circuit that controls oncogenic autophagy in clear cell renal cell carcinoma". In: *Cancer cell* 26.5 (2014), pp. 738–753.
- [96] Ziyang Han, Jonathan J Madara, Andrew Herbert, Laura I Prugar, Gordon Ruthel, Jianhong Lu, Yuliang Liu, Wenbo Liu, Xiaohong Liu, Jay E Wrobel, et al. "Calcium regulation of hemorrhagic fever virus budding: mechanistic implications for host-oriented therapeutic intervention". In: *PLoS pathogens* 11.10 (2015), e1005220.
- [97] Hiroko Toda, Sasagu Kurozumi, Yuko Kijima, Tetsuya Idichi, Yoshiaki Shinden, Yasutaka Yamada, Takayuki Arai, Kosei Maemura, Takaaki Fujii, Jun Horiguchi, et al. "Molecular pathogenesis of triple-negative breast cancer based on microRNA expression signatures: antitumor miR-204-5p targets AP1S3". In: *Journal of human genetics* 63.12 (2018), p. 1197.
- [98] Xiang Li, Yuqiang Niu, Min Cheng, Xiaojing Chi, Xiuying Liu, and Wei Yang. "AP1S3 is required for hepatitis C virus infection by stabilizing E2 protein". In: *Antiviral research* 131 (2016), pp. 26–34.



## DECLARATION

---

Declaration with respect to the doctorate procedure.

Hiermit erkläre ich ehrenwörtlich:

- Mir ist die Promotionsordnung der Fakultät für Mathematik und Informatik (vom 17. Juli 2018) bekannt.
- Die Hilfe eines Promotionsberaters bzw. einer Promotionsberaterin wurde nicht in Anspruch genommen. Dritte haben im Zusammenhang mit dem Inhalt dieser Arbeit weder unmittelbar noch mittelbar geldwerte Leistungen erhalten.
- Die Dissertation habe ich selbst angefertigt, wobei keine Textabschnitte oder Ergebnisse eines Dritten oder eigenen Prüfungsarbeiten ohne Kennzeichnung übernommen und alle von mir benutzten Hilfsmittel, persönliche Mitteilungen und Quellen in meiner Arbeit angegeben wurden sind.
- Die Dissertation (oder Auszüge daraus) wurde noch nicht als Prüfungsarbeit für eine staatliche oder andere wissenschaftliche Prüfung eingereicht.
- Bis jetzt wurde noch keine Dissertation bei einer anderen Hochschule eingereicht.

Bei der Auswahl und Auswertung des Materials sowie bei der Erstellung des Manuskripts wurde ich von folgenden Personen unterstützt: Prof. Dr. Manja Marz und Prof. Dr. Stephan Becker. Für sprachliche und orthographische Aspekte des englischsprachigen Anteils der Arbeit wurde ich von Cilla, Alan und Philipp Wadge unterstützt, für den deutschsprachigen Anteil von Richard Henze.

*Jena, June 2020*

---

Nelly Fernanda Mostajo  
Berrospi